Modelling the transient visual system

Modelling the transient visual system

A. C. den Brinker

Modelling the transient visual system

Modelling the transient visual system

Proefschrift

ter verkrijging van de graad van doctor aan de
Technische Universiteit Eindhoven, op gezag van de
rector magnificus, prof. ir. M. Tels, voor een commissie
aangewezen door het college van dekanen in het
openbaar te verdedigen op vrijdag 17 maart 1989 te
14.00 uur

door

Albertus Cornelis den Brinker

geboren te Heerlen

Dit proefschrift is goedgekeurd door de promotoren:

Prof. Dr. Ir. J.A.J. Roufs

en

Prof. Dr. Ir. P. Eykhoff

I have no answers,
either,
I have got some stories
(on lucky days).

uit: Peter Hammill:
Palinurus (Castaway)

Contents

Introduction

Presumably, man has always been aware of the limitations of his senses. Occasionally, one even feels doubt about what the senses tell about the real world. This shows there exists an awareness about a world outside and a projection of that world via the senses. But this distinction between a world outside and a perceived world has become more acute now that physicists describe a world in terms that is more and more at odds with our daily experience. Terms like 'mass' are used instead of 'weight' and light is described as a 'spectrum of electromagnetic frequencies' while one observes 'colours'.

Therefore, the relation between the world described in physical terms and the world as perceived by our senses gains in scientific interest, also supported by the demands for knowledge about this relation for use in technical equipment. This thesis reflects this interest and, more specifically, it is concerned with the relation between visual stimuli described in physical terms and human percepts. This is still a rather large field and is much more narrowed down in the following chapters.

In this introduction, we will look into three issues that occur again and again in each chapter of this thesis. Therefore, it is worthwhile to start this thesis by considering these items in a more global way than could be done in the various chapters. These items are:
- the processing of visual stimuli,
- descriptive formulations of experimental findings (models),
- interpretations of models.

The processing of visual stimuli

The field of research that is of interest in this thesis is the processing of visual stimuli by the human eye and brain. We restrict ourselves to non-cognitive processes, and to psychophysical data and models. The actual processing by nerve cells is not our direct concern, although there obviously has to be a connection between physiological findings and psychophysical results. But it must always be kept in mind that psychophysical results must presumably be attributed to large masses of nerve cells, and physiological research concentrates on the behaviour of single cells or cooperations of small groups of cells. Psychophysics is essentially a black-box approach: only relations between input and output signals are investigated. The actual implementation by nerve cells is of secondary importance, and the modelling of psychophysical data as is done in this thesis provides in general no information about this.

The input signal in our black-box approach is a *visual stimulus*: the luminance distribution described in physical terms. The output signals are *human percepts* e.g., colour, brightness, apparent contrast, apparent size. Frequently the term

'apparent' appears in names of human percepts, since we often have to distinguish between the physical definition of these terms and the judgments of the human observer.

From this large field we will concentrate on *threshold data* and *the transient system*. Threshold data are the data concerning the relations between the physical quantities of a stimulus (upon a certain background) such that these can just be detected. We concentrate ourselves on threshold data for two reasons, mainly. First, these data are important as limits for technical realization of visual equipment. Secondly, this kind of analysis is a well-established first step in the modelling of nonlinear systems. This is a consequence of the small-signal theory: small variations of input signals around some steady level can usually be described by linear processing. Essentially, this is an engineering approach to the problem, that was started in the temporal domain of the visual perception by the work of De Lange (1952). However, the experimental data as collected by De Lange will not be a starting point for our modelling, as will be discussed in Chapter 1. It is doubtful whether linearity holds in general for threshold data.

Although the visual system acts in general nonlinearly for threshold stimuli, there are certain conditions in which linearity holds. From this finding and from physiology (e.g., Lennie, 1980), the idea of parallel pathways evolved. Nowadays, models for visual processing at threshold level commonly consist of parallel linear filters that cooperate in some nonlinear way.

In the temporal domain usually two temporal channels are distinguished: the transient and sustained channel (Kulikowsky and Tolhurst, 1973; Roufs, 1974; Breitmeyer and Ganz, 1976; Krauskopf, 1980; Roufs and Blommaert, 1981; Green, 1984). Some studies (Mandler and Makous, 1984) point at three separate channels. The sustained channel is tuned to the low temporal frequencies, the transient channel is most sensitive to fast temporal changes. In the spatial domain the sustained channel and the transient channel are sensitive to high-spatial and low-spatial frequencies, respectively (e.g., Breitmeyer and Ganz, 1976; Legge, 1978). These channels are also founded on the different percepts that are observed. For periodic stimuli of high-temporal frequency the percept is flicker, sometimes described as 'agitation' (Roufs, 1974). For periodic signals of low-temporal frequency the percept seems more related to brightness: increases and decreases of the amplitude can be observed. Therefore this percept is sometimes called 'swell' (Roufs, 1974). For pulse and step-like stimuli there is also a clear difference in percept in case of processing by the transient and sustained channel. In the former case a disturbance of the homogeneity of the field is seen, a sudden and hard to localize event. In the latter case a clearer increase (or decrease) of brightness at a localized position in the field is observed.

In this thesis we are mainly concerned with the transient visual channel. The data that is used is considered to be solely contributable to the transient visual system, unless explicitly stated otherwise. As argued in Chapter 1, it is possible to obtain appropriate experimental data to model this channel.

Models

As mentioned above, we are concerned with modelling the transient visual channel. This channel is assumed to act linearly around some steady background level, at least for threshold excitations. Indications for linearity have been found by De Lange (1954), Roufs and Blommaert (1981), Krauskopf (1980), Blommaert and Roufs (1987) and this author (Chapter 2 of this thesis). Roufs and Blommaert (1981) suggested a method (the perturbation technique) for experimentally determining time-domain the impulse response of circular discs. These impulse responses for larger disc sizes are associated with the transient channel (Roufs and Blommaert, 1981; de Ridder, 1987), and will form the starting point of the modelling. Using a parameter estimation program, the parameters of a linear model are determined from the impulse response data. Not only the impulse response but also the step response, the gain, and phase characteristic of the system can be experimentally determined by the perturbation technique. These data can be used as an independent test for the estimated model.

Modelling the system has several advantages:
• the modelled data is condensed into a few parameter values,
• the noise in the data is smoothed,
• predictions can be made with respect to new experiments and the modelling provides therefore an important contribution to generalization,
• hopefully, the model and its estimated parameters give insight into the system (see next section).

In Chapter 3 a chain of linear filters is proposed as a model of the transient channel. The last filter is 'matched' with respect to signals occurring in the earlier stages. This concept is based on an explicit functional argument about the system. In Chapter 4, 5 and 7 a fourth and sixth-order linear filter are taken as a model for the temporal behaviour. The choice of these filters is a very common approach in engineering and is more general than the approach in Chapter 3. The reason to introduce these n-th order filters is that (the macroscopic behaviour of) many physical systems can be described by a differential equation of limited order.

It turns out that both above mentioned models provide a nice description of the impulse response data, and give adequate predictions of threshold-versus-duration curves, subthreshold measurements of gain and phase characteristics and of the high-frequency side of De Lange curves.

Interpretation of models

The results of the estimated models give rise to two different interpretations.

The first interpretation tries to find a relation with physiological data. For instance, an n-th order linear filter is a description in poles and zeros of the system and in general one hopes that it is possible to attribute different poles (and zeros) to different subsystems that actually perform the processing. However, we

have to be extremely careful with this, since physiology is usually concerned with single cell behaviour whereas psychophysics presumably reflects the behaviour of an enormous number of different nerve cells. Even if we can distinguish different subprocesses that agree with physiological events, it must be kept in mind that from modelling the total response only a rough estimate of the subprocesses can be obtained. All details in subprocesses are more or less filtered out in a chain of processes.

Another way of interpreting the estimation results is achieved by comparing the parameters over different experimental conditions. In that case it is necessary to have an estimate of the variance of the estimated parameters. It is found that if the same experimental conditions are used with different observers, the estimated filters can be considered one and the same. This is not a surprising result: it already seems apparent in the data, and secondly, this is a common finding in perceptual research. This enables us to introduce a 'standard filter' and a 'standard subject' in a given experimental condition.

Varying the field size reveals that some of the estimated parameters of the fourth-order filter vary by an amount that cannot be attributed to statistical effects. This leads to the concept that, at least functionally, a subsystem is found that incorporates all spatiotemporal interactions within the transient channel. A simple linear spatiotemporal model is proposed to account for the processing performed by this subsystem (Chapter 6).

Variation of the background level gives similar results: also here specific parameters change by an amount not attributable to statistical effects. From this we derive a nonlinear model that is able to account for the observed changes. This nonlinear model, a fast adaptive closed-loop mechanism, gives a generalization of our results to conditions of arbitrary background levels, and can possibly even account for some suprathreshold phenomena (Chapter 7).

In this respect our modelling reveals relations between conditions that are (a posteriori) hidden in the experimental data. We think that this is the most interesting merit from the modelling.

In conclusion we would like to say that the whole exercise performed in this thesis is a rather tricky business; the collecting of the experimental data, the choice of the model and its parametrization and the interpretations are so linked up, that it is hardly possible to start with an 'unprejudiced' view of this matter. Even though one starts with adhering to viewpoints that may be questionable, it is hoped that the thesis establishes the fruitfulness of the chosen approach, and that the many suggestions in the different chapters act as a catalyst for insight and future research.

An outline of the thesis

In the first chapter we devote attention to experimental data that can be used to model (part of) the visual system. In particular the De Lange curves are

considered, and it is discussed that this kind of experimental data is probably not a good starting point for modelling.

In the second chapter a statistical test is performed on the subthreshold data from a perturbation experiment. It is shown that this statistical test supports the notion that the transient channel is operating linearly, and rejects models containing quadratic elements.

On the basis of the linearity assumption the impulse response data obtained by the perturbation technique are modelled as a linear filter. In Chapter 3 a proposal is made for the linear filter (a pseudo-matched filter) and it is shown that the behaviour of the system agrees well with such model.

A more general filter (a fourth-order linear filter) is proposed in Chapter 4, and an estimation technique is described to estimate the parameters of this filter. A short discussion of the results of the estimation method is included.

In Chapter 5 the estimation results of the fourth-order linear filter are discussed in more detail, and it is shown that by the choice of the filter and its parameters interpretations of the processing within the transient system can be made.

One of the conclusions in Chapter 5 is that a relatively simple spatiotemporal model should be able to account for the spatiotemporal interaction within the transient system. In Chapter 6 we take a closer look at the possibilities that membrane models offer to explain the results from Chapter 5.

The results of the estimation procedure (Chapter 5) with background level are elaborated in the Chapter 7. A sixth-order filter is taken as a model and by comparison of the estimated parameters of the filter it is found that these results can be interpreted as a closed-loop adaptive filter.

References

Blommaert F.J.J., Roufs J.A.J. (1987) Prediction of thresholds and latency on the basis of experimentally determined impulse responses. Biol. Cyb. **56**, 329-344.

Breitmeyer B.G., Ganz L. (1976) Implications of sustained and transient channels for theories of visual pattern masking, saccadic suppression, and information processing. Psychol. Review **83**, 1-36.

Green M. (1984) Masking by light and the sustained-transient dichotomy. Perc. and Psychophysics **35**, 519-535.

Krauskopf J. (1980) Discrimination and detection of changes in luminance. Vision Res. **20**, 671-677.

Kulikowski J.J., Tolhurst D.J. (1973) Psychophysical evidence for sustained and transient detectors in human vision. J. Physiol. **232**, 149-162.

Lange H. de (1952) Experiments on flicker and some calculations on an electrical analogue of the foveal system. Physica **18**, 935-950.

Lange H. de (1954) Relationship between critical flicker frequency and a set of low-frequency characteristics of the eye. J. Opt. Soc. Am. **44**, 380-389.

Legge G.E. (1978) Sustained and transient mechanisms in human vision: tempo-
    ral and spatial properties. Vision Res. **18**, 69-81.

Lennie P. (1980) Parallel visual pathways: a review.   Vision Res. **20**, 561-594
    (1980).

Mandler M.B., Makous W. (1984) A three channel model of temporal frequency
    perception. Vision Res. **24**, 1881-1887.

Ridder H. de (1987) Dynamic properties of human brightness perception.   Dr.
    Thesis Eindhoven University of Technology.

Roufs J.A.J. (1974) Dynamic properties of vision.-IV. Thresholds of decremental
    flashes, incremental flashes and doublets in relation to flicker fusion. Vision
    Research **14**, 831-851.

Roufs J.A.J., Blommaert F.J.J. (1981) Temporal impulse and step responses of
    the human eye obtained psychophysically by means of a drift-corrected per-
    turbation technique. Vision Research **21**, 1203-1221.

chapter 1

Considerations on modelling from De Lange curves[1]

A.C. den Brinker
F.J.J. Blommaert

Abstract

Starting with the pioneering work of De Lange[1], many attempts have been made to model temporal human vision on the basis of thresholds for sinusoidally modulated light. In this way it is hoped to acquire a general function from which thresholds for other time-varying stimuli can be predicted. Recently several new studies appeared. Reconsidering these attempts we argue that this kind of approach often suffers from assumptions which are not or not fully acknowledged.

1.1 Introduction

As proposed by Sperling[2] and Levinson[3] at the Flicker Symposium held at Amsterdam in 1963, a curve which describes the log of the modulation- or amplitude sensitivity as a function of the log frequency for sinusoidally modulated light is called a De Lange characteristic or De Lange curve. Such a curve is often seen as a fundamental characteristic of the temporal properties of the visual system. This stems from the notion that linear systems theory may be applicable to the visual system, at least for threshold excitations around some steady background level.

De Lange[1,4,5] showed that starting from a De Lange characteristic the sensitivity of the system to other periodic stimuli of high temporal frequency content can successfully be predicted. The extension of this idea is that one might be able to predict the sensitivity for arbitrary stimuli, especially aperiodic ones, on the basis of a De Lange curve.

As this idea has been put forward in various studies over the years, some of them recently, one wonders about the assumptions and fruitfulness of such an approach. We therefore reconsider the assumptions that are usually made in the prediction of thresholds for aperiodic stimuli, and argue that the linear approach is not as straightforward as often suggested. Other measurements might be more appropriate to characterize temporal properties of vision.

In the second Section of this paper we turn our attention to several studies that model the visual system starting from a De Lange curve, and focus on the similarities and differences in these papers. Next a closer look is taken at the assumptions underlying the modelling. In Section 3, predictions of these models for threshold-versus-duration curves are discussed, and compared to experimental

---

data. As a last point we discuss an alternative experimental approach which aims at a more direct determination of impulse responses and phase spectra. This kind of approach involves restrictions, as will be discussed.

1.2 Models on temporal processing

If a De Lange curve is taken for modelling the visual system around threshold by using linear system theory, one should have some indication that the system is actually behaving linearly. There is ample evidence for linear processing at threshold level (cf. De Lange[4]); on the other hand there are also indications for temporal processing in different channels[6,7,8]. Furthermore, there is always noise to consider, which cannot be accounted for in a linear model either.

Nevertheless, under the assumptions that the visual system acts as a single temporal channel, and that the noise can be neglected, the De Lange curve is equal to the amplitude-gain characteristic (TMTF, Temporal Modulation Transfer Function) of the unknown linear filter. These assumptions (single channel and negligible noise) will be discussed in more detail further on.

One way to start modelling the visual system is to postulate a certain impulse response or an equivalent network, and take the parameters such that the absolute value of the Fourier transform of this impulse response fits the De Lange curve. Early examples of this approach are the studies of Kelly[9], who used a diffusion stage followed by a pulse encoder, Matin[10] and Sperling and Sondhi[11], who used a network consisting of a cascade of RC elements with parametrically controlled time constants, and Roufs[12], who postulated a minimal phase network (using a ten-stage lowpass filtering network plus two differentiating sections). More recent examples can be found in the work of Watson and Nachmias[13] and Bergen and Wilson[14], who used the impulse response of a ten-stage lowpass filter added to a delayed and inverted replica of itself, of Georgeson[15], who took a single cycle of a raised cosine with halfwidth T, plus an inverted delayed and attenuated copy of the same waveform with a delay T, and of Ohtani and Ejima[16], who used a combined differentiating and integrating network.

A weak point in most of these studies might be that the choice of the impulse response (or the network) is rather arbitrary. To comment on this, we have to distinguish between two different kinds of stimuli.

On the one hand there is the case of targets with fine detail. A lowpass character is found in a De Lange curve which does not seem dependent on either background or spatial frequency[15,16], except for a multiplication factor (overall sensitivity). For a lowpass gain characteristic (not having a very high fall-off) there is little choice in the shape of the impulse response: it has to be something like a positive 'bump', although in principle small negative parts of the impulse response are permitted. How this 'bump' is described is not so essential for purposes of prediction. However, from the point of view of a systems approach, there are preferences. For instance, one would prefer an n-th order linear filter description to a description

in the form of one period of a raised cosine[15].

On the other hand we have the condition of low spatial frequency stimuli. At high background intensities a De Lange curve shows a (nearly) bandpass character, which changes into lowpass at low background levels. In this case the choice of the impulse response to fit a De Lange curve is essentially arbitrary: roughly speaking, it may consist of several positive and negative 'bumps' which can be arranged in various ways to obtain the same amplitude-gain characteristic. Fascinatingly, all cited authors agree that the impulse response should be (almost) biphasic, with the first phase positive and most pronounced. The argumentation of this choice is, as far as we know, physiologically inspired: the processing of visual informa- tion in cones[17], horizontal[18], bipolar[19] and ganglion cells[20] shows biphasic impulse responses, as far as the linear part of the cell responses is concerned. Although cells are the basic units for perception, it is not clear how these cell responses contribute to a resulting overall perceptual response. Therefore, postulating a biphasic impulse response as a model for the perceptual impulse response is an unwanted restriction.

A way to circumvent the arbitrariness of the choice of an impulse response was sought by Stork and Falk[21]. They did not consider a specific choice of impulse response to fit the De Lange data, but wanted to reconstruct the phase spectrum from the De Lange curve without any new assumption. They stated that on the basis of the causality of the impulse response the phase spectrum of the filter could be retrieved from a De Lange curve by means of the Kramers-Kronig relations, without any new assumption.

The notion that there is an unique connection between causality and the Kramers- Kronig relation is incorrect, and is not even supported by the reference[22] that Stork and Falk[21] used. The Kramers-Kronig relation is equivalent to a minimal phase assumption, as was acknowledged by Swanson et al.[23], who used the Stork and Falk[22] scheme to derive impulse responses from their De Lange curves for lumi- nance and chromatic stimuli. However, it is questionable whether minimal phase is an appropriate assumption for chromatic temporal responses, as was already recognized by De Lange[5]. With chromatic stimuli[23] it is expected that difference signals from different colour-sensitive pathways determine the responses. It is well known that a transfer resulting from the difference of two minimal phase transfer functions generally exhibits a non-minimal phase behaviour (cf. electrical bridge circuits).

The fact that causality does not imply a minimal phase relation, is shown with a counter example in Fig. 1. An amplitude spectrum (Fig. 1a), which can be associated with different phase spectra (Fig. 1b), can lead to different causal impulse responses (Fig. 1c).

The foregoing discussion can be extended to the general conclusion that it is impossible to derive an impulse response or a phase spectrum from an amplitude spectrum (TMTF) without any further assumptions. And in as much as a biphasic impulse response is an arbitrary choice, so is the assumption of a minimal phase.
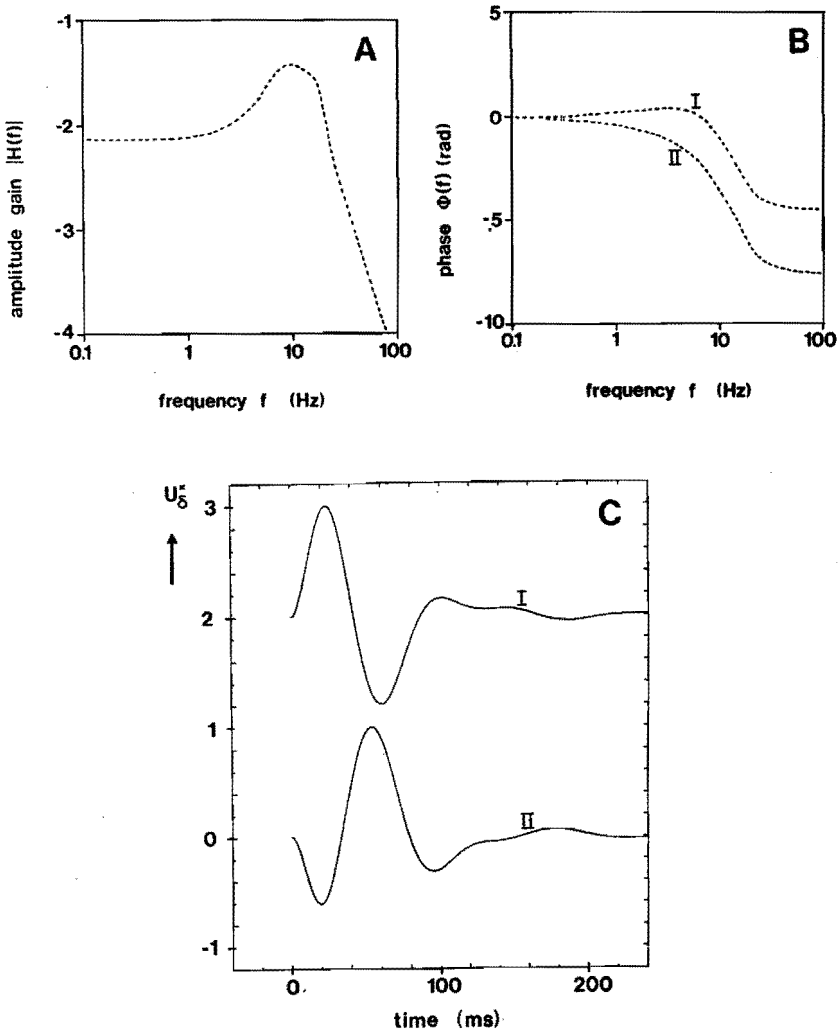
Figure 1: **A.** Amplitude-gain characteristic of a fourth-order linear filter. **B.** Two phase-spectra belonging to the amplitude-gain curve of Fig. 1a. The upper curve (I) is a phase spectrum with the zeros of the transfer function in the left half-plane; for the lower curve (II) the zeros have been mirrored with respect to the origin of the *s*-plane. **C.** Normalized impulse responses derived from the amplitude and phase spectra of Figs. 1a and 1b. For clarity, the upper curve is shifted over two units.

Sustained and transient channels

The channel idea emerged from the electrophysiologically defined sustained and transient cells[24] (for a review see Lennie[25]), and was soon adopted in psychophysics [6,26,13,8]. It was found that different temporal behaviour is coupled to different sensitivities for spatial patterns: the sustained behaviour is found for stimuli with fine detail, the transient system is associated with spatially coarser targets. The discussion on this subject is not yet concluded. A recent overview of arguments in this debate can be found in Watson[27].

As already mentioned, for fine-detail targets all the De Lange curves appear quite similar. However, for spatially coarser targets the characteristics change with spatial frequency and background level, and different percepts are observed at low and high temporal frequencies[7]. So, in the region of low spatial frequencies, there is not only a problem with the choice of the impulse response, but also with the question of whether a De Lange curve can be attributed to one channel only.

The influence of noise

The approaches to modeling the visual system, as mentioned above, all assume that a De Lange curve equals the amplitude-gain characteristics of the linear filter. This implies that there is no (or negligible) noise, or that the noise identically influences the measured sensitivity to different frequencies. That the influence of noise is not negligible can be readily shown experimentally: the sensitivity to a gated sinusoid is dependent on the duration of the signal[28]. This means that if a De Lange curve is used to model the temporal behaviour, the conjecture is made that the noise affects the sensitivity of different frequencies by an equal amount (on a logarithmic scale). For two special noise conditions this conjecture is not hard to prove (see Appendix), viz. if either a large part of the power spectrum of the noise is above the frequency domain of the linear filter, or if the autocorrelation function of the noise has time constants larger than the observation time which is used in the measurement of the De Lange curve (i.e. the dominant part of the power spectrum of the noise is located at very low frequencies).

However, both noise conditions are probably not realistic assumptions for the noise in the visual system. There is no reason to assume that frequencies to which the filter is sensitive are absent in the noise spectrum. It is more likely that all three frequency components mentioned are present in the power spectrum of the noise.

Low and medium frequency noise components might explain the differences in the slopes of the psychometric functions that are found using a fast measurement technique (Blommaert and Roufs[29]; $\beta = 6 - 8$ if one uses Watson's[27] description for the psychometric function) or a more time-consuming one (where $\beta = 3 - 4$ may be found[27]).

Nevertheless, since significant noise is also found in fast measurements of psy-

chometric functions, one must assume that part of the noise is located around the frequencies to which the eye is most sensitive. This means that this noise might give unequal reduction in sensitivity at different frequencies of a De Lange curve.

1.3 Prediction of threshold-versus-duration curves

From the modeled visual system, predictions can in principle be made for thresholds of arbitrary time-varying stimuli. For validation of models, pulses with variable durations are often used. Usually, predictions of thresholds for fine-detail targets are in satisfactory agreement with experimental data if noise is incorporated in the model. For spatially coarser targets there is less agreement between these predictions and experimental data[15,16]. We will therefore turn our attention to these cases.

Examples of experimental data that make up such curves for not too small field sizes with a completely dark surround are shown in Fig. 2. These curves (taken from Blommaert and Roufs[29]) show a linear relation between sensitivity and duration for small durations (Bloch's law) and a duration-independent threshold intensity for long durations.
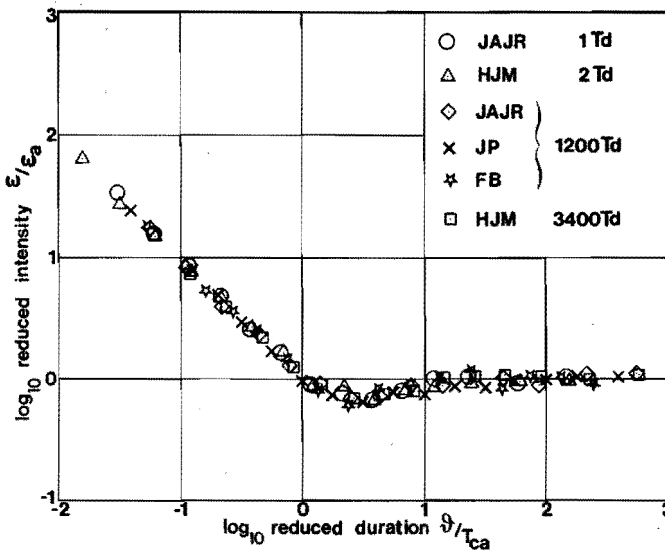
Figure 2: Reduced threshold-versus-duration curve for a 1 degree disk without surround. The individual curves were shifted horizontally and vertically such that the asymptotes at short and long durations coincided (for details see Blommaert and Roufs[29], reprinted with permission).

Bloch's law can be explained by a processing in the visual system that starts with a linear filter (with no transfer at the very high frequencies) followed by any

nonlinear processing[30,31]. The independence of the threshold at long duration rules out a lowpass filter; a lowpass filter will not provide a steady threshold at long durations if noise is taken into account[32]. This means that the linear filter must have a (nearly) bandpass character.

The most remarkable element in such curves is that under certain conditions, these curves show a pronounced dip (about 0.15 log unit) at intermediate durations [33,29,23]: this is the threshold version of the Broca-Sulzer brightness phenomenon[34]. This dip, occurring at low spatial frequencies, cannot be explained by a biphasic impulse response and deterministic processing. Furthermore, the influence of noise is probably too small to account for the dip. Since Gorea and Tyler[35] ignored other than mono- and biphasic impulse responses, they concluded that no linear model would be able to predict this dip. (That this is not the case if triphasic impulse responses are used was shown by Blommaert and Roufs[29].) Therefore, Gorea and Tyler introduced a nonlinear model, consisting of a linear filter with a biphasic impulse response, followed by a nonlinear double integrator. Apart from the fact that they fitted the biphasic impulse response directly to the De Lange curve, thus neglecting the contributions of their nonlinear operator, and apart from an incorrect derivation of the nonlinear parameter from the psychometric function, their model is still unable to predict a threshold-versus-duration curve showing a dip of the correct magnitude except for very unlikely values of the nonlinear parameters. In short, none of the models discussed up to now is able to explain the dip in the threshold-versus-duration curve from a biphasic impulse response.

1.4 Concluding remarks

Summarizing the foregoing, impulse responses can be derived from a De Lange characteristic if three conditions are fulfilled:
• noise should contribute equally at different temporal frequencies
• the temporal properties of one channel only are reflected in the De Lange curve
• a choice is made on either the phase spectrum, the impulse response or a network that is used as a model.
If this procedure is followed and it is found that predictions do not agree with experimental data, the mentioned conditions have to be reconsidered. This was actually done by Roufs[7], Georgeson[15], and Ohtani and Ejima[16]. These authors agree in that they attribute the discrepancies to the action of two different channels. The most detailed analysis of a two-channel concept can be found in the work of Roufs[7]. He postulated a bandpass filter for the transient channel and succeeded in unifying experimental results on periodic and aperiodic stimuli with substantial temporal high frequency content. In a later stage this idea was pursued further in attempts to determine phase behaviour[36] and impulse responses[33] of the separate channels by using a subthreshold summation technique. The impulse responses determined in this way showed a triphasic character (like the impulse response in Fig. 1c), and the phase spectrum exhibited a non-minimal phase relation. These

findings cast doubt upon the usual assumption of a biphasic impulse response or a minimal phase relation. However, the analysis of the properties of individual channels has the disadvantage that only predictions within a single channel can be accounted for. This means that this approach is only a partial way out of the problem that is posed by modelling the visual system from a De Lange characteristic, since new unknown factors are introduced, i.e. interactions between channels.

References

[1] H. de Lange, "Experiments on flicker and some calculations on an electrical analogue of the foveal system." Physica **18**, 935-950 (1952).

[2] G. Sperling, "Linear theory and the psychophysics of flicker." In: *Flicker*, eds. H. E. Henkes and L. H. van der Tweel. The Hague: Junk, 1964.

[3] J. Levinson, "Nonlinear and spatial effects in the perception of flicker." In: *Flicker*, eds. H. E. Henkes and L. H. van der Tweel. The Hague: Junk, 1964.

[4] H. de Lange, "Relationship between critical flicker frequency and a set of low-frequency characteristics of the eye." J. Opt. Soc. Am. **44**, 380-389 (1954).

[5] H. de Lange, Attenuation characteristics and phase-shift characteristics of human fovea-cortex systems in relation to flicker fusion phenomena. Ph.D thesis, Delft, 1957.

[6] J. J. Kulikowski and D. J. Tolhurst, "Psychophysical evidence for sustained and transient detectors in human vision." J. Physiol. **232**, 149-162 (1973).

[7] J. A. J. Roufs, "Dynamic properties of vision-IV. Thresholds of decremental flashes, incremental flashes and doublets in relation to flicker fusion." Vision Res. **14**, 831-851 (1974).

[8] M. Green, "Masking by light and the sustained-transient dichotomy." Perception and Psychophysics **35** (6), 519-539 (1984).

[9] D. H. Kelly, "Visual responses to time-dependent stimuli. II. Single-channel model of the photopic visual system." J. Opt. Soc. Am. **51** (7), 747-754 (1961).

[10] L. Matin, "Critical duration, the differential luminance threshold, critical flicker frequency and visual adaptation, a theoretical treatment." J. Opt. Soc. Am. **58**, 404-415.

[11] G. Sperling and M. M. Sondhi, "Model for visual luminance discrimination and flicker detection." J. Opt. Soc. Am. **58**, 1133-1145.

[12] J. A. J. Roufs, "Dynamic properties of vision-II. Theoretical realationships between flicker and flash thresholds." Vision Res. **12**, 279-292 (1972).

[13] A. B. Watson and J. Nachmias, "Patterns of temporal interaction in the detection of gratings." Vision Res. **17**, 893-902 (1977).

[14] J. R. Bergen and H. R. Wilson, "Prediction of flicker sensitivities from temporal three-pulse data." Vision Res. **25**, 577-582 (1985).

[15] M. A. Georgeson, "Temporal properties of spatial contrast vision." Vision Res. **27**, 765-780 (1987).

[16] Y. Ohtani and Y. Ejima, "Relation between flicker and two-pulse sensitivities for sinusoidal gratings." Vision Res. **28**, 145-156 (1988).

[17] S. J. Daly and R. A. Normann, "Temporal information processing in cones: effects of light adaptation on temporal summation and modulation." Vision Res. **25**, 1197-1206 (1985).

[18] M. Kawasaki, K. Aoki and K.-I. Naka, "Effects of background and spatial pattern on incremental sensitivity of catfish horizontal cells." Vision Res. **24**, 1197-1204 (1984).

[19] K.-I. Naka, "The cells horizontal cells talk to." Vision Res. **22**, 653-660 (1982).

[20] C. Enroth-Cugell and R. M. Shapley, "Adaptation and dynamics of cat retinal ganglion cells." J. Physiol. **233**, 271-309 (1973).

[21] D. G. Stork and D. S. Falk, "Temporal impulse responses from flicker sensitivities." J. Opt. Soc. Am. A **4** (6), 1130-1135 (1987).

[22] H. M. Nussenzveig, *Causality and Dispersion Relations.* New York: Academic, 1972.

[23] W. H. Swanson, T. Ueno, V. C. Smith and J. Pokorny, "Temporal modulation sensitivity and pulse-detection thresholds for chromatic and luminance perturbations." J. Opt. Soc. Am. A **4** (10), 1992-2005 (1987).

[24] B. G. Cleland, M. W. Dubin and W. R. Levick, "Sustained and transient neurones in the cat's retina and lateral geniculate nucleus." J. Physiol. **217**, 473-496 (1971).

[25] P. Lennie, "Parallel visual pathways: a review." Vision Res. **20**, 561-594 (1980).

[26] B. G. Breitmeyer and L. Ganz, "Implications of sustained and transient channels for theories of visual pattern masking, saccadic suppression and information processing." Psychol. Review **83**, 1-36 (1976).

[27] A. B. Watson, "Temporal sensitivity." In: *Handbook of Perception and Human Performance, Vol.I. Sensory Processes and Perception.* Eds. K. R. Boff, L. Kaufman and J. P. Thomas. New York: Wiley, 1986.

[28] J. A. J. Roufs, "Dynamic properties of vision-VI. Stochastic threshold fluctuations and their effect on flash-to-flicker sensitivity ratio." Vision Res. **14**, 871-888 (1974).

[29] F. J. J. Blommaert and J. A. J. Roufs, "Prediction of thresholds and latency on the basis of experimentally determined impulse responses." Biol. Cyb. **56**, 329-344 (1987).

[30] J. A. J. Roufs, "Time dependent brightness of pixels." Eurodisplay, 1981. Proc. of the First European Display Research Conf., 120-129.

[31] H. de Ridder, *Dynamic properties of human brightness perception.* Ph.D thesis, Eindhoven University of Technology, 1987.

[32] J. A. J. Roufs and H. Bouma, "Towards linking perception research and image quality." Proc. SID **21**, 247-269 (1980).

[33] J. A. J. Roufs and F. J. J. Blommaert, "Temporal impulse and step responses of the human eye obtained psychophysically by means of a drift-correcting perturbation technique." Vision Res. **21**, 1203-1221 (1981).

[34] A. Broca and D. Sulzer, "La sensation lumineuse en function de temps." J. de Physiologie et de Pathologie Générale **4**, 632-640 (1902).

[35] A. Gorea, and C. W. Tyler, "New look at Bloch's law for contrast." J. Opt. Soc. Am. A **3**, 52-61 (1986).

[36] J. A. J. Roufs, H. A. L. Piceni and J. A. Pellegrino van Stuyvenberg, "Phase and gain analysis of the visual transient system." IPO Annual Progress Report **19**, 49-56 (1984).

[37] W. Weibull, "A statistical distribution function of wide applicability." J. Appl. Mech. **18**, 292-297 (1951).

[38] J. A. J. Roufs and H. A. L. Piceni, "The effect of noise on the analysis of the transient human visual system." To be submitted to Biol. Cyb.

Appendix. Contributions of noise to a De Lange curve

In this appendix the effect of noise on the sensitivity of the visual system to a gated sinusoid is approximated for two special cases. First a high-frequency noise with a cut-off frequency f_{cN} is considered. Second, the effect of low-frequency noise is evaluated.

We start with the scheme in Fig. 3: the input signal is a gated sinusoid with duration T. This duration T is much larger than the period $1/f$ of the lowest frequency f in the De Lange curve. The slow onset and offset are used to eliminate transient phenomena at the start and end of the presentation. The time constants of the gating onset and offset functions are much smaller than the presentation time T. Within T the input signal is described by $\varepsilon \sin(2\pi ft)$, and $\varepsilon > 0$. The gated sinusoid is the input to a linear filter with transfer $H(f) = |H(f)| \exp(-j\phi(f))$, $|H(f)|$ being the amplitude spectrum and $\phi(f)$ the phase spectrum of the linear filter. The output $s(t)$ of the linear filter is considered to be equal to $\varepsilon |H(f)| \sin(2\pi ft - \phi(f))$, within time interval T. Noise $n(t)$ is added to the output of the linear filter. The last stage of the processing is a detection mechanism with a symmetric threshold values $(-d, +d)$.
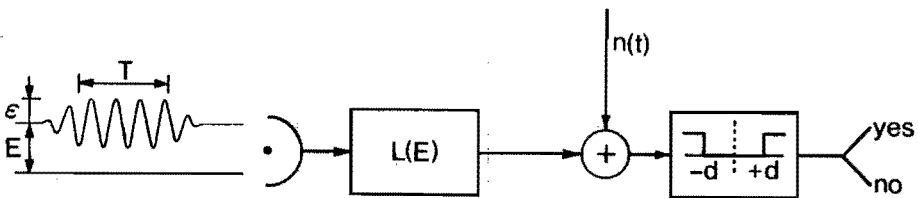
Figure 3: Model for noise analysis.

Taking a Weibull distribution[37] and under the assumption that the cut-off frequency f_{cN} of the noise is much larger than the cut-off frequency of the linear filter,

the noise behaviour can be translated into a deterministic nonlinear operator. For the threshold value ε_{th} of a gated sinusoid it is found that[38,16]

$$
\begin{aligned}
\log \varepsilon_{th} = & -\log(|H(f)|/d) - \tfrac{1}{\beta} \log(f_{cN}) \\
& -\tfrac{1}{\beta} \log(T) - \tfrac{1}{\beta} \log\left(\tfrac{1}{\pi} \int_0^\pi |\sin\rho|^\beta \, d\rho\right),
\end{aligned}
\tag{1}
$$

where β is the parameter from the Weibull distribution.

From this equation we see that the effect of noise is identical for each frequency f, as long as the same presentation time T is used.

We find that the substitution of the stochastic behaviour of the noise by a nonlinear deterministic rule is only applicable under the assumption of high-frequency noise. Consequently, this description of the noise is not as *plausible*[27] as sometimes thought.

The effects of low-frequency noise will now be considered where, similar to the case of high-frequency noise, we again consider intervals in which the noise is uncorrelated. If the time constants of the autocorrelation function of the noise are much larger than T, the threshold determination in each interval T is a deterministic event with threshold $d - n$ (with noise n approximated as steady over the complete presentation time). Repeating such an experiment with the same frequency f and duration T, we find in each experiment a different value for the noise n. However, the distribution of n is not dependent on f, so:

$$
\mathcal{E}[\log \varepsilon_{th}] = -\mathcal{E}\left[\log\left(\frac{|H(f)|}{d-n}\right)\right] = -\log\left(\frac{|H(f)|}{d}\right),
\tag{2}
$$

in a first order approximation of any distribution with $\mathcal{E}[n] = 0$ ($\mathcal{E}$ stands for expected value).

An extension of this low-frequency noise can be described qualitatively. Consider noise with time constants of the autocorrelation smaller than the presentation time T, but larger than that of the period of even the lowest frequency in a De Lange curve. The presentation time T can then be divided into a number of intervals with duration T_{ac} (T_{ac} about the largest time constant of the autocorrelation function). This rough approximation shows a deterministic behaviour within T_{ac} and independent noise contributions in the different intervals. In that case the effect of the noise is dependent on the presentation time T, but independent of the presented frequency f. Furthermore, one would expect to see a sequence of peaks (over periods of roughly T_{ac}), contrary to the case of high-frequency noise, where detection would consist of observing independent peaks randomly distributed over the presentation interval T.

However, the most interesting case of noise with a significant part of its spectrum located around the frequencies to which the linear filter is optimally sensitive cannot be treated in the rough approximations as before. Nevertheless, one thing is clear: such noise will give different sensitivity increases to different input frequencies. Essential in those cases is the precise form of the autocorrelation function (or the power spectrum) of the noise.

chapter 2

Linear and quadratic models for threshold data of the transient visual system[1]

A.C. den Brinker

Abstract

In this paper two models are considered for the transient visual system at threshold. One is a linear model and the other a model containing a quadratic element. Both models are commonly used based on experimental results from different sources. It is shown that both models act in a similar way for the experiments using a perturbation technique as is the case at IPO. It is, however, possible to distinguish between these models in an experiment with a perturbation technique using a statistical test. This test is discussed and performed and it is shown that it supports the linear and rejects the quadratic model.

2.1 Introduction

Data obtained from a psychophysical threshold experiment (Roufs and Blommaert, 1981) are interpreted and modelled as the impulse response from a linear system. Within the sets of linear models there is one, which we will call a pseudo-matched filter, which fits the data. This model has some resemblances to two nonlinear models: the Reichardt model (Reichardt, 1957; 1961; Reichardt and Varjú, 1959), and the Rashbass model (Rashbass, 1970; 1974). It is shown that the measured data can also be interpreted as being derived from these nonlinear models. In these cases the measurement data are interpreted not as an impulse response, but as the autocorrelation of the impulse response of the linear stage of these models. Additional data (e.g. step responses and block responses) also fit into the linear and nonlinear models. Therefore the problem is how to distinguish between the linear and the nonlinear models. It is pointed out that a measurement performed by Elsner (1986) is probably not decisive in distinguishing between these linear and nonlinear models. It is shown that a perturbation experiment makes it possible to discriminate between the linear and nonlinear models by using a simple statistical test.

2.2 A qualitative comparison

In this section the similarities in behaviour of the Rashbass, the Reichardt, and the pseudo-matched filter model are shown with regard to certain stimuli.

---

[1]Parts of this chapter appeared in IPO Annual Progress Report **21**, 53-62, 1986.

The Reichardt model (Reichardt, 1961) was originally developed for the movement detection of insects, but later these models were also applied to human movement detection. Here only the main part of this model (Figure 1A) is used and all refinements are omitted. This main part consists of two equal linear filters D, plus a cross-correlator.
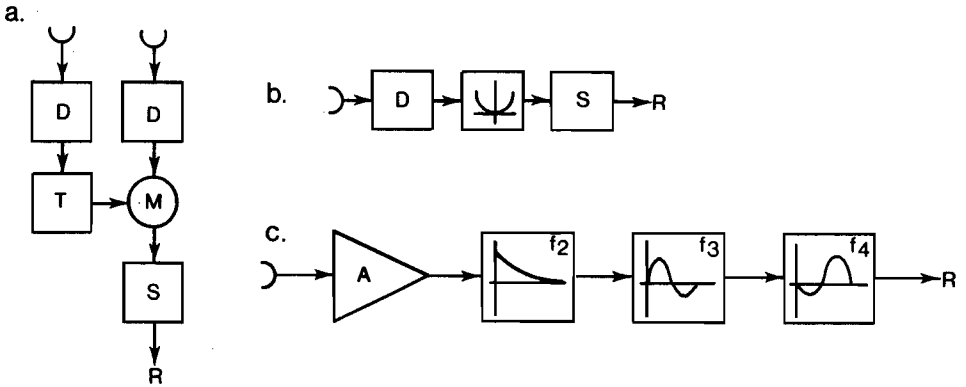
Figure 1: **A.** A simplified version of the Reichardt model. This model consists of two identical linear filters D, a time delay T, a multiplier M, and an ideal integrator S.
B. The Rashbass model. D is a linear filter, which is followed by a quadratic element, and an integrator S.
C. The pseudo-matched filter model, consisting of a series of linear filters f_i ($i = 2, 3, 4$) and an amplifier A.

For non-moving stimuli (e.g. flashed discs) the excitation at different points of the retina has the same time variation. The maximum response of the cross correlator will therefore occur for a time delay $T = 0$. Since the time courses at the two inputs of the simplified Reichardt model are equal, the multiplier can be substituted by a quadratic element, simultaneously omitting the second input of Figure 1A. This is depicted in Figure 1B. This model is called the Rashbass model (Rashbass, 1970; 1974). This means that the simplified Reichardt model acts in the same way as the Rashbass model for short time delays T, and non-moving stimuli. We will not discuss whether a small time delay is appropriate within the Reichardt model; the point here is that if small delays are used in the Reichardt model, then this model is equivalent to the Rashbass model for static stimuli.

The pseudo-matched filter model is sketched in Figure 1C. The fourth filter $f_4(t)$ has the same impulse response as the third filter $f_3(t)$ except for a reversal of the time axis and a time delay to make this filter causal. The essential part is

constituted by these last two filters. By omitting the amplifier A and the first-order filter $f_2(t)$, this can be made to act in a way similar to the Rashbass model, but only if a Dirac function is chosen as excitation. To this end the impulse response $f_3(t)$ and the impulse response of the linear filter D have to be equal. The filter D in the Rashbass model and the filter $f_3(t)$ in the pseudo-matched filter model are both biphasic.

There is a strong connection between matched filtering and correlation techniques. In detection tasks a correlator is often used. If the incoming signal is known by its form, then an appropriate filter, a matched filter, acts in the same manner as a correlator for such a signal (Papoulis, 1977).

The concluding remark for this section is therefore that all three models (Figure 1) are expected to act in a very similar manner when using a non-moving stimulus, with a Dirac function as the principal part of its time course. We will show this in more detail in the rest of this paper, and also discuss a measurement that makes a definite distinction possible between the linear and nonlinear model and nevertheless contains a Dirac pulse as the principle part of its time course.

2.3 The linear model in a perturbation experiment

Consider a linear model followed by a threshold mechanism. The threshold mechanism is symmetrical with output 1 if the absolute value of the input signal is larger than the threshold value d and the output is zero otherwise. The following analysis is not restricted to the pseudo-matched filter model, but applies to any linear model. The model is deterministic; there are no noise sources present (Figure 2A). The impulse response of the linear filter can be measured using a perturbation technique (see also Roufs and Blommaert, 1981).

The impulse response of the linear filter L is called $v(t)$. The step response is called $w(t)$, so that

$$w(t) = \int_0^t v(\sigma)\,d\sigma. \tag{1}$$

We now take $\varepsilon h_{in}(t)$ as the input signal of the linear filter, where $h_{in}(t)$ is an amplitude-normalized function (the peak of h_{in} being normalized) and ε is the amplitude. We define $h(t)$ as the response of the linear filter to the input signal $h_{in}(t)$, so

$$h(t) = h_{in}(t) * v(t), \tag{2}$$

where $*$ denotes a convolution. The signal in front of the threshold mechanism is then $\varepsilon h(t)$. The lowest value of ε at which detection occurs is called ε_1. This means that

$$\varepsilon_1 \max |h(t)| = d. \tag{3}$$

In actual measurements there is considerable noise and we take that value of ε as the threshold value for which the detection probability equals 0.5. The (first) moment at which the extreme value of $h(t)$ is reached is called t_{ex}.
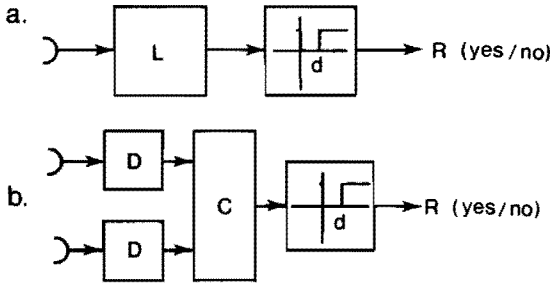
Figure 2: **A.** The linear filter L and the threshold mechanism.
B. The simplified Reichardt model. $v(t)$ the impulse response of the linear filter D, T the time delay. Ideal integration over total time. Time delay and integration are done in C.

Now take $\varepsilon\{h_{in}(t) + qg_{in}(t - \tau)\}$ as the input signal. The function $g_{in}(t)$ is an amplitude-normalized function, q is a proportionality factor and τ is a time delay. Assume

$$g(t) = g_{in}(t) * v(t), \tag{4}$$

then the signal before the detector becomes $\varepsilon\{h(t) + qg(t - \tau)\}$. The lowest value of ε for which detection occurs is called ε_c. On the assumption that

$$h(t_{ex}) \gg qg(t), \qquad \text{for all } t, \tag{5}$$

it is true that

$$\varepsilon_c\{h(t_{ex}) + qg(t_{ex} - \tau)\} = d, \tag{6}$$

if $|h(t)|$ has one sharp peak that is dominant over all other peaks of $|h(t)|$. The lowest detectable amplitude ε_c is a function of τ and q, given $h(t)$ and $g(t)$. By combining (6) and (3), we obtain

$$\frac{g(t_{ex} - \tau)}{h(t_{ex})} = \frac{1}{q} \left\{ \frac{\varepsilon_1}{\varepsilon_c(\tau)} - 1 \right\}. \tag{7}$$

The right-hand side is a function of the measurement data only. The function $h(t)$ is called the probe and the function $g(t)$ is the test signal. Expression (7) shows that the form of the test signal $g(t)$ can be measured by varying τ.

This perturbation technique is used for the measurement of the impulse and step response of the linear filter. First take

$$h_{in}(t) = g_{in}(t) = H(t) - H(t - \vartheta),$$

$$h(t) = g(t) \simeq \vartheta\, v(t),$$

$$q \ll 1,$$

with $H(t)$ the Heaviside function, and ϑ much smaller than the time constants of the linear filter. Then the normalized impulse response $v^*(t_{ex} - \tau)$ can be calculated from the measurements according to (7), yielding

$$v^*(t_{ex} - \tau) \equiv \frac{v(t_{ex} - \tau)}{v(t_{ex})} = \frac{1}{q}\left\{ \frac{\varepsilon_1}{\varepsilon_c(\tau)} - 1 \right\}. \tag{8}$$

In the second place this method can be used to measure the form of the step response by taking

$$\begin{aligned} h_{in}(t) &= H(t) - H(t - \vartheta), \\ g_{in}(t) &= H(t), \\ h(t) &= \vartheta v(t), \\ g(t) &= w(t), \end{aligned}$$

where, as in the previous case, ϑ is much smaller than the time constants of the system. Now a scaled version of the step response $w^o(t_{ex} - \tau)$ is found, that is

$$w^o(t_{ex} - \tau) = \frac{w(t_{ex} - \tau)}{\vartheta\, v(t_{ex})} = \frac{1}{q}\left\{ \frac{\varepsilon_1}{\varepsilon_c(\tau)} - 1 \right\}. \tag{9}$$

The relation between this step response $w^o(t)$ and the normalized impulse response $v(t)$ is given by

$$w^o(t_{ex} - \tau) = \frac{1}{\vartheta} \int_0^{t_{ex} - \tau} v^*(\sigma)\, d\sigma. \tag{10}$$

2.4 The linear model and the norm factors

From $v^*(t)$ the response $v(t)$ can be expressed in threshold units d:

$$\frac{v(t)}{d} = \frac{v^*(t)}{\varepsilon_\delta \vartheta}, \tag{11}$$

and similarly the response $w(t)$ can be expressed in threshold units d by

$$\frac{w(t)}{d} = \frac{w^*(t)}{\varepsilon_s}, \tag{12}$$

with ε_δ and ε_s the smallest values of ε for which the impulse response and the step response, respectively, are detected, and $w^*(t)$ is the amplitude-normalized version of $w(t)$ (and $w^o(t)$). The values $(\varepsilon_\delta \vartheta)^{-1}$ and ε_s^{-1} are called norm factors NF_δ and NF_s:

$$\begin{aligned} NF_\delta &= (\varepsilon_\delta \vartheta)^{-1}, & (13) \\ NF_s &= \varepsilon_s^{-1}. & (14) \end{aligned}$$

From (11) and the linearity of the system the response $R(t)$ to an arbitrary input signal $r(t)$ can be expressed in d units:

$$R(t) = NF_\delta \; r(t) * v^*(t). \tag{15}$$

Using the norm factors a check on the assumption of the linearity of the system can be made. From (1) and (11) we find

$$w^o(t) = \int_{-\infty}^t \frac{v^*(\sigma)}{\vartheta} d\sigma = \varepsilon_\delta \frac{w(t)}{d}, \tag{16}$$

and especially

$$w^o(T_{ex}) = \frac{\varepsilon_\delta}{\varepsilon_s}, \tag{17}$$

using (12) and where T_{ex} is defined by $w^*(T_{ex}) = 1$. (17) states that the maximum of $w^o(t)$, which can be measured according to (9), can be predicted from the ratio of the sensitivities of the system to a short pulse and a step input.

Also the normalized impulse and step response are related by the norm factors. From (10) it is found

$$\left. \frac{dw^o}{dt} \right|_{t_{ex}} = \vartheta^{-1}, \tag{18}$$

$$\left. \frac{dw^*}{dt} \right|_{t_{ex}} = \frac{NF_\delta}{NF_s}. \tag{19}$$

Equation (17) (or (19)) can be used as an indication of the linearity hypothesis of the system. The procedure is as follows: the impulse response $v^*(t_{ex} - \tau)$ is measured. A continuous function is fitted to these data (e.g. Chapter 4). From this fit the step response $w^o(t)$ (or $w^*(t)$) can be calculated and compared to the measured values ε_δ and ε_s, according to (17) (or (19)). Note also that NF_δ/NF_s is the interception of the two asymptotes in the block response data (see Figure 4), i.e. the critical duration T_{ca} (Roufs, 1974a).

There are a few problems with this check. First of all the norm factors, or amplitudes ε_δ and ε_s, are normally not derived from measurements using a drift correction as described by Roufs and Blommaert (1981). These data are therefore subject to large hour-to-hour and day-to-day variations which can be as much as a factor 2. Furthermore ϑ is used either to calculate the maximum in (16) or is used in NF_δ in (19). Although this value may be set very accurately electronically, this is fed to some light source which may not be so good at reproducing the exact area belonging to the Dirac probe.

Still, we will evaluate this quantitatively. As an example the simultaneous fit of the impulse response and the step response was taken (an adapted version of Figure 12 from Roufs and Blommaert, 1981). These fits were obtained by first averaging over the Fourier coefficients of the impulse response and the Fourier

coefficients of the impulse response calculated from the step response, and then applying an inverse transform to these averages. In Figure 3 v^* is called U_δ^* and w^* is called U_s^*. From Figure 3 the derivative of U_s^* at t_{ex} can easily be estimated by drawing a straight line through the continuous line of the step response at $\tau = 0$ (as is indicated by the dashed line). In this way we find for subject FB

$$\frac{NF_\delta}{NF_s} \simeq 80s^{-1},$$

$$\left.\frac{dU_s^*}{dt}\right|_{t_{ex}} \simeq 67s^{-1}.$$

Making allowances for the precision of the measured data as mentioned above, this must be regarded as a good quantitative agreement. Of course this is in no way a proof of the linearity of the system.

For the impulse response of subject HR (100Td, 1 degree field) we obtain from the fourth-order linear filter fit (Chapter 4) for the slope of the step response at $\tau = 0$

$$\left.\frac{dw^*}{dt}\right|_{t_{ex}} = 24 \, s^{-1}.$$

From the block response we find

$$\frac{NF_\delta}{NF_s} = T_c^{-1} \simeq 27 \, s^{-1}.$$

This is also in good agreement.

The linearity assumption is not rejected by the independent measurement of the norm factors. For clarity we would like to stress that the check performed on the linearity is not trivial. The norm factors are measured exactly at threshold level. On the other hand the impulse and step response are measured by a subthreshold perturbation technique. For instance the impulse response of FB (Figure 3A) is measured with $q = 0.15$, which means the measured impulse response is 6 times below the threshold level. We conclude that the test performed on the linearity is a severe one.

2.5 The cross-correlator and a perturbation technique

As explained earlier, only the main part of the Reichardt model will be used in this section to outline what happens in an experiment using a perturbation technique. From the discussion in Section 2 it is clear that this also applies to the Rashbass model for the stimuli used here. The model is shown in Figure 2B. The impulse response of the linear filter is called $v(t)$, the step response $w(t)$, and relation (1) holds. The time delay is called T.

The cross-correlation ψ_{xy} of two signals $x(t)$ and $y(t)$ is defined by

$$\psi_{xy}(T) = \int_{-\infty}^{\infty} x(t)y(t-T)dt = \psi_{yx}(-T). \tag{20}$$
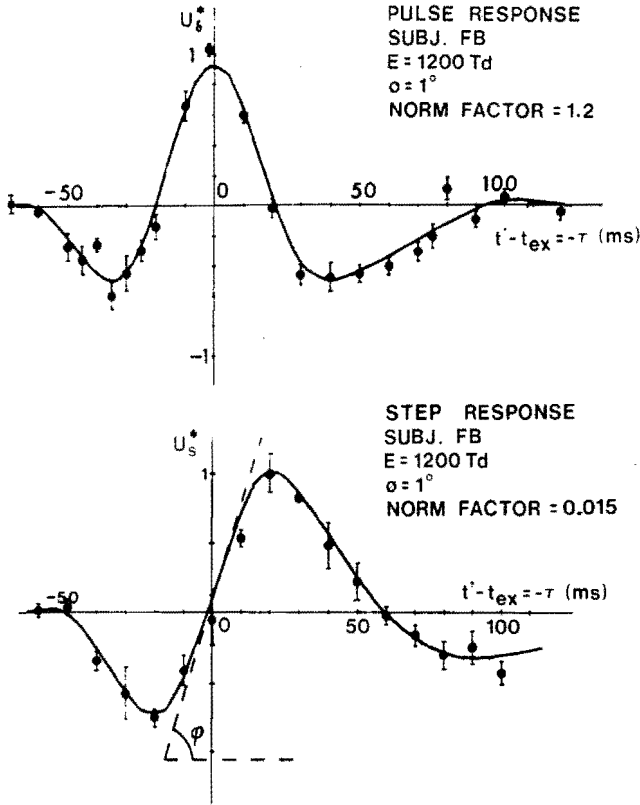
Figure 3: Measured impulse and step response of subject FB at a background level of 1200Td, and for a field size of 1 degree with a dark surround (Roufs and Blommaert, 1981). From the slope of the step response at $\tau = 0$ (the dashed line) a check on the linearity assumption can be made. The slope $\tan \varphi = dU_s^*/dt \simeq 67$ at $\tau = 0$.

The cross-correlation of a signal with itself is called the autocorrelation ψ_{xx} and

$$\psi_{xx}(-T) = \psi_{xx}(T). \tag{21}$$

We introduce $\hat{\psi}_{xx}$ as the maximum of ψ_{xx}:

$$\hat{\psi}_{xx} \equiv \psi_{xx}(0) \geq \psi_{xx}(T), \qquad \text{for every } T. \tag{22}$$

The equal sign of (22) holds only for some $T \neq 0$ if $x(t)$ is periodic. For a signal $f(t)$ which contains $g(t - \tau)$ as perturbing function of $h(t)$ according to

$$f(t) = h(t) + qg(t - \tau), \tag{23}$$

the autocorrelation can be expressed in the autocorrelation terms ψ_{hh}, ψ_{gg} and the cross-correlation term :

$$\psi_{ff}(T) = [\psi_{hh}(T) + q^2\psi_{gg}(T)] + q[\psi_{hg}(T+\tau) + \psi_{gh}(T-\tau)]. \tag{24}$$

Only the last two terms, the cross-correlation terms, are dependent on the time shift τ.

Assume the transient system consists of an infinity of mechanisms as sketched in figure 1A (simplified Reichardt model) all with different T, and $h(t)$ is a non-periodic function. As in the linear model analysis, we assume $h_{in}(t)$ and $g_{in}(t)$ to be amplitude-normalized functions. The responses of the linear filter to $h_{in}(t)$ and $g_{in}(t)$ are $h(t)$ and $g(t)$, respectively. Again amplitudes have to be taken into account. ε_1 and ε_c are defined as the amplitudes for excitations exactly at threshold level:

$$\varepsilon_1^2 \hat{\psi}_{hh} = d, \tag{25}$$

$$\varepsilon_c^2[\hat{\psi}_{hh} + q^2\hat{\psi}_{gg}] + 2q\varepsilon_c^2\psi_{hg}(\tau) = d. \tag{26}$$

By combining (26) and (25), we have

$$\psi_{hg}^0(\tau) \equiv \frac{\psi_{hg}(\tau)}{\hat{\psi}_{hh}} = \frac{1}{2q}\left[\left(\frac{\varepsilon_1}{\varepsilon_c(\tau)}\right)^2 - 1 - q^2\frac{\hat{\psi}_{gg}}{\hat{\psi}_{hh}}\right] \tag{27}$$

On the right-hand side of this equation only measurement data occur except for the ratio $q^2\hat{\psi}_{gg}/\hat{\psi}_{hh}$. This equation (27) should be compared to (7) of the linear model.

We take the same excitations as for the analysis of the linear model. By first taking a short rectangular pulse with duration ϑ (approximating a Dirac function) as probe and as test signal, it follows that

$$h(t) = g(t) \approx \vartheta\,v(t),$$
$$q \ll 1.$$

The normalized autocorrelation $\psi_{vv}^*(\tau)$ of $v(t)$ is found by applying (27), so that

$$\psi_{vv}^*(\tau) \equiv \frac{\psi_{vv}(\tau)}{\hat{\psi}_{vv}} = \frac{1}{2q}\left[\left(\frac{\varepsilon_1}{\varepsilon_c(\tau)}\right)^2 - 1 - q^2\right]. \tag{28}$$

Again taking a short rectangular pulse as probe but now a step as test, we obtain

$$h(t) \simeq \vartheta\,v(t), \tag{29}$$
$$g(t) = w(t), \tag{30}$$

and again applying (27), we have

$$\psi_{vw}^0(\tau) \equiv \frac{\psi_{vw}(\tau)}{\hat{\psi}_{vv}} = \frac{1}{2q}\left[\left(\frac{\varepsilon_1}{\varepsilon_c(\tau)}\right)^2 - 1 - q^2\frac{\hat{\psi}_{ww}}{\vartheta^2\hat{\psi}_{vv}}\right]. \tag{31}$$

From the relation between $w(t)$ and $v(t)$,

$$w(t) = \int_0^t v(\sigma)\,d\sigma,$$

together with the definition of ψ_{vv}^* and ψ_{vw}^o we find an integral relation, comparable to (10), that is

$$\psi_{vw}^o(\tau) = \frac{1}{\vartheta} \int_{-\infty}^{\tau} \psi_{vv}^*(\sigma)\,d\sigma. \tag{32}$$

The interpretation of the measurement of the step response is only clear if the factor $q^2\hat{\psi}_{ww}/\hat{\psi}_{vv}$ is small enough. This is not known beforehand, and can only be assumed and later checked. This factor cannot be made arbitrarily small by taking q small, because in that case the test signal would disappear in the noise.

For every τ the measurements give a value for $\varepsilon_1/\varepsilon_c$. With this value we can compute $v^*(t_{ex} - \tau)$ according to (7) and also $\psi_{vv}^*(\tau)$ according to (28). Performing this calculation for the data measured at IPO gives two plots, both showing a figure with a positive central phase around $\tau = 0$ and two smaller negative phases on both sides of the positive phase, see Figure 6A and 6D.

2.6 The cross-correlator model and the norm factors

Just as with the linear model a relation can be found between the normalized autocorrelation function $\psi_{vv}^*(\tau)$ and the amplitudes ε_δ and ε_s for detection of an impulse and step excitation, respectively:

$$(\varepsilon_\delta\vartheta)^2\hat{\psi}_{vv} = d, \tag{33}$$

$$(\varepsilon_s)^2\hat{\psi}_{ww} = d. \tag{34}$$

Also from (33) and (34) it is found that

$$\psi_{vw}^o(\tau) = \frac{\varepsilon_\delta^2\vartheta\,\psi_{vw}(\tau)}{d},$$

and subsequently $\psi_{ww}^o(\tau)$ is defined by

$$\psi_{ww}^o(\tau) = \frac{1}{\vartheta} \int_{-\tau}^{\infty} \psi_{vw}^o(\sigma)\,d\sigma = \varepsilon_\delta^2\vartheta\,\psi_{vw}(\tau)/d.$$

As with (17) and (19) it is found

$$\left.\frac{d\psi_{vw}^o(\tau)}{d\tau}\right|_{\tau=0} = \vartheta^{-1}, \tag{35}$$

$$\psi_{ww}^o(0) = (\varepsilon_\delta/\varepsilon_s)^2. \tag{36}$$

Because of all the simplifications made in the original model, (36) is quite an unrealistic approximation. With suitable adjustments for nonideal multiplication, integration, and windowing in the integration, it is always possible to make a more realistic model in which the predicted amplitude of ε_s is in accordance with the measured value. The conclusion is that the norm factors cannot be used to reject or support the models containing a quadratic element.

2.7 Block response data

Taking a block response with variable duration ϑ as an input for the transient
system, and measuring the sensitivity, a figure such as the one sketched in Figure 4
is found (taken from Roufs and Bouma, 1980).
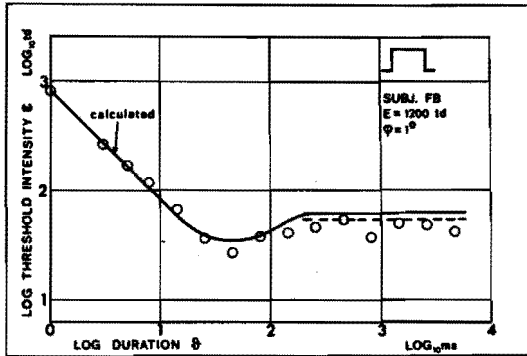
Figure 4: Threshold intensity as function of the block duration. Data of
subject FB (1200Td, 1 degree field). The line is the prediction of the linear
model, the dashed line the correction of the prediction for stochastic effects
at long flash durations (probability summation). From: Roufs, J.A.J. and
Bouma, H.: Towards linking perception research and image quality. Proc.
SID **21**, 247-269 (1980). Reprinted with permission.

Bloch's law is found for small ϑ. A constant sensitivity is measured for large
ϑ. Both in the linear model and in the nonlinear models this is predicted, if the
integrator in the nonlinear models has a finite integration time.

The only thing that might be critical is the dip (see also Roufs, 1974a), occurring
at intermediate values of ϑ. This dip is predicted in the linear model: a triphasic
transient impulse response means a biphasic step response (see Figure 3B), with a
negative first phase. This causes the dip in the figure according to the linear model.
Furthermore, this dip is in excellent quantitative agreement with the measured
impulse response (see also Blommaert and Roufs, 1987).

Simulations with the Rashbass model showed that this dip also is predicted in
this model, as a consequence of a finite window in the integrator. Suitable choices
for the extent of the window can account for the strength of the dip (Blommaert,
1974).

We conclude that the threshold-versus-duration curve is in agreement with the
linear model. On the other hand the nonlinear models are neither rejected nor
supported by these data, since the integration window in this model cannot be
estimated from the perturbation experiment and is still a free parameter.

2.8 A measurement for distinguishing between the linear and nonlinear models

We have shown that the norm factors and the threshold-versus-duration curve do agree with the linear model. Latency responses can also be predicted from the linear model (Roufs, 1974b; Blommaert and Roufs, 1987). On the other hand the cross correlator model can be made to fit the norm factors and the threshold-versus-duration curve, because one of the parameters of the nonlinear model, the nonideal integration, cannot be estimated reliably from the measurements with a perturbation technique. Because of this free parameter, it is difficult to make adequate predictions for the above mentioned measurements. Parameters can always be found that will show predictions and measurements to be in agreement. Thus such predictions neither reject nor support the nonlinear models.

As can be seen from the discussion in Section 2, the linear and nonlinear models are expected to act in a similar way when the main part of the input signal consists of a pulse. Other inputs may well make a good distinction between these models. A step as probe and an impulse as test signal, for instance, predicts the measurement of the impulse response, while the cross-correlator model predicts the measurement of the cross-correlation of impulse response and step response. However, from the triphasic impulse response it is also predicted that the step response is biphasic with, in absolute value, an almost equal maximum and minimum (see Figure 3B). Therefore, applying a step as a probe and interpreting the results in the linear model is contradictory to one of the assumptions for the perturbation experiment, namely the existence of one clearly dominant extreme. Also, when using a step as probe input to the visual system, the sustained channel may make a considerable contribution to the overall response. Since it is not yet known how to model the sustained channel, nor how these two channels interact, we feel that such an experiment would fall short in its interpretation. Nevertheless, this kind of experiment was performed by Elsner (1986), who actually used a sawtooth step, but the slow decay of the sawtooth ensures a response very similar to a stepresponse. Another complicating factor here is that they used reaction time measurements, which may be something quite different to the threshold experiment mentioned earlier. Elsner and Hauske found a behaviour that suits the Rashbass model well. However, we maintain that, if it is not known whether the same system is measured, nor if other channels are operating, plus the assumption for applying the perturbation technique in the linear case being invalid, these data have no unambiguous interpretation.

The problem of another channel also operating is a very real one. Therefore all excitations for measuring the transient channel are always of short duration. For the measurements of the Rashbass model it was explicitly stated that only short luminance excursions from the baseline were used (Broekhuysen et al., 1976). In Section 2 it was already mentioned that for these stimuli, which contain fast changes, the linear and quadratic models are to be expected to act in a very similar

manner.

Up till now we have no effective means of separating different temporal channels, except for smallest spatial stimuli. We have always found that a large field (e.g. 1 deg.) stimulus without surround is a suitable configuration in which to have little contribution from sustained channels. However, for stimuli of low temporal modulation the transient response will eventually be zero. Thus, for long duration after onset, the sustained response will always be larger than the transient response. This means that the transient system can only be measured with stimuli of high temporal modulation. Hence a measurement with which to make a distinction between models for the transient system at threshold level must necessarily be closely related to the perturbation experiment.

We recall to mind relations (8) and (28) for the linear model calculating the impulse response and for the cross-correlation model (Fig. 1A) calculating the autocorrelation of the impulse response, respectively:

$$v^*(t_{ex} - \tau) = \frac{1}{q}\left[\frac{\varepsilon_1}{\varepsilon_c(\tau)} - 1\right], \tag{37}$$

$$\psi_{vv}^*(\tau) = \frac{1}{2q}\left[\left(\frac{\varepsilon_1}{\varepsilon_c(\tau)}\right)^2 - 1 - q^2\right]. \tag{38}$$

The values of ε_1 and ε_c are dependent on the input functions. This means that ε_c is dependent on both q and τ. The value of $v^*(t_{ex} - \tau)$ at a certain τ should not be dependent on q if the transient system acts as a linear model, for all q for which the perturbation requirement applies (see also Roufs and Blommaert, 1981). The same is true for $\psi_{vv}^*(\tau)$ if the transient system acts as a the mechanism sketched in Fig. 1A. From (37) and (38) it can be seen that the measured values of $\varepsilon_1/\varepsilon_c$ are dependent on q in different ways for the linear or the cross-correlator model. It is also shown in Figure 5 that, for each ratio $\varepsilon_1/\varepsilon_c$, v^* and ψ_{vv}^* can be calculated. This gives a different plot of v^* versus ψ_{vv}^* for each q-value. Thus we can test if the dependence of $\varepsilon_1/\varepsilon_c$ on q is according to a linear model, a cross-correlator model or neither. The quantitative difference between the the autocorrelation and the impulse response interpretation at different q is not large, given the noise on the measurements. But since there are measurements available for twenty values of τ, these differences become significant, as will be shown below.

We therefore define the variables Δv_i and $\Delta \psi_i$ according to

$$\Delta v_i = v_1^*(t_{ex} - \tau_i) - v_2^*(t_{ex} - \tau_i), \tag{39}$$

$$\Delta \psi_i = \psi_{vv1}^*(\tau_i) - \psi_{vv2}^*(\tau_i), \tag{40}$$

where v_1^* and v_2^* are the values calculated according to (37) and ψ_{vv2}^* and ψ_{vv1}^* according to (38) from experiments at the same sampling moment τ_i using two different q-values: q_1 for v_1^* and ψ_{vv1}^*, and q_2 for v_2^* and ψ_{vv2}^*. From the variance of
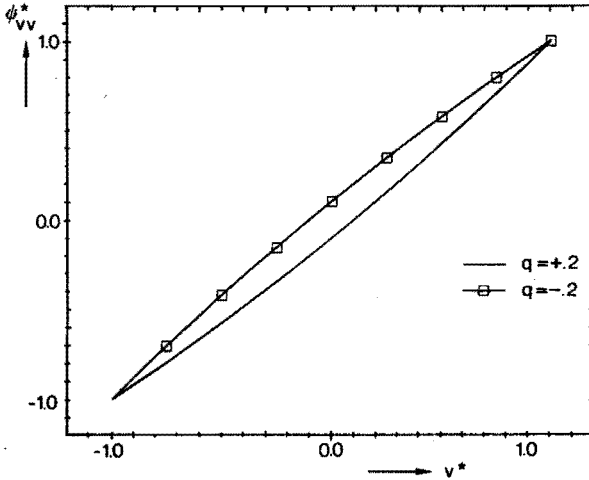
Figure 5: Relation between $v^*(t_{ex} - \tau)$ and $\psi_{vv}^*(\tau)$ for $q = 0.2$ and $q = -0.2$. A different relation between normalized impulse response and normalized autocorrelation exists for each q. The linear and cross-correlator model can be discriminated on the basis of the interval between the lines of the relation $v^*(t_{ex} - \tau)$ versus $\psi_{vv}^*(\tau)$ for different q.

$\varepsilon_1/\varepsilon_c$ the variance of v_1^*, ψ_{vv1}^*, v_2^* and ψ_{vv2}^* can be calculated and the variance of Δv_i and $\Delta \psi_i$ likewise. These variances $\sigma_{\Delta v_i}^2$ and $\sigma_{\Delta \psi_i}^2$ are taken as

$$\sigma_{\Delta v_i}^2 = \sigma_{v_1^*(\tau_i)}^2 + \sigma_{v_2^*(\tau_i)}^2, \tag{41}$$

$$\sigma_{\Delta \psi_i}^2 = \sigma_{\psi_{vv1}^*(\tau_i)}^2 + \sigma_{\psi_{vv2}^*(\tau_i)}^2. \tag{42}$$

The expected values of these two variances $\sigma_{\Delta v_i}^2$ and $\sigma_{\Delta \psi_i}^2$ are approximately equal, as can be shown from an analysis of the error propagation using a Taylor series expansion of (37) and (38), giving

$$\frac{\mathcal{E}[\sigma_{\psi_{vv}^*}^2]}{\mathcal{E}[\sigma_{v^*}^2]} = \left(\frac{\mathcal{E}[\varepsilon_1]}{\mathcal{E}[\varepsilon_c]}\right)^2 \simeq 1, \tag{43}$$

where $\mathcal{E}[\ ]$ denotes the expected values of a stochastic variable and where the approximation sign stems from the perturbation requirement. It can be shown in a perturbation experiment that the expected values of the variances at different sampling instants τ_i are approximately equal. Therefore the variances at different sampling moments can be averaged, and a mean variance is introduced for Δv_i and $\Delta \psi_i$

$$\sigma_{\Delta v}^2 \equiv \frac{1}{M} \sum_{i=1}^{M} \sigma_{\Delta v_i}^2 \qquad \text{and} \qquad \sigma_{\Delta \psi}^2 \equiv \frac{1}{M} \sum_{i=1}^{M} \sigma_{\Delta \psi_i}^2, \tag{44}$$

and from (43) it is found that

$$\sigma_{\Delta v}^2 \simeq \sigma_{\Delta \psi}^2. \tag{45}$$

Now a null hypothesis test can be performed for the linear and quadratic model. If the system acts as a linear model or like the autocorrelator model, we expect

$$\mathcal{E}\left[\Delta v_i\right] \equiv 0 \qquad \text{or} \qquad \mathcal{E}\left[\Delta \psi_i\right] \equiv 0, \qquad (46)$$

respectively. This test is performed by comparison of the mean values $\overline{\Delta v}$ and $\overline{\Delta \psi}$ of Δv_i and $\Delta \psi_i$ respectively, according to

$$\overline{\Delta v} = \frac{1}{M} \sum_{i=1}^{M} \Delta v_i \qquad \text{and} \qquad \overline{\Delta \psi} = \frac{1}{M} \sum_{i=1}^{M} \Delta \psi_i \qquad (47)$$

with the standard deviation σ_Δ of the mean, which is given for both (see (43)) by

$$\sigma_\Delta = \frac{\sigma_{\Delta v}}{\sqrt{M}} \simeq \frac{\sigma_{\Delta \psi}}{\sqrt{M}}.$$

It was found for measurement data of subject JAJR, at q-values $q = +0.2$ and $q = -0.2$ (see Roufs and Blommaert, 1981) that $\overline{\Delta v} = 0.013$, $\overline{\Delta \psi} = -0.142$ and the estimator of the standard deviation $\sigma_{\Delta v}$ was $s_{\Delta v} = 0.046$. From these values we see that $\overline{\Delta v}$ is inside the standard deviation interval of the mean, while $\overline{\Delta \psi}$ is outside the highly significant interval of 2.5 times the standard deviation of the mean.

The whole statistical procedure is shown in Figure 6. In Figure 6A and 6B the calculated normalized impulse responses are shown for the two q-values. In Figure 6D and 6E the calculated normalized autocorrelations are shown. The difference of the calculated impulse responses Δv_i and the autocorrelations $\Delta \psi_i$ is shown in Figure 6C and 6F respectively, together with the (estimated) standard deviations $s_{\Delta v_i}$ and $s_{\Delta \psi_i}$ ($= \sqrt{M} s_\Delta$, where M gives the number of samples). The dotted lines are the plus and minus the mean standard deviations (located round the baseline). In Figure 6C the differences Δv_i are located around the baseline, while in Figure 6F most of the values $\Delta \psi_i$ are located beneath the baseline, and often more than the standard deviation.

2.9 Conclusion

In this chapter, linear models for the transient visual system at threshold level are compared to "quadratic" models. Quadratic models are the models containing a quadratic element (the Rashbass model) and those containing an autocorrelator (the Reichardt model). It is suggested that the linear model and these nonlinear models act similarly for most of the commonly used excitations: perturbation measurements with a Dirac pulse as probe and threshold measurements of pulses with variable duration. For reasons of simplicity we would prefer the linear model to a nonlinear one when there is no significant difference in behaviour. Furthermore, we have shown that even in a perturbation measurement with suitable excitation,
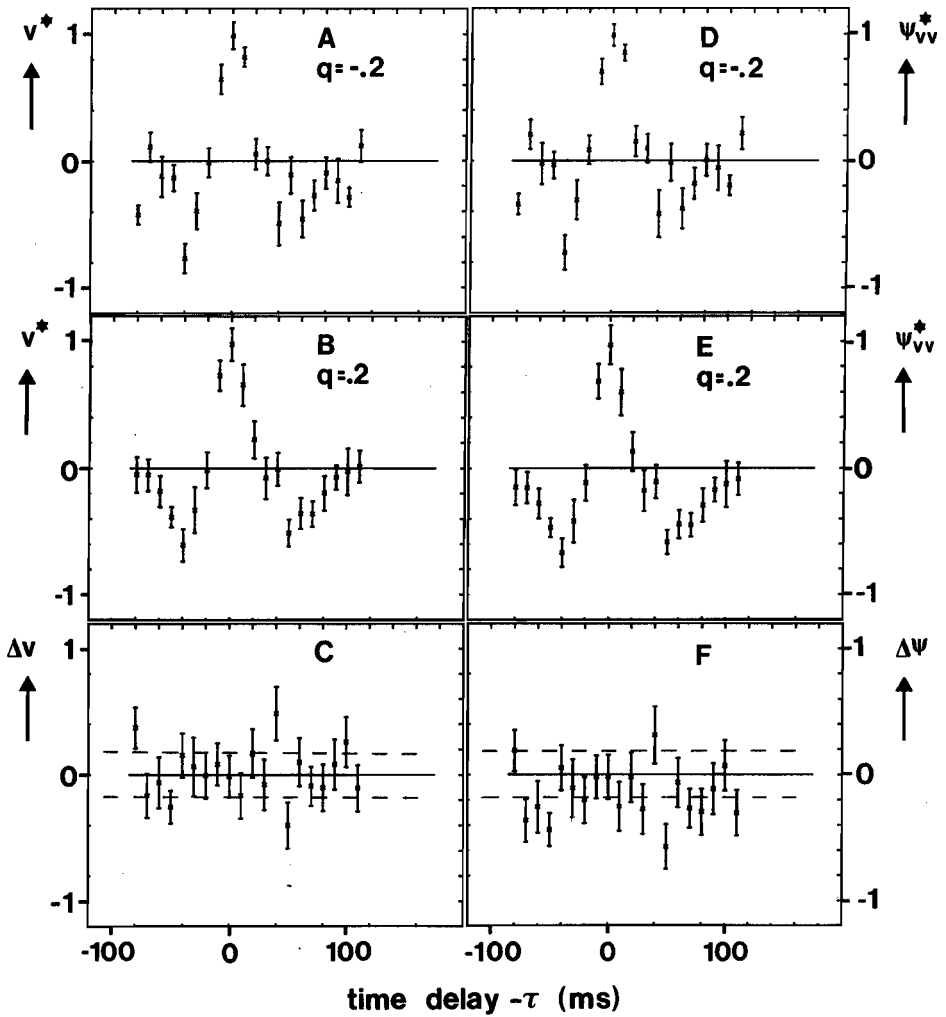
Figure 6: **A.** Impulse response interpretation $v_1^*(\tau_i)$ of the measured data where $q = -0.2$.
B. Impulse response interpretation $v_2^*(\tau_i)$ of the measured data where $q = +0.2$.
C. Difference Δv_i of the calculated values from **A** and **B**.
D. Autocorrelation interpretation $\Delta\psi_{vv1}^*(\tau_i)$ of the measured data where $q = -0.2$.
E. Autocorrelation interpretation $\Delta\psi_{vv2}^*(\tau_i)$ of the measured data where $q = +0.2$.
F. Difference $\Delta\psi_i$ of the calculated values from **D** and **E**.

a difference in behaviour can be predicted and also measured. These experimental data favour the linear model, which agrees with the conclusions of Roufs and Blommaert (1981), who based their arguments on the asymmetry of the responses with respect to the $\tau = 0$ axis. We think that the difference in behaviour for positive and negative disturbances is (statistically) so significant that even changed versions of the quadratic models (e.g. taking into account integration windows, nonideal multiplication) will not be able to account for the measured differences.

Acknowledgements

References

Blommaert, F.J.J.: Comparison of two dynamical models of the eye. IPO-report **265** (1974).

Blommaert, F.J.J. and Roufs, J.A.J.: Prediction of thresholds and latency on the basis of experimentally determined impulse responses. Biol. Cyb. **56**, 329-344 (1987).

Broekhuysen, M., Rashbass, C. and Veringa, F.: The threshold of visual transients. Vision Research **16**, 1285-1289 (1976).

Elsner, T.: Systemtheoretische Modellierung der visuellen Wahrnemung bei Detektion. Dissertation an der Technischen Universität München, 1986.

Papoulis, A.: *Signal analysis.* New York: McGraw-Hill (1977).

Rashbass, C.: Visibility of transient changes in luminance. Journal of Physiology **210**, 165-186 (1970).

Rashbass, C.: Transformations of waveform under which incremental visual thresholds are invariant. Vision Research **14**, 97-99 (1974).

Reichardt, W.: Autokorrelationsauswertung als Funktionsprinzip des Zentralnervensystems. Zeitschrift für Naturforschung **12B**, 447-457 (1957).

Reichardt, W.: Autocorrelation, a principle for the evaluation of sensory information by the central nervous system. In: W.A.Rosenblith: *Sensory communication.* New York: Wiley (1961).

Reichardt, W., and Varjú, D.: Übertragungseigenschaften im Auswertesystem für das Bewegungssehen. Zeitschrift für Naturforschung **14B**, 724-735 (1959).

Roufs, J.A.J.: Dynamic properties of vision-IV. Thresholds of decremental flashes, incremental flashes and doublets in relation to flicker fusion. Vision Research **14**, 831-851 (1974a).

Roufs, J.A.J.: Dynamic properties of vision-V. Perception lag and reaction time in relation to flicker and flash thresholds. Vision Research **14**, 853-869 (1974b).

Roufs, J.A.J., and Blommaert, F.J.J.: Temporal impulse and step responses of the human eye obtained psychophysically by means of a drift-corrected perturbation technique. Vision Research **21**, 1203-1221 (1981).

Roufs, J.A.J. and Bouma, H.: Towards linking perception research and image quality. Proc. SID **21**, 247-269 (1980).

chapter 3

A pseudo-matched filter model applied to the transient system of the visual perception[1]

Albertus C. den Brinker
Hans A. L. Piceni
Frans E. W. Vervuurt

Abstract

A pseudo-matched filter configuration is presented as a model for the transient system of the human visual perception. This model has close resemblances to the Reichardt [1] and the Rashbass [2] model, but on the other hand the pseudo-matched filter model is linear. The choice of the model is based on the shape of the psychophysically measured impulse response and on physiological and functional arguments. The parameters of the model are estimated for different data sets. The behaviour of the model agrees with the experimental data in all essential aspects, and can be used for prediction and further modelling of the human visual system.

3.1 Introduction

An important branch in psychophysical research is concerned with the measurement of the characteristics of the visual system at threshold level. Even these small signals are not processed linearly in the visual system, and it is usually assumed that the visual system can be modelled by different channels operating in parallel. In the temporal domain there are usually two channels postulated: the sustained and the transient channel [3,4,5,6]. Roufs and Blommaert [7] showed that the impulse response of these temporal channels can be measured separately. This paper discusses the parameter estimation of a linear model on the basis of data [7,8] from impulse responses of the transient channel.

Performing this type of estimation a compact description of the measurement data is obtained, and predictions on the basis of the model can be made. Of more importance is the possibility of models to give insight into the system that is being modelled.

A linear filter configuration is chosen as a model of the transient channel. We prefer to call this model a pseudo-matched filter model. A matched filter optimizes the detection performance of the overall system for a certain specified input signal in the presence of white noise at the input of the matched filter. The transient channel is also a detection mechanism in which non-negligible noise is present, as in all biological systems. Furthermore, a matched filter model has close resemblances

---

to autocorrelation processes. In this way the model is reminiscent of the models of Reichardt [1] and Rashbass [2].

It has been shown [7] that the linear model for the transient system proposed by Roufs [4,7] and the nonlinear model of Rashbass [2] yield a vastly similar behaviour for pulse-like stimuli. Rashbass [9] showed that these two models can be seen as the extreme cases of a large set of models that are now commonly used for visual processing. We argue that there is a second reason for the quadratic model of Rashbass and the linear model of Roufs to exhibit quite similar behaviour. This is done in the sequel of this paper by showing that a linear interpretation of the measurement data can be found within the class of filters based on the matched filter theory. It is well known that there are strong similarities between matched filtering and autocorrelation processes [10] (see also chapter 2) for certain specific input signals.

The pseudo-matched filter model we propose here is fit to experimental data. The data on which the parameter estimations are performed are derived from psychophysical experiments. These experiments are detection tasks, i.e. a subject states whether he has seen or not seen a certain stimulus. A perturbation technique is used to obtain impulse responses from such experiments. This technique is described by Roufs and Blommaert [7]. Using this technique some a priori information on the impulse response is available. This information must be incorporated into the model that is being fit, resulting in some restrictions on the degrees of freedom of the chosen model.

The impulse response data [7,8] are interpreted as being derived from a continuous system. The model being fitted to these data consists of three linear filters operating in cascade. Two of these filters are designed according to the matched filter theory, as will be explained later.

The method used to obtain the parameters of this model is the well-known least-squares estimation. The objective function, which is being minimized during the estimation process, is a nonlinear function of the parameters of the three filters. For the estimation of the filter parameters standard routines from the NAG-library are used [11]. We do not find it opportune to write our own programs to this end [12,13].

The chapter is organized in the following way. The data are presented in Section 2, and the model in Section 3. Section 4 describes the nonlinear parameter estimation process and its implementation. The results of this parameter estimation are presented in Section 5. Comparisons of predictions of the behaviour of the model to experimental data are shown in Section 6. We conclude with a discussion (Section 7).

3.2 The impulse response data

The response of the eye to a certain stimulus is generally supposed to be processed in different channels operating in parallel [3,4,5,6]. In the temporal domain two

channels are usually assumed to intermediate between the physical stimulus and the human percept. These are the sustained and transient channel. The transient channel is tuned to low spatial frequencies and fast temporal changes (cf. [14]).

The available data consist of impulse responses of seven subjects at 1200 Td and four subjects at a 100 Td background [7,8]. These data are obtained from threshold measurements of flashed discs (1 degree visual angle) upon a circular background of the same extent and a certain luminance projected foveally. The surround of the disc is completely dark. It is assumed that in this way the transient channel of the eye is most stimulated [4,7], and so the measured impulse responses are solely attributable to the transient channel.

The normalized impulse responses were measured with the perturbation technique [7]. The perturbation technique uses a two-pulse temporal excitation, where the response of one pulse (the probe flash) is perturbed by the response of a second (smaller) pulse (the test flash). This causes an increase or decrease in the threshold amplitude of the probe flash. The change in threshold amplitude caused by the test flash can be determined as a function of the time delay τ between the two pulses. (Positive τ means that the disturbing pulse is delayed in respect to the probe pulse.) In this way the shape of the perturbing signal, i.e. the response of the system to the test flash, can be obtained. For further details on this technique see [7]. The absolute sensitivity of the system for a single flash (the norm factor NF, see [7]) can be measured separately.

There are, however, some consequences of this method with respect to the obtained data that we need to discuss. First, the method requires rather time-consuming experiments. For this reason the number of samples (with a different τ) that is being measured, is as low as possible. The number usually ranges from about twenty to thirty samples. In most cases an extra tail of four or five samples was added to the measured data, with mean values equal to zero and standard deviations taken as the mean of the standard deviations of the actually measured samples. This tail is added in the region where the impulse response is approximately zero to facilitate the estimation process and to prevent severe oscillations of the estimated impulse responses in this region. Secondly, as a result of the perturbation technique the position of the starting point of the impulse response (let's say $t = 0$) is lost. The origin of the time axis is located exactly on the extremum of the impulse response (see Figure 1). Note also that the time scale is plotted in the independent variable $-\tau$. It was preferred to stick close to the same variable as used in the original measurements, which is τ. To obtain the direction of a normal time axis (later events on the righthand side) the variable $-\tau$ had to be taken. Thirdly, the extremum should be exactly equal to one. Actual measurement of this extremum gives a value close to but not exactly one, because of the noise in the system (see Figure 1 at $\tau = 0$ ms). Since the response axis of the experimental data is normalized the amplification of our model will not be a free parameter in the estimation process.
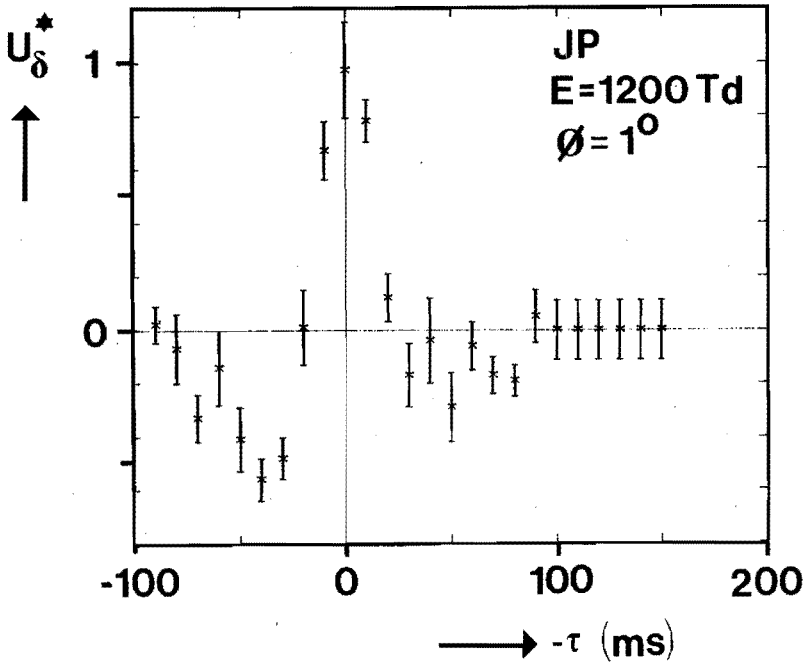
Figure 1: An example of data obtained from a psychophysical experiment using a perturbation technique, for the measurement of the impulse response. The points represent the mean value, the bars represent twice the standard deviation of the mean. Subject JP, E = 1200 Td and stimulus diameter is one degree.

The data show that the impulse response is nearly symmetrical with respect to the extremum. This is a well known feature of matched filter responses [10]. In the model (see Section 3) the impulse responses of the three filters are chosen in such a way that the overall impulse response is approximately symmetrical. As a consequence of the symmetry in the impulse response the phase characteristic of the system and the model will have a large linear component. Independent measurement of the (relative) phase characteristic of the transient visual channel confirms this property [15,16].

3.3 The pseudo-matched filter model

In this section the model is presented. The choice of the model's components is based on the measured data and physiological and functional arguments. This model has certain similarities to earlier proposed models, notably the Reichardt model [1] and the Rashbass model [2,9]. This is described in chapter 2.
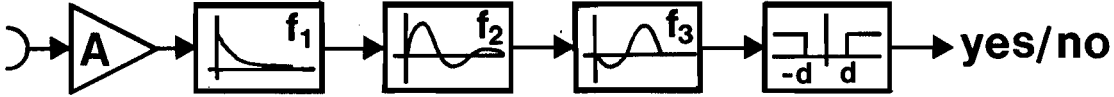
Figure 2: The pseudo-matched filter model, consisting of an amplifier A and three linear filters operating in cascade (for details see text).

As a model of the transient channel of the visual perception an amplifier A and a cascade of three linear filters f_1, f_2, f_3 is proposed (see Figure 2). The first filter is a first-order filter with impulse response $f_1(t)$:

$$f_1(t) = \exp(-at)H(t), \tag{1}$$

where $H(t)$ is the Heaviside function:

$$H(t) = \begin{cases} 0, & t < 0, \\ 1, & t \geq 0. \end{cases} \tag{2}$$

The second filter is a second-order filter and its impulse response $f_2(t)$ is given by

$$f_2(t) = \exp(-b_1 t)\sin(\omega_0 t)H(t), \tag{3}$$

where b_1 is the damping parameter ($b_1 > 0$) and ω_0 the angular frequency. The third filter has a biphasic impulse response $f_3(t)$, where the second phase is positive and most pronounced:

$$f_3(t) = -\exp(-b_2 t)\sin(\omega_0 t)\{H(t) - H(t-T)\} \tag{4}$$

where $T = 2\pi/\omega_0$ and $b_2 < 0$. This is an exponentially growing sinusoid truncated after one period T. Note that if $b_2 = -b_1$ the impulse responses $f_2(t)$ and $f_3(t)$ are each others mirrored images with respect to a vertical axis, except for a shift in time, an amplification factor, and the truncation in time:

$$f_3(t) = f_2(-t + T)\exp(b_1 T)H(t), \qquad b_2 = -b_1. \tag{5}$$
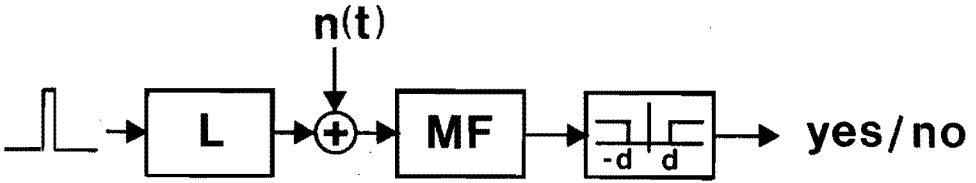
Figure 3: The matched filter model, consisting of a transmission channel and a matched filter MF (for details see text).

Therefore we will call filter f_3 pseudo-matched on the impulse response of filter f_2.

The overall impulse response of the three linear filters and the amplifier is called $f(t)$ and is given by a convolution $*$ according to

$$f(t) = A f_1(t) * f_2(t) * f_3(t). \tag{6}$$

Consider a simplification of Figure 2, where the amplifier and the first filter have been omitted (Figure 3). Suppose the input signal consists of pulses only, and there is a linear medium L with a second-order impulse response $x(t) = f_2(t)$. Suppose further there is a white noise source $n(t)$. If we want to make a detection mechanism, the optimal linear filter is a matched filter [17]. This filter has an impulse response that is a mirrored version of the input signal with respect to the vertical axis. The signal to noise ratio SNR_{opt} at the output of this (optimal) matched filter would be [10]:

$$SNR_{opt} = 2E/N_0, \tag{7}$$

where
$E \quad = \quad \int_{-\infty}^{\infty} x^2(t)\, dt$, the energy of the input signal,
$N_0 \quad = \quad$ the spectral density of the white noise signal $n(t)$.
This optimal SNR is not affected by any time delay in the impulse response of the matched filter. This property is used to obtain a matched filter with a causal impulse response. Naturally, this is only possible for signals of finite duration. Since we assumed that $x(t) = f_2(t)$ the optimal filter can only approximately realized. This was done by taking the filter MF (see Fig. 3) with an impulse response $y(t)$ equal to

$$y(t) = x(T - t)H(t), \tag{8}$$

which means $y(t) = f_3(t)$, under the condition that $b_2 = -b_1$. The signal to noise ratio SNR at the output of filter MF can be calculated and is found to be

$$SNR = SNR_{opt}(1 - \exp\{-4\pi b_1/\omega_0\}). \tag{9}$$

From (9) it can be seen that the signal to noise ratio is not seriously impaired by the truncation of the mirrored version of $x(t)$ as long as $4\pi b_1 > \omega_0$. The results from the fits of the overall impulse response $f(t)$ to the measured data (Section 4) are always such that this holds. For instance, with $b_1 = -b_2 = 30$ s^{-1} and $\omega_0 = 80$ rad/s we find a reduction of only 1 percent in the *SNR* as a consqunce of the truncation. Similarly, if b_1 and $-b_2$ have the same order of magnitude (and $b_1 < \omega_0$; $-b_2 < \omega_0$) the *SNR* is still close to the optimum [18]. Besides the filters f_2 and f_3, Fig. 2 depicts an amplifier and an extra filter f_1. The amplifier A does not change the *SNR*, and if the parameter a of filter f_1 is such that $a > \omega_0$ the reduction of the *SNR* as a consequence of this filter is small [18].

The choice of the filters in Fig. 2 has to be seen in connection with the impulse response data and some physiological findings. First of all, the measured impulse response as described in Section 2 is nearly symmetrical round its extremum $\tau = 0$. As stated before, this is a feature of matched filter responses. Secondly, the data is triphasic. By chosing the second and third filter as above, (see formulas (3) and (4)), an approximation to a triphasic impulse response is ensured. b_2 not necessarily being equal to $-b_1$ provides some additional freedom to fit the model to the experimental data, with only a small impairment of the *SNR* [18].

The first filter (f_1) is chosen because it can account for the small asymmetry in the impulse response data. Furthermore, it ensures that the high-frequency fall-off is 1.5 log units per octave (with a small ripple caused by the truncation), which agrees well with the de Lange characteristics of stimuli with large spatial extent [19,20]. A magnification factor does not exist in any of the filters; this is separately modelled in the amplifier. As already noted, our data has an extremum exactly equal to one. So this amplification will not be a free parameter when the model is fitted to the impulse response data.

The model is also physiologically inspired. Apart from the amplifier, the ordering in Figure 2 is such as might be present in the visual system. The first-order filter is a (maybe gross) approximation of a receptor cell response [21]. The second filter is conceived as an approximation to the (linear part of the) response of the retina cells behind the receptor: many physiological measurements show a biphasic impulse response of these cells (cf. [22]). The responses of these cells are transmitted to the cortex and we assume that in this transmission the largest amount of internal noise is introduced (this is illustrated by the noise source $n(t)$ in Fig. 3). Suppose further that the cells in the cortex are functionally interconnected in such a way as to minimize noise influences in their detection operation. Then, under the condition of linearity of the transient channel around threshold level ([23,7,24,8] and chapter 2), the overall effect of these cortex cells *necessarily* can be modeled by an impulse response that looks like that of filter 3. In this way the chain of filters in Fig. 2 is not only chosen to get resemblance to the experimentally determined impulse response (Fig. 1), but it is also related to physiological data (filters 1 and 2) and based on an explicit functional reason (filter 3).

3.4 The parameter estimation process

The model outlined in Section 3 is to be fit to the impulse response data [7,8]. From noise analysis of experiments using a perturbation technique it can be shown that the expected value of the noise at the various sampling instants τ_i is approximately equal (see Appendix). Therefore, the residuals at different τ_i need not be weighted differently in the objective function Ψ (i.e. the function that is to be minimized). The objective function is taken to be the sum of unweighted and squared residuals:

$$\Psi = \sum_{m=1}^{M} \{f(-\tau_m + t_{ex}) - U_\delta^*(-\tau_m)\}^2, \tag{10}$$

where

M	=	number of samples,
τ_m	=	m-th sample time, $m = 1, \ldots, M$,
$U_\delta^*(-\tau_m)$	=	measured (amplitude normalized) response at $-\tau_m$,
t_{ex}	=	time of occurence of the extremum of the fitted impulse response $f(t)$.

This function Ψ depends on the parameters A, a, b_1, b_2, ω_0. Since the experimentally determined impulse response is normalized (see Section 2) the amplification A is chosen in such a way that the extremum of the impulse response $f(t)$ equals one. As a result A is a function of the other parameters:

$$A = A(a, b_1, b_2, \omega_0). \tag{11}$$

We did not find an analytical expression for this relation. With any parameter set (a, b_1, b_2, ω_0) the extremum, which we call K, can be searched for numerically. Then A can be set to

$$A = K^{-1}, \tag{12}$$

and so the maximum is scaled to unity.

We can either search for the maximum of the impulse response $f(t)$, or for zeros of the derivative df/dt. The latter approach was adopted in the computer programs using routine C05AZF from the NAG-library [11]. A search for zeros of the derivative was preferred to a search for the maximum, since the former method provides better accuracy in the value of t_{ex}. This value t_{ex} is also needed, since the time axis of the measurement data is shifted by this amount (see Section 2). Just like A, t_{ex} is a function of the filter parameters: $t_{ex} = t_{ex}(a, b_1, b_2, \omega_0)$. An explicit relation for this relation was not found since $df/dt = 0$ holds not only for t_{ex} but for an infinite number of values of t.

Although we did not find an analytical expression for A, we were still able to formulate first and second derivatives of $f(t)$ explicitly with respect to the parameters. This is possible since a relation between the change in t_{ex} and changes in the parameters can be established. This means that all first and second derivatives of Ψ can be formulated even though a numerical search for t_{ex} (and A) is performed.

This allowed us to use routine E04HEF from the NAG-library [11], which is an estimation routine in which first and second derivatives are not approximated by finite differences, but have to be formulated explicitly.

Having implemented the optimization programs in the above mentioned way, we soon found that the parameter a was ill conditioned in the estimation process. This is a direct consequence of the model: the first-order filter (see Section 3) was merely introduced to obtain a sufficient fall-off in the gain characteristic. This means that a is always larger than the other parameters and it has only minor influence on the shape of the impulse response and is consequently poorly conditioned in the optimization procedure. Therefore we excluded parameter a from the optimization by setting $a = 2\omega_0$. This ensures that the influence of this parameter is exactly as outlined above: it affects only the frequencies roughly above the cut-off frequency (under the condition that $b_1, -b_2 < \omega_0$) and has only minor effect on the shape of the impulse response. In this way the optimization program was restarted, with only three free parameters: b_1, b_2, ω_0.

A problem in least-squares optimization is always the possible occurence of local minimi of the function Ψ. Fortunately, there is only a small number of parameters (three) and a good guess for the initial parameters can be obtained directly from the experimental data. Twice the width of the positive phase can act as a first guess of the period time T $(= 2\pi/\omega_0)$. This means about 80 rad/s for the angular frequency ω_0 at the 1200 Td level and about 50 rad/s at 100 Td for all subjects. Parameters b_1 and $-b_2$ can be chosen equal and roughly estimated from the ratio of positive and negative phase. This is always somewhere between 10 to 30 (1/s). With these rough guesses for the initial parameters we never found any local minimi, which was checked by trying different starting parameters.

3.5 Results of the estimation process

The results of the fit of the model of Figure 2 to data sets from two different subjects on different background levels are shown in Figure 4. For most subjects a reasonable fit is obtained. In general the fits are especially good for the first negative and the positive phase, but poor for the second negative phase. This can also be seen in Figure 4A. Note also that the time axis $-\tau$ from Figure 1 is corrected by t_{ex} so an ordinary time axis $t = t_{ex} - \tau$ is obtained, where $t = 0$ indicates the start of the impulse response.

The agreement between experimental data and the fit is numerically shown in Table 1. In this table the standard deviation s_m estimated from the measurements is compared to the standard deviation s_e estimated from the result of the fitting procedure. s_m is derived from the measured variance averaged over the different samples according to

$$s_m^2 = \frac{1}{M} \sum_{i=1}^{M} s^2(\tau_i), \qquad (13)$$
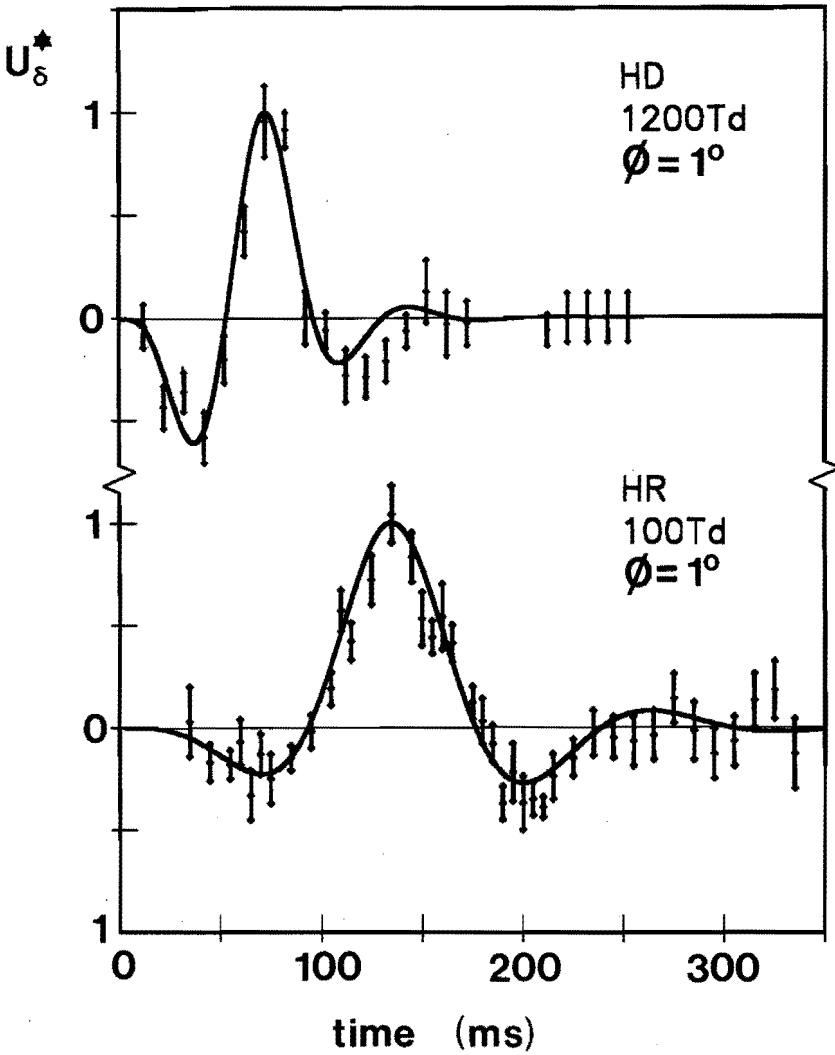
Figure 4: Two examples of estimated impulse responses of the pseudo-matched filter model.
A. Subject HD, 1 degree field at 1200 Td.
B. Subject HR, 1 degree field at 100 Td.

where $s(\tau_i)$ is the measured standard deviation at the i-th sampling moment (see also Figure 1). The standard deviation s_e is estimated from the (final) fit of the model to the measured data according to

$$s_e^2 = \frac{\Psi}{M - N}, \tag{14}$$

where Ψ is the objective function at the final estimate, M the number of samples and N the number of degrees of freedom in the estimation [25,26,11]. The estimated standard deviation is in most cases larger than the measured standard deviation, reflecting the poor fit of the second negative phase.

	back-ground (Td)	s_m	s_e	Ψ
JR74	1200	.120	.149	.488
JAJR	1200	.086	.129	.364
FB	1200	.074	.162	.761
JP	1200	.112	.112	.278
LT	1200	.139	.130	.369
HD	1200	.118	.125	.362
IH	1200	.106	.122	.326
LT	100	.109	.127	.353
HR	100	.113	.116	.502
JW	100	.170	.222	1.432
KS	100	.140	.146	.857

Table 1: Measured standard deviation s_m and the standard deviation s_e calculated from the fit (see text). The sum of squared residuals is given by Ψ.

The estimated parameters and their variances (s_i, $i = 1, 2, 3$) are shown in Table 2. The confidence intervals of the parameters can be calculated from the variances [25,26,11]. For the true parameter value θ_i^o the following inequality holds:

$$\theta_i - \sqrt{var\theta_i}\; t_{\beta/2,M-N} < \theta_i^o < \theta_i + \sqrt{var\theta_i}\; t_{\beta/2,M-N}, \tag{15}$$

where

$$\begin{aligned}
\theta_i &\quad \text{the i-th estimated parameter, } 1 \leq i \leq N, \\
var(\theta_i) &\quad \text{the estimated variance of } \theta_i, \\
\theta_i^o &\quad \text{the true value of the i-th parameter,} \\
t_{\beta/2,M-N} &\quad 100\beta/2 \text{ percentage point of the t-distribution.}
\end{aligned}$$

The size of the confidence intervals points out the well and poorly conditioned parameters. This is about the same for all datasets. The frequency parameter ω_0 is a very well conditioned parameter; its confidence interval is relatively small (about 10%). The damping parameters (b_1, b_2) have a (relatively) larger variance.

	$A \cdot NF$ $10^6(\text{Td}^{-1}\text{s}^{-5})$	a (s^{-1})	$b_1 \pm s_1$ (s^{-1})	$b_2 \pm s_2$ (s^{-1})	$\omega_0 \pm s_3$ (rad/s)
JR74	92.5	149	45.5± 25.6	5.9± 6.4	74.5± 5.6
JAJR	74.5	179	42.9± 19.3	9.5± 6.8	79.5± 5.8
FB	50.3	181	33.4± 14.6	15.4± 9.5	90.4± 7.6
JP	66.6	167	45.3± 18.3	10.5± 6.5	83.7± 5.5
LT	64.8	169	24.3± 7.9	15.1± 10.4	84.6± 5.5
HD	207.3	181	41.5± 17.2	10.5± 8.5	90.7± 6.7
IH	25.4	174	32.4± 11.6	28.5± 13.6	86.9± 7.2
LT	1.6	110	29.3± 11.2	16.0± 6.0	55.1± 4.3
HR	0.2	100	19.6± 4.2	22.4± 6.3	49.9± 2.9
JW	2.9	117	18.9± 7.1	8.0± 6.6	58.5± 4.2
KS	1.0	100	15.8± 7.7	9.7± 8.0	49.9± 4.5

Table 2: Parameters of the pseudo-matched filter for seven subjects at a 1200 Td level and four subjects at a 100 Td level (upper and lower part of the table respectively). In all cases the stimulus diameter is 1 degree.

The estimated parameters are also shown in Figure 5. From this figure (and Table 2) it can be seen that the estimated filter parameters cluster in specific areas in the complex plane, fairly independent of the subjects (see also the variances in Table 2) but strongly dependent on background luminance. From comparison of Figures 5A and 5B we see that only a significant change (given the variances) in the angular frequency parameter ω_0 occurs: an increase in frequency with an increase in background level. As a consequence of our assumptions (i.e. $a = 2\omega_0$) the parameter a changes by the same proportional amount with the background as ω_0. There seems to be a trend in the damping parameter b_1 to higher values at higher levels (see Figure 5), but this is within the confidence regions (see Table 2).

In Figure 6 an example (subject LT, $E = 1200$ Td, $1°$ field diameter) is shown of the confidence regions of the three estimated parameters. Essentially, the confidence region is a three-dimensional figure, and Figure 6 shows only the cross-sections of this hyper ellipsoid with the parameter planes. However, Figure 6 gives a good impression of this three-dimensional hyper ellipsoid. This was checked by the singular value decomposition (SVD) of the Hessian matrix at the final estimated parameters. The SVD can be used to obtain information on well and
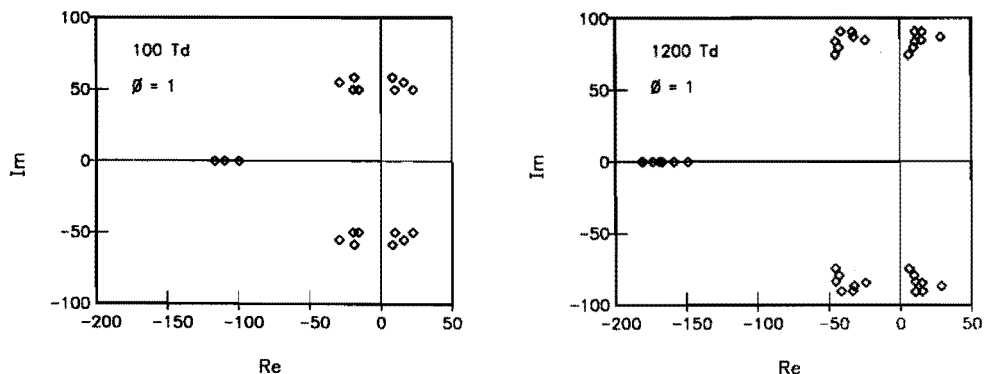
Figure 5: The estimated parameters for different subjects of a field of 1 degree diameter. **A.** 4 subjects at 100 and **B** seven subjects at 1200 Td background level.

poorly conditioned directions in the parameter space [25,26,11]. Essentially, the SVD ranges N orthogonal combinations of parameters from best to poorliest conditioned. In almost all cases the best parameter directions (from the point of view of the estimation process) are approximately the directions of the model parameters. This means that there are no directions in the parameter space with confidence intervals that are much larger than those shown in Figure 6. This guarantees furthermore that we had a well-defined optimization process, especially since the order of magnitude of the variances of the three estimated parameters is equal (see Table 2 and Figure 6).

3.6 Predictions from the model

Threshold-versus-duration curves

In Figure 7 the detection threshold ε is plotted versus the duration ϑ of a rectangular pulse. The solid line gives the prediction of the model estimated in the previous section for subject JR, at a background level of 1200 Td, and a 1 degree field without surround. The dots show the measured value of ε for the same conditions [8]. Figure 7 shows that the predicted curve agrees well with the measured data, with a small underestimate of the threshold amplitude at long durations. This is a direct consequence of the poor fit of the estimated model to the second negative phase of the experimental data.
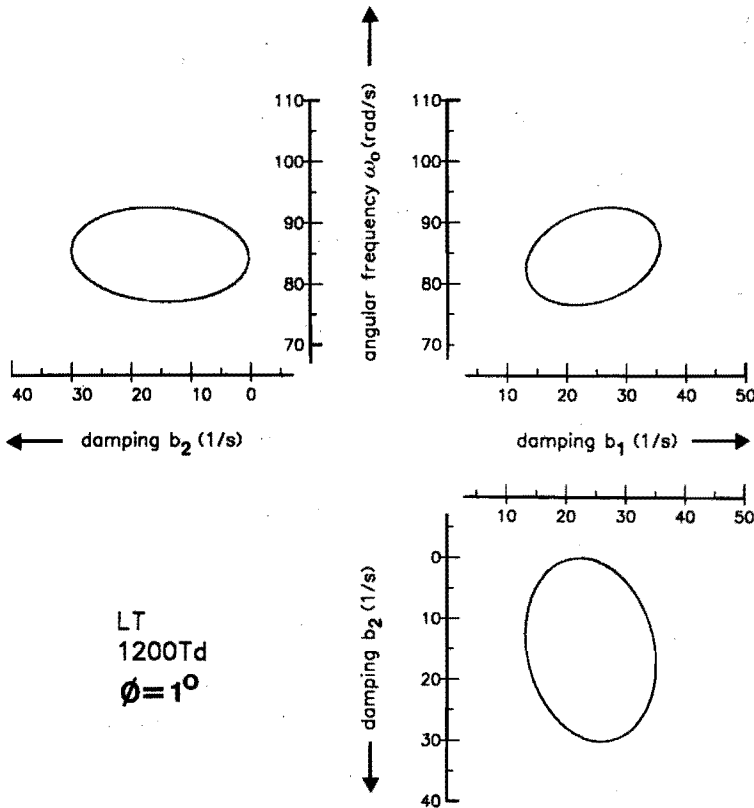
Figure 6: An example of the estimated confidence regions (see text). Subject LT, 1200 Td and a 1 degree field.

Frequency characteristics

From subject LT estimated impulse responses are available at two different background levels. From these estimated impulse responses the gain characteristics were calculated. The gain characteristics of the estimated linear models are shown in Figure 8. The figure is to some extent comparable to the de Lange characteristics (amplitude sensitivity versus frequency of a sinusoid, cf. [19,20]). However, a direct quantitative comparison is not possible. First of all, we do not have these experimental data of subject LT. Secondly, we assume that the de Lange curve is an envelope of different channels (cf. [4]) and thirdly, a de Lange curve incorporates stochastic effects (cf. [27]). Nevertheless, Fig. 8 allows a qualitative comparison with the high-frequency side of a de Lange curve. The gain character-
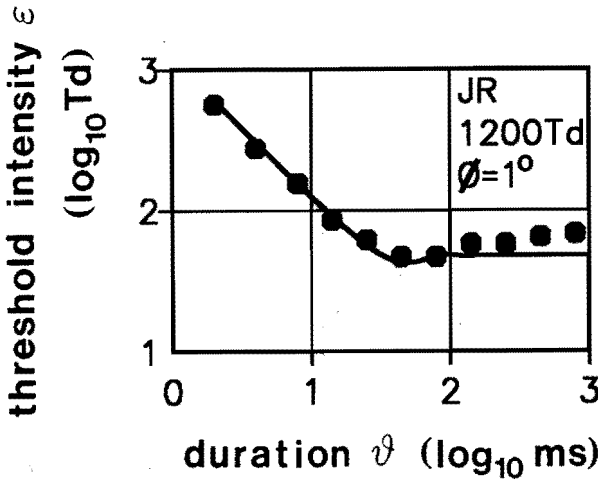
Figure 7: Prediction and experimental data of a threshold-versus-duration curve. Subject JR, 1200 Td and a 1 degree field.

istics show that at the higher background level the peak value of the gain curve is lower and the cut-off frequency is higher and that the high-frequency asymptotes of both levels (virtually) coincide. This is in agreement with the experimental data [19,20], while the slope of the high-frequency asymptote also agrees well with the experimental results.

For subject JP the gain and phase characteristics were measured using a sub-threshold summation technique, in the same way as the impulse responses were determined [15,16]. The advantages of this method are the possibility of measuring the amplitude sensitivity of the *transient* visual system (i.e. without contributions from other channels), and of revealing the (relative) phase characteristic. This means that a quantitative comparison of the frequency behaviour of the estimated linear model with experimental data is possible. We did not allow any vertical shifts in the predicted curve since the model is fully specified by its parameters, including the gain (see Table 2), and the contributions of probability summation in the measurement data should only be negligible as a consequence of the perturbation technique.

Figure 9A shows the gain characteristic of the model (continuous line) and the subthreshold measured data (dots) of the amplitude sensitivity of the transient channel. The predicted curve and the experimental data are in good agreement, except for the lowest frequencies. This is a direct consequence of the underestimation of the second negative phase of the impulse response; a more pronounced second negative phase results in smaller predicted values of the low-frequency side
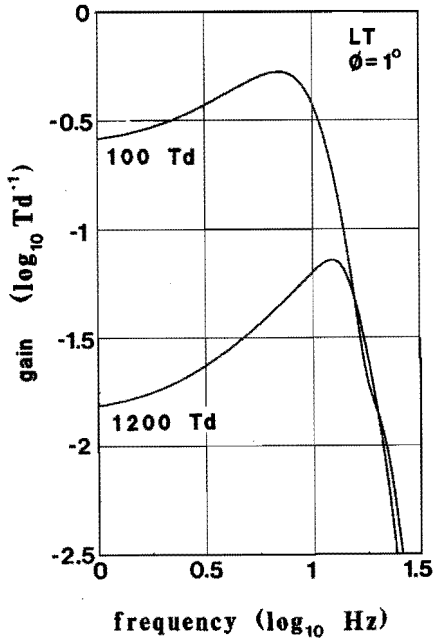
Figure 8: Gain characteristics of the pseudo-matched filter model. Subject LT, 1 degree field, 100 and 1200 Td background level.

of the gain characteristic. Figure 9B shows the phase characteristic of the model (continuous line) and the experimental data (dots). Both show a nearly linear dependence on frequency.

3.7 Discussion

In this paper we have presented a model for the transient channel of the visual system. The model consists of a cascade of linear filters, and is based on physiological and functional arguments. These arguments provide a conceptually attractive model. The functional argument, i.e. the fact that the system performs according to a nearly optimal detection unit, is in our view the most important one. However, the choice of the filters might contain weak points: the filter model is somewhat too rigid to contain all details of actual occurring physiological responses. Providing possibilities for further detail in the first and second filter would mean introducing extra parameters. In view of the parsimony principle we decided to take filters with the smallest number of parameters possible and so with very little possibility of detail.
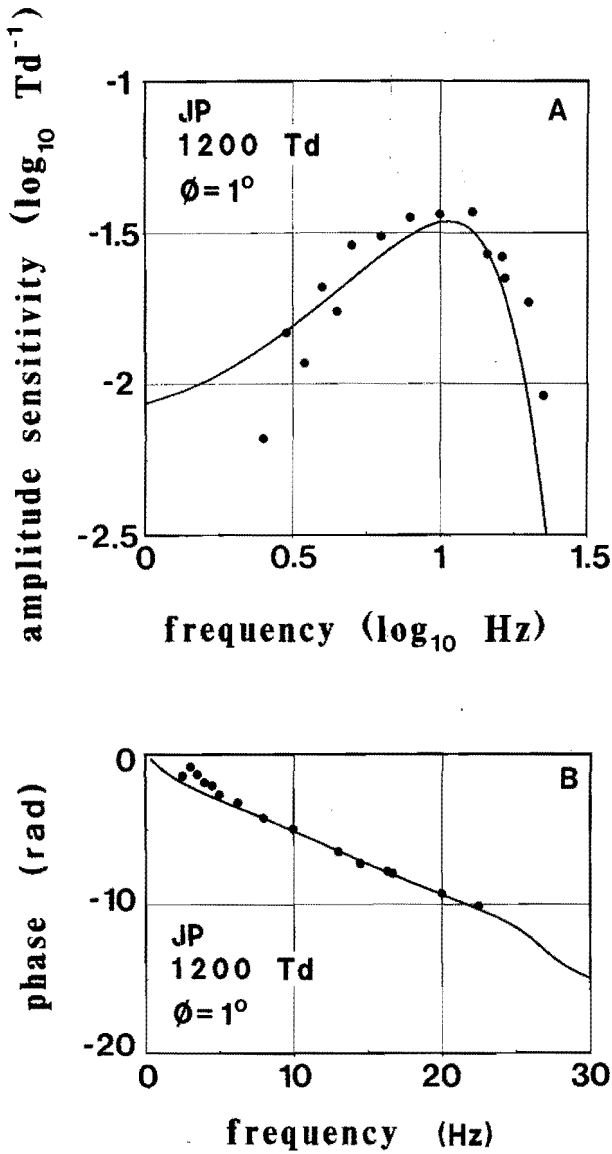
Figure 9: Gain and phase characteristics of the pseudo-matched filter model and experimental data of the subthreshold measurement of these characteristics. Experimental data replotted from [15]. Subject JP, 1 degree field at 1200 Td background.

The model was fitted to experimentally determined impulse responses of the transient channel of the visual system. In most cases the model's parameters were found so a reasonable fit was obtained (considering the variance in the measurement data). However, the second negative phase of the impulse response is mostly underestimated by the model. This is a consequence of the rigid choice of the linear filters. Other filters that are slight modifications of the ones proposed here may provide a better fit to the impulse response data without losing the concept of the model. Since the concept is considered of more importance than its actual implementation and because probably only slight modifications in the model are sufficient to provide better fits, we continued to examine the behaviour of the model.

It was found that under the same conditions (background level and field diameter) the estimated model was essentially the same for different subjects. Comparison of the results from the fits at different background levels showed that from the three parameters in the model only the angular frequency changed by more than the estimated standard deviation. This means the model is also incorporates a very simple description of changes in background level.

Finally it was shown that the model is in agreement with other psychophysical data. This was shown by predicting the threshold-versus-duration curve and the sensitivity to sinusoidal stimuli. The model's threshold-versus-duration curves agree well with the experimental data. From the prediction of gain characteristic it was found that the low-frequency side is overestimated. This is a direct consequence of the underestimation of the second negative phase of the impulse response rather than a discrepancy. The phase characteristic shows a linear dependence on frequency. This does not only agree with the experimental results, but may also be an attractive system property. In view of the idea of parallel operating channels, linear phase characteristics would provide an easy means to establish timing between transient and sustained channel. Sustained channels (see the impulse responses of point sources [7]) also show linear phase behaviour over the essential part of their frequency spectrum.

In short, we conclude that a chain of filters incorporating a matched filter is an attractive frame for analysing and understanding the temporal behaviour of the transient channel of the visual sytem.

Acknowledgements

References

[1] W. Reichardt, "Autocorrelation, a principle for the evaluation of sensory information by the central nervous system." In: W. A. Rosenblith, *Sensory*

communication. New York: Wiley, 1971.

[2] C. Rashbass, "Visibility of transient changes of luminance." *J. Physiol. Lond.,* vol. 210, pp. 165-186, 1970.

[3] J. J. Kulikowski and D. J. Tolhurst, "Psychophysical evidence for sustained and transient detectors in human vision." *J. Physiol.,* vol. 232, pp. 149-162, 1973.

[4] J. A. J. Roufs, "Dynamic properties of vision-IV. Thresholds of decremental flashes, incremental flashes and doublets in relation to flicker fushion." *Vision Res.,* vol. 14, pp. 831-851, 1974.

[5] B. G. Breitmeyer and L. Ganz, "Implications of sustained and transient channels for theories of visual pattern masking, saccadic suppression, and information processing." *Psychol. Review,* vol. 83, pp. 1-36, 1976.

[6] M. Green, "Masking by light and the sustained-transient dichotomy." *Perception and Psychophysics,* vol. 35 (6), pp. 519-539, 1984.

[7] J. A. J. Roufs and F. J. J. Blommaert, "Temporal impulse and step responses of the human eye obtained psychophysically by means of a drift-correcting perturbation technique." *Vision Res.,* vol. 21, pp. 1203-1221, 1981.

[8] F. J. J. Blommaert and J. A. J. Roufs, "Prediction of thresholds and latency on the basis of experimentally determined impulse responses." *Biol. Cyb.,* vol. 56, pp. 329-344, 1987.

[9] C. Rashbass, "Unification of two contrasting models of the incremental threshold." *Vision Res.,* vol. 14, pp. 97-99, 1976.

[10] A. Papoulis, *Signal analysis.* New York: McGraw-Hill, 1977.

[11] Numerical Algorithms Group Ltd., *Fortran Minimanual, Mark 9.* NAG Central Office, Oxford, UK, 1981.

[12] A. van den Bos and P. Eykhoff, "Model building and parameter estimation as means for intelligent measurements." *5-th International IMEKO Symposium Intelligent Measurement,* Jena, DDR, June 1986.

[13] P. E. Gill, W. Murray and M. H. Wright, *Practical Optimization.* London: Academic Press, 1981.

[14] G. E. Legge, "Sustained and transient mechanisms in human vision: temporal and spatial properties." *Vision Res.,* vol. 18, 69-81, 1978.

[15] J. A. J. Roufs, H. A. L. Piceni and J. A. Pellegrino van Stuyvenberg, "Phase and gain of the visual transient system." *IPO Annual Progress Report,* vol. 19, 49-56, 1984.

[16] J. A. J. Roufs, J. A. Pellegrino van Stuyvenberg and H. A. L. Piceni, "Phase and gain analysis of subthreshold-flicker and flash responses." *Perception,* vol. 13, p. A15, 1984.

[17] G. L. Turin, "An introduction to matched filters." *IRE transac. on inf. theory,* vol. IT-6, pp. 311-329, 1960.

[18] F. E. W. Vervuurt, "Pseudo-matched filter models for the transient visual system." Internal Report (in Dutch) ET-12-88, Eindhoven, University of Technology, 1988.

[19] D. H. Kelly, "Visual responses to time-dependent stimuli. I. Amplitude sensitivity measurements." *J. Opt. Soc. Am.*, vol. 51, pp. 422-429, 1961.

[20] J. A. J. Roufs, "Dynamic properties of vision-I. Experimental relationship between flicker and flash thresholds." *Vision Res.*, vol. 12, pp. 261-278, 1972.

[21] M. G. F. Fuortes and A. L. Hodgkin, "Changes in time scale and sensitivity in the ommatidia of Limulus." *J. Physiol.*, vol. 172, pp. 239-263, 1964.

[22] K.-I. Naka, "The cells horizontal cells talk to." *Vision Res.*, vol. 22, pp. 653-660, 1982.

[23] H. de Lange, "Relationship between critical flicker frequency and a set of low-frequency characteristics of the eye." *J. Opt. Soc. Am.*, vol. 44, pp. 380-389, 1954.

[24] J. Krauskopf, "Discrimination and detection of changes in luminance." *Vision Res.*, vol. 20, pp. 671-677, 1980.

[25] Y. Bard, *Nonlinear parameter estimation*. New York: Academic Press, 1974.

[26] J. R. Wolberg, *Prediction Analysis*. New York: D.Van Nostrand Co.Inc., 1967.

[27] J. A. J. Roufs, "Dynamic properties of vision.-VI. Stochastic threshold fluctuations and their effect on flash-to-flicker sensitivity ratio." *Vision Res.*, vol. 14, pp. 871-888, 1974.

Appendix

Consider the output of a linear filter L detected by a deterministic mechanism with threshold d. The detection process, however, is stochastic because of the noise source $n(t)$, see Figure 10. The noise $n(t)$ is assumed stationary and white. For the mean and the variance σ_0^2 of $n(t)$ we take

$$\mathcal{E}[n(t)] = 0 \qquad (16)$$

$$\mathcal{E}[n(t)^2] = \sigma_0^2, \qquad (17)$$

where $\mathcal{E}[\ ]$ denotes the expected value. It is assumed that the high threshold assumption is valid, i.e. $\sigma_0 \ll d$. For a pulse to be detected in the deterministic case ($\sigma_0 = 0$), a certain amplitude ε_1 is taken

$$\varepsilon_1 \,\Delta t\, U_\delta(t_{ex}) = d, \qquad (18)$$

where Δt is the duration of the pulse (Δt much smaller than the time constants of the linear filter), $U_\delta(t)$ is the impulse response of the linear filter and t_{ex} is the time of occurence of the extremum of the impulse response. In the stochastic case and assuming a high threshold and one clear dominant extremum of $U_\delta(t)$, equation (18) has to be corrected for the noise contribution at t_{ex}:

$$\varepsilon_1 \,\Delta t\, U_\delta(t_{ex}) = d - n(t_{ex}), \qquad (19)$$

The measured value of ε_1 will be a stochastic variable too.
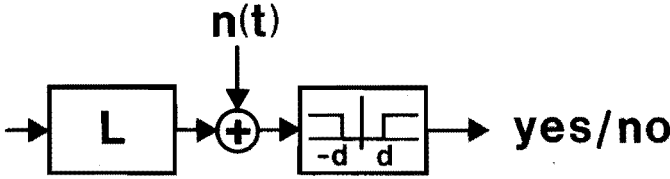
Figure 10: The linear model L (impulse response $U_\delta(t)$), the additive
noise $n(t)$ and the detection mechanism (with threshold d).

For the detection of an impulse response perturbed by an amplitude normalized
function $f(t)$ under the same assumptions as earlier, an equation is found similar
to (19):

$$\varepsilon_c\{\Delta t\, U_\delta(t_{ex}) + q\, f(t_{ex} - \tau)\} = d - n(t_{ex}),\tag{20}$$

where q is a constant so

$$q\, f(t_{ex} - \tau) \ll U_\delta(t_{ex}),\qquad\qquad \text{for all } \tau.\tag{21}$$

ε_c will have a stochastic nature too. From (19) and (20) it is found that a
constant ratio exists between the mean ε_{01} and ε_{0c} and their standard deviation
(σ_1 and σ_c)

$$\frac{\sigma_1}{\varepsilon_{01}} = \frac{\sigma_c}{\varepsilon_{0c}} = \frac{\sigma_0}{d}.\tag{22}$$

This ratio is called the Crozier coefficient. This ratio is constant over a large
number of stimulus conditions [27]. The normalized disturbance is calculated
according to [7]

$$g(t_{ex} - \tau) = \frac{f(t_{ex} - \tau)}{\Delta t\, U_\delta(t_{ex})} = q^{-1}\{\frac{\varepsilon_1}{\varepsilon_c(\tau)} - 1\}.\tag{23}$$

This function will be stochastic with mean $g_0(\tau)$ and variance $\sigma_{g(\tau)}^2$. Using a Taylor
series expansion around ε_{01} and ε_{0c}, it is found

$$g_0(\tau) \simeq q^{-1}\left\{\frac{\varepsilon_1}{\varepsilon_c} - 1\right\}_{\varepsilon_{01},\varepsilon_{0c}} = q^{-1}\{\frac{\varepsilon_{01}}{\varepsilon_{0c}} - 1\},\tag{24}$$

$$
\begin{aligned}
\sigma_{g(\tau)}^2 &\simeq \sigma_1^2\left(\frac{\partial g}{\partial \varepsilon_1}\right)^2_{\varepsilon_{01},\varepsilon_{0c}} + \sigma_c^2\left(\frac{\partial g}{\partial \varepsilon_c}\right)^2_{\varepsilon_{01},\varepsilon_{0c}} \\
&= 2\left(\frac{\sigma_0}{qd}\right)^2 [1 - q\, g_0(\tau)]^2 \\
&\simeq 2\left(\frac{\sigma_0}{qd}\right)^2.
\end{aligned}\tag{25}
$$

The last approximation stems from the perturbation requirement (21). From (25) it is seen that at each sampling moment the noise is approximately the same. The measured noise at different moments τ can therefore be compared directly to each other, and the introduction of a mean measured noise σ_m^2 (eq. 13) is justified.

chapter 4

Nonlinear parameter estimation applied to psychophysically measured impulse responses [1]

Albertus C. den Brinker
Jacques A. J. Roufs

Abstract

A technique is presented for the estimation of the impulse response, based on data from a psychophysical experiment on threshold vision. A two-step method is used for the estimation of the model parameters. The first step is a Hankel matrix approach, the second an unweighted least-squares method. Results of this estimation technique are presented. The model with the estimated parameters corroborates other psychophysical data. The estimates obtained are adequate for the intended purposes of simulation and modelling.

4.1 Introduction

Much research in the field of human visual perception is directed at visual threshold characteristics. It is usually assumed that these characteristics result from different channels operating in parallel. Each channel is tuned to some specific temporal and spatial frequency range. These channels are assumed to act linearly for small excursions from a steady background. In the temporal domain there are usually two channels postulated (e.g., [1,2,3,4]). One is tuned to temporally low frequencies and is called the sustained channel, the other to higher temporal frequencies and is called the transient channel [1,2,3,4]. Roufs and Blommaert [5] have shown that the temporal channels (the sustained and the transient channel) can be isolated from each other, and that the impulse responses of these channels can be measured psychophysically.

This paper discusses the parameter estimation of a linear model based on psychophysical measurements of the impulse responses of the transient channel. The linear model is an n-th order filter described by the poles and zeros of the transfer function (see Section 4). The reasons for this type of estimation are threefold. In the first place, it allows a convenient and simple description of the results of the measurements, because the model condenses all insight and knowledge on the system into a few parameters. In this case some 25 experimental data are translated into five parameters which describe a function that smoothes and interpolates the original data. Also, the parameters give insight in the behaviour of the system,

---

[1] This chapter is the (slightly modified version of the) text from an article with the same title. It is in press by IEEE Transactrions on Biomedical Engineering.

e.g., the poles represent the eigen functions of the system, i.e. the possible output signals in absence of an excitation. Secondly, this description enables us to predict the response of the modelled system for other excitations [6]. An example of a threshold-versus-duration curve will be shown in Section 6. Thirdly, in the long run we want to model (part of) the behaviour of the responses of the retina in a model with distributed parameters. In such a spatiotemporal model, the parameters from these estimations can be used to identify and model certain parts of this larger system. How the estimated parameters may be used in connection with a distributed parameter model will be given elsewhere (chapters 5 and 6).

The data on which the parameter estimations are performed here are derived from psychophysical experiments. Data from such experiments are rather noisy, as are all measurement data from biological systems. Furthermore, the experiments to obtain these data are time-consuming. Therefore the number of samples available is small. A small number of relatively noisy samples is an extra complicating factor in the process of estimating the modelled system.

An impulse response of a certain channel of the visual system cannot be measured directly by psychophysical means. However, from psychophysical detection experiments (where a subject states whether he has seen or not seen a certain stimulus) using a perturbation technique [5], a normalized impulse response can be obtained. The absolute sensitivity of the system can be measured separately.

The use of the perturbation technique has been extensively described by Roufs and Blommaert [5]. In essence, this technique uses a two-pulse temporal excitation, where the response of one of the pulses is perturbed by the response of the other (smaller) pulse. This causes an increase or decrease in threshold amplitude of the larger pulse. The change in threshold amplitude caused by the smaller pulse can be measured as a function of the time delay τ between these two pulses. From such data the shape of the perturbing signal can be retrieved [5]. As a consequence of this technique some a priori information on the experimental results is available. This information must be incorporated into the model, resulting in some restrictions on the degrees of freedom of the model chosen.

The data are interpreted as being derived from a continuous system: the signals are not quantized and are functions of a continuous time variable. The model being fitted to these data is an n-th order continuous linear filter, with some restrictions on its structure.

The method used to obtain the parameters of this model is the well known least-squares estimation. The objective function, which is being minimized during the estimation, is a nonlinear function of the parameters of the n-th order filter. A problem with such nonlinear parameter estimations is that the objective function may have (many) local minima. In order to limit the chance that the minimization of the objective function is trapped in such a local minimum, a fairly good initial estimate of the parameters is helpful.

For this reason the parameter estimation considered here consists of a two-step method. As a first step an estimation procedure is used that is not sensitive

to local minima. To this end a Hankel approximation (see Section 3) is used. Thus an acceptable estimate for the initial parameters of the model is obtained. As the second step the least-squares method is used for the nonlinear parameter estimation of the ultimate model.

There are several reasons for using this second step. Firstly, the Hankel approach leads to a time-discrete model. Although an equivalent continuous system can be formulated, this still means that non-equidistant datapoints cannot be taken into account in the first step. Secondly, the optimization criterion in the Hankel estimation cannot easily be given in terms of known criteria (e.g., least-squares, maximum deviation). Thirdly, there is no possibility to introduce a priori information in the first step, e.g., that the impulse response is continuous at its starting moment.

Estimations using this Hankel matrix approach have shown that the results obtained are quite close to the minimum, in an unweighted least-squares sense, for a model having the same degree of freedom [7]. So in this way the nonlinear least-squares estimation of the second step can be started with a fairly good initial guess of the optimal parameters.

The paper is organized in the following way. Section 2 discusses the data sets and the specific consequences of the measurement technique. Section 3 deals with the Hankel matrix approach, the way in which the data are used, and the method used to translate the results of this estimation into the parameters of a continuous model. Section 4 describes the continuous model used in the second estimation step as well as the restrictions on the parameters based on a priori information. The implementation of the estimation process in computer programs is briefly indicated in Section 5. In Part 6 some actual results of the estimations are presented, as well as some problems encountered.

4.2 The impulse response data

The response of the eye to a certain stimulus is generally supposed to be processed in different channels operating in parallel [1,2,3,4]. In the temporal domain two channels are usually assumed to intermediate between the physical stimulus and the human percept. These are the sustained and the transient channels [1,2,3,4].

The experimentally determined impulse responses [5,6] of different subjects at two different background levels, were obtained by the so-called perturbation technique [5]. The impulse response data are derived from flashed discs of a diameter of 1 degree visual angle, superimposed on an equally large disc of a given luminance. The disc was projected foveally and the surround of the disc was always completely dark. It was found [2,5,6] that the transient system is dominant for this spatial configuration when only fast temporal excitations (flashes) are used (as is the case with the perturbation technique, see Section 1).

There are, however, some consequences of this method with respect to the measured data [5,6] that we need to discuss. First, the method requires rather

time-consuming experiments. For this reason the number of datapoints that is usually measured is taken as low as possible. The number usually ranges from about twenty to thirty. In most cases an extra tail of some 4 or 5 samples was added to the measured data, with mean values equal to zero and standard deviations taken as the mean of the standard deviations of the actually measured samples. This extra tail was added in the region where the impulse response is approximately zero, and ensures that the estimated filter has the properties of a stable system (Bounded Input-Bounded Output). Secondly, there is the offset of the time axis. As a result of the perturbation technique the position of the starting point of the impulse response (say $t = 0\,s$) is lost. A time axis is obtained in which the origin of the axis is located exactly on the extremum of the impulse response (see Fig. 1). Note also that the time scale is plotted in the independent variable $-\tau$. It was preferred to stick close to the same variable as used in the original measurements, which is τ. To obtain the direction of a normal time axis (later events situated on the right-hand side) the variable $-\tau$ had to be taken. Thirdly, the extremum should be exactly equal to one, since a normalized impulse response is obtained with the method used . Actual measurement of this extremum gives a value close to but not exactly one, because of the noise in the system (see Fig. 1A at $\tau = 0\,ms$).

The system is not fully specified by its normalized impulse response $U_\delta^*(t)$. The amplification factor of the filter is not constrained by the experimental procedure. This constant can be measured separately. We suppose that after the linear filter considered here, an ideal detector with an unknown threshold level is operating. By measuring the intensity ε at the detection level of a pulse with a duration ϑ that is short compared to the time constants of the filter, the normalizing constant can be expressed in units of the internal detection mechanism. The normalizing constant is called the norm factor NF and is equal to $\varepsilon^{-1}\vartheta^{-1}$. The norm factor multiplied by the normalized impulse response gives the impulse response of the system in threshold units per second. Consequently the response $R(t)$ of the linear filter to an arbitrary input $\varepsilon_{in} f_{in}(t)$ can be expressed as a convolution:

$$R(t) = \int_{-\infty}^{t} \varepsilon_{in} f_{in}(\rho)\, NF\, U_\delta^*(t - \rho)\, d\rho = \frac{\varepsilon_{in}}{\varepsilon\vartheta} \int_{-\infty}^{t} f_{in}(\rho)\, U_\delta^*(t - \rho)\, d\rho, \qquad (1)$$

where $f_{in}(t)$ is an amplitude-normalized signal and ε_{in} is the amplitude. The response $R(t)$ is in this way expressed in threshold units, e.g., $R(t) = 2$, the response is twice as large as the internal threshold level. Alternatively the intensity ε_{in} of an arbitrary stimulus to reach the threshold can be calculated.

The data of the normalized impulse response (see Fig. 1A) show an oscillatory behaviour. This points to a bandpass or nearly bandpass character of the system. Furthermore, from the data it can be seen that the experimentally determined impulse response is (probably) continuous at the unknown starting point. It is also (probably) slowly starting, i.e. the first derivative equals zero at the starting point. This is true for most biological responses.

These remarks have consequences for the model that is being fitted to these
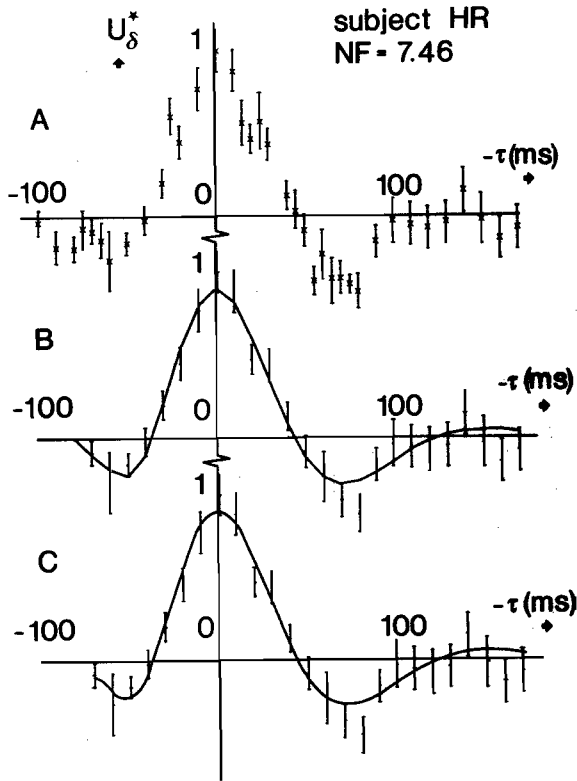
Figure 1: **A.** An example of data obtained from a psychophysical experiment using a perturbation technique, for the measurement of the impulse response. The points represent the mean value, the bars represent twice the standard deviation of the mean. **B.** The data of Fig. 1A (midpoints of the vertical error bars) used in the Hankel estimation (the non-equidistant samples of Fig. 1A are omitted), together with the Hankel realization of order four based on these data. **C.** Data of Fig. 1B (midpoints of the vertical error bars) for the Hankel estimation, and the continuous impulse response calculated from the Hankel realization. The impulse response starts with a time delay equal to the sampling time (see (3)).

data. It implies that there are a number of restrictions on the chosen model, and thus that this will result in a reduced number of degrees of freedom in the model. This will be dealt with in section 4.

4.3 The Hankel matrix approach

In this section the first part of the two-step method in the estimation procedure is discussed. It should provide the initial values of the parameters for the second step. Our aim is to use the estimated model for simulations. The method of deriving the estimate (e.g., equation error method, output error method) determines the possible applications of these estimates [8,9]. As shown in [9] an equation error method will not give an adequate estimate for purposes of simulation with the experimental data at hand. For models to be used in simulations the output error model is to be preferred [8], since in that case the predicted (i.e. model) response does not depend on the foregoing system (i.e. measured) responses. Since an output error method will be used in the second step, the estimation in the first step should also be closely linked to an output error method step, and should not be sensitive to local minima. The Hankel matrix approach is such a method.

A Hankel realization is an estimate of a discrete n-th order model from a sequence of impulse response points. The realization is a state space model. The way in which the parameters of the n-th order discrete state space model are derived from the data of the impulse reponse can be found in Van den Hof [10].

The parameters of this state space model can be translated into the parameters q_i and R_i of a discrete transfer function according to

$$\hat{F}(z) = \sum_{i=1}^{n} \frac{R_i}{z - q_i}, \tag{2}$$

$\hat{F}(z)$ being the transfer function in the z-domain, q_i and R_i being the (discrete) poles and residues, respectively.

To use this discrete model estimation, the data are assumed to be obtained from a discrete system. Therefore all non-equidistant samples are omitted and, if necessary, interpolated samples are used. Furthermore, an ad hoc assumption has to be made for the starting point of the impulse response. This has to be an integer multiple of sampling intervals used in the experiments. If the data are not obtained by equidistant sampling this method cannot be used.

In Fig. 1B only the data from Fig. 1A are plotted that are used in the Hankel estimation. The non-equidistant samples are omitted, as well as the data before the assumed starting point (which was taken $8 * 10\,ms$ before the extremum). This method gives an estimate of the parameters R_i and q_i of a discrete system. The time-discrete impulse response associated with the estimated parameters is also plotted in Fig. 1B.

From this discrete model a corresponding continuous model can be calculated. The continuous model is described by its transfer function $H(s)$ in the Laplace domain s :

$$H(s) = \exp(-sT) \sum_{i=1}^{n} \frac{R_i}{s - p_i}, \tag{3}$$

where p_i, R_i are the poles and the residues, respectively, of the continuous transfer function, and T is the time delay (equal to one sampling interval). From the discrete model parameters q_i the parameters p_i can be derived:

$$q_i = \exp(-p_i T), \tag{4}$$

$$Re\{p_i\} = T^{-1} \ln |q_i|, \tag{5}$$

$$Im\{p_i\} =$$
$$T^{-1} \arctan(Im\{q_i\}/Re\{q_i\}) \quad , \text{ if } Re\{q_i\} > 0 ,$$
$$T^{-1} \arctan(Im\{q_i\}/Re\{q_i\}) + \pi \quad , \text{ if } Re\{q_i\} < 0 \text{ and } Im\{q_i\} > 0 ,$$
$$T^{-1} \arctan(Im\{q_i\}/Re\{q_i\}) - \pi \quad , \text{ if } Re\{q_i\} < 0 \text{ and } Im\{q_i\} < 0 . \tag{6}$$

In Fig. 1C the continuous impulse response is plotted, along with the data (the midpoints of the vertical error bars) used for the Hankel estimation. The continuous impulse response coincides with the impulse response of the discrete model at the sampling points.

From these estimations it is possible to obtain an estimate for the order of the model in the second step. This can be done by simply performing the estimation for several orders, and evaluating (e.g.) the sum of square errors. The poles (see formula (4)) are used as an initial guess of the parameters of the continuous model described in the next part. The residues cannot be used directly to get an initial estimate of the remaining parameters of the continuous model because of the restrictions on these parameters. This will be elaborated on in Section 6.

In view of the noisiness of the experimental data and of the problems that are caused by the sensitivity of a least-squares optimization to local minima, the Hankel matrix approach is a convenient starting point. To be more specific, we can distinguish three advantages of using the Hankel matrix approach as a first step. We already mentioned that the Hankel method can easily provide an estimate of the order of the system. Secondly, also already mentioned, initial values for the parameters in the second step (the least-squares optimization) are provided. As a third point we would like to draw attention to the fact that the estimated poles and zeros also provide an indication of the surplus of poles with respect to zeros of the system. This is of considerable importance, since if it were tried to fit a filter that has not an appropriate difference in poles and zeros by means of an least-squares output error method, the least-squares technique will fail. If there are too many zeros, the norm of at least one zero will be large with respect to the norms of the poles and the other zeros, thus creating a badly conditioned problem. This problem is especially acute in a least-squares estimation, since when the process proves to be badly conditioned, it is unknown whether this is a consequence of an inappropriate choice of the model (e.g., a wrong number of poles and zeros), or simply caused by a bad choice of initial parameters. On the other hand, a too small number of zeros will lead to a bad fit. In short, an estimate of the surplus

of the number of poles with respect to the zeros is provided by the Hankel matrix approach, and would be a cumbersome problem in a least-squares estimation. E.g., from the fourth order Hankel realizations it was found that, for almost all cases, the estimation results gave only one zero with a norm that was in the region of the norms of the poles.

In conclusion, the first step in the suggested two-step approximation procedure is used to provide the numbers of relevant poles and zeros and the values of the initial parameters in the least-squares estimation. If there is some other source that yields this information, then the Hankel matrix approach can be substituted by this other source. This may be either a priori knowledge about the modelled system, or may consist of another estimation procedure that is not sensitive to local minima, and is (also) closely linked to a least-squares method.

As already stated, the important advantage of this method is that no local minima occur. The method has the following disadvantages: in the first place the restrictions we want to impose on the realization cannot be implemented. These restrictions are that the extremum of the impulse response equals one, the extremum occurring at $\tau = 0\,ms$, a continuous impulse response and a continuous first derivative. Secondly, the samples that are not equidistant cannot be taken into account. Thirdly, an ad hoc assumption has to be made for the time at which the impulse excitation took place. To overcome these drawbacks a second estimation procedure is added to the first. This second procedure is described in the next part.

4.4 The continuous model, transfer function, parameters and the restrictions

A general continuous causal n-th order linear filter can be described by the transfer function $F(s)$ in the s-domain, i.e. the Laplace transform $\mathcal{L}$ of the impulse response $f(t)$:

$$F(s) = \mathcal{L}\{f(t)\} = \int_0^\infty f(t)\exp(-st)\,dt, \qquad (7)$$

$$F(s) = \frac{\sum_{i=0}^n C_i s^i}{\prod_{i=1}^n (s - p_i)}. \qquad (8)$$

The reason for the choice of the parameters C_i in the numerator is that in that case the restrictions mentioned earlier can be imposed on the model in a simple manner.

Since the impulse response is a real valued signal, and the system is stable, the only restrictions on the poles are that they occur in complex conjugated pairs, and that the real part of the poles is non-negative.

The reason for the choice of the denominator in the form of a product containing the poles as parameters is that it can easily be translated into an impulse response in the form of damped sinusoids. If we were to chose to describe the denominator

in a form containing the natural frequencies Ω_{oi} and the damping ratios ξ_i as the parameters, then

$$p_i = -\xi_i \Omega_{oi} \pm j\Omega_{oi}\sqrt{1 - \xi_i^2} \ , \ j = \sqrt{-1}, \tag{9}$$

and a restriction has to be imposed on ξ_i: $0 \leq \xi_i \leq 1$. This would result in an undesirable constraint on the optimization problem that can be avoided by the choice of the parameters in the form of the poles p_i. If we were to chose to describe the denominator in the form of a summation by

$$\prod_{i=1}^{n}(s - p_i) = \sum_{i=0}^{n} E_i s^i \ , \ E_n = 1, \tag{10}$$

with E_i, (i=0,...,n-1) as the parameters, a search has to be made for the zeros of an n-th degree polynomial every time the impulse response is compared with the data in order to calculate the objective function in each iteration step.

We have found that for our data the Hankel approximations always gave the largest possible number of complex pole pairs, i.e. always only one real pole, if the order is uneven. The estimated complex pole pairs for our impulse response data [5,6] were never located near the real axis, but always contained a considerable imaginary component. The data are such that the poles are always estimated so as to have a real part less than zero. This means there is no need to impose any restrictions on the poles from the stability point of view.

The restrictions on the parameters C_i can simply be derived. Assuming there is no impulsive component in the impulse response, that the impulse response is continuous, and that also its derivative is continuous at the starting point means, respectively

$$C_n = 0, \tag{11}$$

$$C_{n-1} = 0, \tag{12}$$

$$C_{n-2} = 0. \tag{13}$$

$F(s)$ is now simplified to the form:

$$F(s) = C_{n-3}\frac{\sum_{i=0}^{n-3} D_i s^i}{\prod_{i=1}^{n}(s - p_i)}, \tag{14}$$

where

$$D_i = C_i/C_{n-3} \ , \ i = 0, \ldots, n - 3. \tag{15}$$

It is obvious that the restriction of the extremum of the impulse response being equal to one results in a restriction on C_{n-3}, that is to say C_{n-3} is a function of the other parameters:

$$C_{n-3} = C_{n-3}(p_i, D_k) \ , \ k = 0, \ldots, n - 4 \ , \ i = 1, \ldots, n. \tag{16}$$

The analytic expression (16) for C_{n-3} is, however, hard to derive for the general case. Before imposing the restriction on the extremum, the transfer function is translated into the impulse response $f(t)$.

The impulse response associated with $F(s)$ according to (14) can be written as

$$f(t) = \mathcal{L}^{-1}\{F(s)\} = \sum_{i=1}^{n} Res_i \exp(p_i t) H(t), \tag{17}$$

where $H(t)$ is the Heaviside function defined by

$$H(t) = \begin{cases} 0 & , t < 0 \\ 1 & , t \geq 0. \end{cases} \tag{18}$$

The residues Res_i can be calculated from the set (p_i, C_{n-3}, D_k), $i = 1, \ldots, n$; $k = 0, \ldots, n - 4$, by

$$Res_i = \lim_{s \to p_i} (s - p_i) F(s) = C_{n-3} \frac{\sum_{k=0}^{n-3} D_k p_i^k}{\prod_{k=1, k \neq i}^{n} (p_i - p_k)}, \tag{19}$$

assuming that all poles p_i are distinct.

As said before, the analytical expression for C_{n-3} as a function of the other parameters is hard to derive. We circumvent this problem numerically. Given any set (p_i, D_k), $i = 1, \ldots, n$, $k = 0, \ldots, n - 4$, the residues Res_i can be calculated according to (19), apart from the factor C_{n-3}. If C_{n-3} is set at a certain numerical value, e.g. unity, a numerical search for the extremum of $f(t)$ can be made for any parameter set. The value of the extremum found in this way is called K ; K may be positive or negative. C_{n-3} is set to

$$C_{n-3} = K^{-1}. \tag{20}$$

The impulse response $f(t)$ is thereby scaled to unity.

During the search for K the numerical value of t_{ex}, the moment at which the extremum of the impulse response of the model occurs, is found also. This value t_{ex} equals of course exactly the shift between the time axis of the impulse response that is being fitted, and the time axis of the measurements. The loss of the starting point in the measurements does not give rise to an extra degree of freedom: the shift between the origin of the $-\tau$ axis and the filter response axis t is not arbitrary, but is uniquely given by the condition that the extremum of the filter response should coincide with $\tau = 0$. The expression $f(-\tau + t_{ex})$ given by

$$f(-\tau + t_{ex}) = \sum_{i=1}^{n} Res_i \exp(p_i t_{ex}) \exp(-p_i \tau) H(-\tau + t_{ex}), \tag{21}$$

can now be compared with the data.

The number of degrees of freedom N in an n-th order model is (in formula (14))

$$N = 2n - 3. \tag{22}$$

Because of the restrictions on the numerator of the transfer function the minimum order of the model is three.

4.5 Objective function and implementation for the second estimation step

From noise analysis of experiments using a perturbation technique it can be shown that the expected value of the noise at the various sampling instants τ_i is approximately independent of τ [5]. For this reason an unweighted least-squares objective function Ψ is chosen:

$$\Psi = \sum_{m=1}^{M} \{f(-\tau_m + t_{ex}) - U_\delta^*(-\tau_m)\}^2, \tag{23}$$

where

$\begin{aligned}
M &= \quad \text{number of samples}, \\
\tau_m &= \quad m\text{-th sample time}, m = 1, \ldots, M, \\
U_\delta^*(\tau_m) &= \quad \text{measured response at } \tau_m.
\end{aligned}$

In contrast to the Hankel matrix approach non-equidistant samples are included in the optimization process of (23). There are no constraints on the values of the parameter set (p_i, D_k). The poles p_i are complex valued, but always occurring in complex conjugated pairs. The computer programs for estimation purposes work with real-valued parameters only. Therefore p_i is split into its real and imaginary parts and these act as actual parameters in the programs. There are no constraints on the values of these real and imaginary parts. But it means that the number of complex pole pairs has to be stated if the programs are not to become too complex. The Hankel realization always showed a maximum number of complex pole pairs given any order, i.e. all poles are complex or there is only one real pole. The least-squares estimation programs incorporate this assumption.

For the estimation process we used subroutines from the NAG library [11]. The estimation is an unconstrained nonlinear least-squares problem. Only function values of Ψ are supplied, no analytic derivatives of Ψ with respect to its parameters are used. The subroutines E04FDF and E04FCF from the NAG library are meant for such a problem [11]. These routines use a modified Gauss-Newton method to search for the minimum of the objective function [12]. Programs were written in Fortran and implemented on a VAX 11/750 computer.

4.6 Results and discussion

The results of the Hankel estimation have been mentioned several times before. They show a good fit of the model to our data (see the example in Fig. 1B) for each data set, for orders ranging from 4 to 6.

The poles of the Hankel realization are used to calculate an initial guess of the poles in the least-squares estimation step. The values of the initial guess of the poles and the ultimately obtained poles from the second estimation step agree well.

Essentially, from the residues of the Hankel estimation no adequate information can be derived for an initial guess of the D_k parameters in the second step, because

of all the restrictions imposed. For a fourth-order filter, enough additional information is present to get an idea about what the initial value for these parameters should be.

The data show that the realization approximately must have a bandpass character. Consequently at least one zero of the continuous transfer function is small with respect to the poles. Furthermore, from measurements of the phase characteristics it is known that the system has a non-minimum phase characteristic [13]. This means that at least one zero is lying in the right-half of the s-plane.

Turning our attention to a model of order four, sufficient information exists for the initial guess of the D_0 parameter. With a fourth order model there is only one (real valued) zero z_1 outside infinity. From (14) it follows that this zero has the value

$$z_1 = -D_0/D_1 = -D_0. \tag{24}$$

The two considerations mentioned above (a zero small with respect to the poles, and a zero in the right half plane) apply to this one zero. In this way we can make a reasonable guess for the D_0 parameter. For higher orders than four it is much harder to attain an initial value for the D parameters on the basis of such considerations.

In Figs. 2 and 3 several results of the two-step method of estimation are shown. The measured data are from different subjects and at two different background luminance levels[2] (1200 Td for Fig. 2, 100 Td for Fig. 3). The fourth-order models fit reasonably well. This can also be shown numerically. In Tables 1 and 2 the measured standard deviation s_m derived from the variance averaged over the different datapoints is compared with the standard deviation s_e estimated from the realization:

$$s_e^2 = \frac{\Psi}{M - N}, \tag{25}$$

where Ψ is the objective function at the final estimate, M the number of datapoints, and N the number of free variables in the least-squares estimation [14,15]. The estimated standard deviation s_e should not be much larger than the measured standard deviation s_m. This would mean that the estimate is not an adequate representation of the measured data. On the other hand, s_e must not be much smaller than s_m, otherwise the estimation process would not perform one of its main functions, which is to dispose of (part of) the noise that is present in the measured data.

The least-squares fits are in most cases better than the Hankel estimates, even though the number of free parameters is larger in the Hankel estimation. The reason for this is that the Hankel estimation does not minimize a least-squares criterion, and is in this respect always sub-optimal.

---

[2] The number of trolands (Td) is given by multiplying the luminance in $Cd\ m^{-2}$ by the pupil area in mm^2.

	s_m	s_e from Hankel	s_e from least-squares
JR74	.120	.157	.144
JAJR	.090	.105	.099
FB	.074	.145	.127
JP	.112	.144	.131
LT	.139	.110	.115
HD	.118	.134	.138

Table 1: Measured (s_m) and estimated (s_e) standard deviations for six different subjects at 1200Td.

	s_m	s_e from Hankel	s_e from least-squares
LT	.109	.122	.096
HR	.113	.114	.116
JW	.170	—	.247

Table 2: Measured (s_m) and estimated (s_e) standard deviations for three different subjects at 100Td.

In Fig. 4 an example of a pole-zero plot is shown. The differences in estimated parameters of different subjects at the same background level are relatively small. For different background levels there is a consistent change in estimated parameters. Such an analysis of the estimated parameters under different conditions will be carried out in chapter 5.

In all estimates the zero z_1 is located in the right-half plane. The system therefore has a non-minimum phase characteristic. This is consistent with independent measurements of the phase [13]. The ratio of z_1 and the smallest norm of the poles is far from being constant over the different subjects. It ranged between 0.1 and 1.1. At the higher background level the zero became relatively smaller, indicating poorer d.c. response at higher light levels.

Probably a still better fit would be possible with a least-squares estimation of a higher order fit to the data. As yet such higher order fits have not been tried. There is still a problem with the fourth-order least-squares estimations, i.e. the estimation of the D_0 parameter. It is found that for most data the estimation is hardly sensitive to variations in this parameter. The D_0 parameter determines the output of the system to a step response for long times after onset. If the system is (nearly) bandpass, it is obvious that this value is hard to estimate from impulse

Figure 2: Fourth-order estimates of the ultimate model (14) for six different subjects at a background luminance of 1200 Td. Data from subjects JR74 (4A), JAJR (4B), FB (4C), JP (4D), LT (4E), and HD (4F). For clarity Figs. A and D are shifted 2.4 units and Figs. B and E 1.2 units in the vertical direction.

response data. This can also be seen from (19). For order four the numerator is $p_i + D_0$. D_0 being small with respect to $|p_i|$ means it has hardly any influence on the residues. Consequently the influence of D_0 on the objective function is very small in these cases. With such an ill-determined parameter in the fourth-order model, it was not found advisable to try even higher order fits.

One way to solve this problem would be to fix the D_0 parameter in those cases where the zero z_1 is small with respect to $|p_1|$. We could, for instance, assume the zero to be lying in the origin of the s-plane, which is to say assuming the system to be bandpass. In this manner we can eliminate such an ill-determined parameter. Another way to overcome this problem might be to make simultaneous fits using
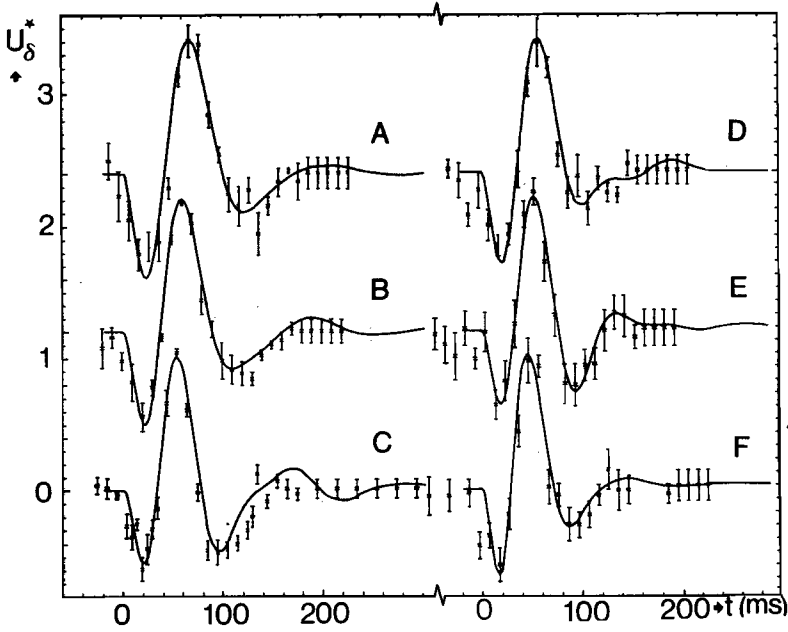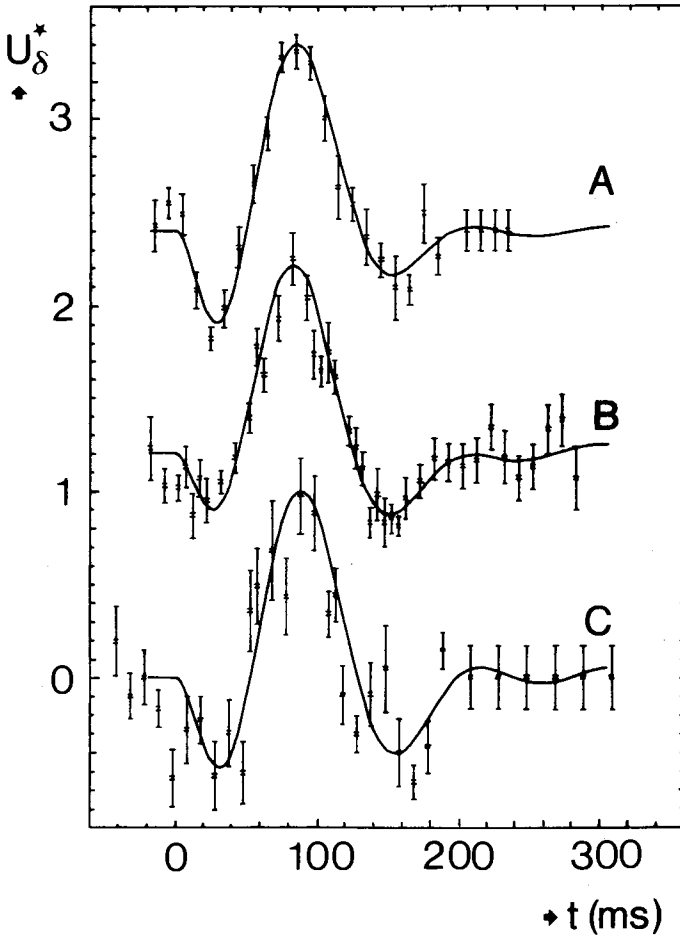
Figure 3: Fourth-order estimates of the ultimate model for three different subjects at a background luminance of 100 Td. Data from subjects LT (5A), HR (5B), and JW (5C). For clarity Figs. A and B are shifted vertically 2.4 and 1.2 units respectively.

data in which the D_0 parameter is not so badly conditioned, e.g., using data from step responses.

The research will be continued in this direction, also taking into account the reliability of the estimated parameters. However, up till now we are content with the fourth order descriptions of the measurement data. The most important features of the experimental data can be represented in such a simple description, and these features are also consistent with other psychophysical data. Furthermore,
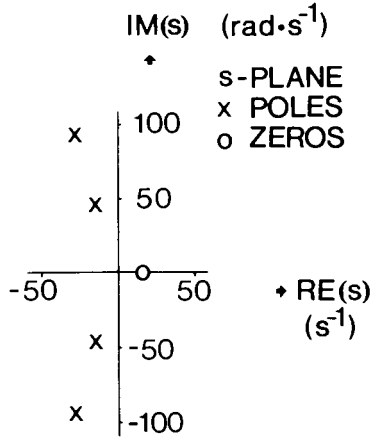
Figure 4: Pole-zero plot of the fourth-order ultimate model for subject **JAJR**.

with these descriptions the response of this system to any time excitation can be predicted, and also the modelling of more complex systems (as a formal analogy of the performance of the human eye) comes within closer reach.
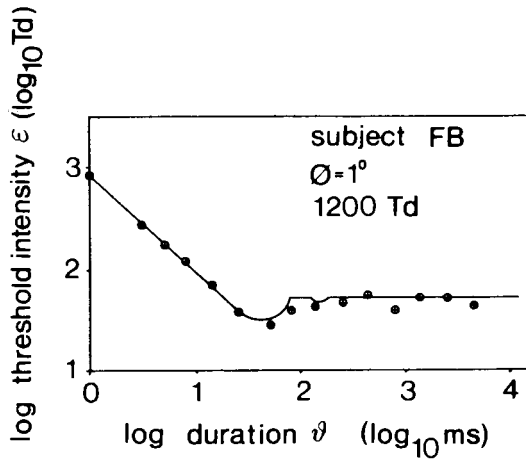
Figure 5: Threshold of rectangular flashes as a function of the duration ϑ for subject FB. The circles are the experimental data, the continuous line is the prediction derived from the estimated impulse response.

An example of a prediction of the model is shown in Fig. 5, where the detection amplitude is plotted versus the duration of rectangular pulses. The circles give the experimental data of subject FB for the same experimental conditions for

which the impulse response has been measured (1 degree field, 1200Td). The continuous line is the threshold value predicted from the estimated linear filter on basis of the experimentally determined impulse response. Since the model is completely described by the normalized impulse response and the norm factor, there are no degrees of freedom to fit the prediction to these data. From Fig. 5 it can be seen that the estimated impulse response gives an adequate prediction of this threshold-versus-duration curve, even for long durations. This confirms the assumed linearity [2,5,6] of the transient visual system (see also [16,17]).

The small irregularities in the predicted threshold curve for long durations are due to the nonlinear detection unit. The response of the filter to a pulse is the difference of two step responses. The first starts at the onset of the pulse and has a positive amplitude, the second at the offset of the pulse and has a negative amplitude. For pulses of long duration the response to the offset adds to the tail of onset response, which is a small oscillatory signal. Thereby the detection sometimes occurs at the maximum of the onset response, and sometimes on the minimum of the offset response, depending on the pulse duration. This produces the irregularities in the prediction. These irregularities probably do not occur in reality, but are a consequence of the low order of the filter that is used to approximate the real system, together with the nonlinear behaviour of the threshold unit.

Acknowledgements

References

[1] J. J. Kulikowski and D. J. Tolhurst, "Psychophysical evidence for sustained and transient detectors in human vision." *J. Physiol.*, vol. 232, pp. 149-162, 1973.

[2] J. A. J. Roufs, "Dynamic properties of vision-IV. Thresholds of decremental flashes, incremental flashes and doublets in relation to flicker fusion." *Vision Res.*, vol. 14, pp. 831-851, 1974.

[3] B. G. Breitmeyer and L. Ganz, "Implications of sustained and transient channels for theories of visual pattern masking, saccadic suppression, and information processing." *Psychol. Review*, vol. 83, pp. 1-36, 1976.

[4] M. Green, "Masking by light and the sustained-transient dichotomy." *Perception and Psychophysics,* vol. 35 (6), pp. 519-539, 1984.

[5] J. A. J. Roufs and F. J . J . Blommaert, "Temporal impulse and step responses of the human eye obtained psychophysically by means of a drift-correcting perturbation technique." *Vision Res.,* vol. 21, pp. 1203-1221, 1981.

[6] F. J. J. Blommaert and J. A. J. Roufs, "Prediction of thresholds and latency on the basis of experimentally determined impulse responses." *Biol. Cyb.,* vol. 56, pp. 329-344, 1987.

[7] P. Berben, "The estimation of a state space model according to a weighted quadratic error function." ER Report, Eindhoven University of Technology, 1985.

[8] M. Gevers and G. Bastin, "What does system identification have to offer." *Proc. 6-th IFAC Symposium, Identification and System Parameter Estimation,* vol. I, pp. 77-84. Eds. G. A. Bekey and G. N. Saridis. Oxford: Pergamon, 1983.

[9] A. A. H. Damen, R. L. Moses, P. M. J. Van den Hof and Y. Tomita, "Bounds on the simulation power of equation error estimates." *Proc. 25-th IEEE Conf. on Decision and Control,* vol. 3, pp. 1646-1647, Athens, Greece, 1986.

[10] P. Van den Hof, "Approximate realization of noisy linear multivariable systems." *Journal A,* vol. 25, pp. 21-26, 1984.

[11] Numerical Algorithms Group Ltd., *Fortran Minimanual, Mark 9.* Oxford (UK): NAG Central Office, 1981.

[12] P. E. Gill and W. Murray, "Algorithms for the solution of the nonlinear least-squares problem." *SIAM J. Numer. Anal.,* vol. 15, no. 5, pp. 977-992, 1978.

[13] J. A. J. Roufs, H. A. L. Piceni and J. A. Pellegrino van Stuyvenberg, "Phase and gain analysis of the visual transient system." *IPO Annual Progress Report,* vol. 19, pp. 49-56, 1984.

[14] Y. Bard, *Nonlinear parameter estimation.* New York: Academic Press, 1974.

[15] J. R. Wolberg, *Prediction Analysis.* New York: D. Van Nostrand Co. Inc., 1967.

[16] H. de Lange, "Relationship between critical flicker frequency and a set of low-frequency characteristics of the eye." *J. Opt. Soc. Am.,* vol. 44, pp. 380-389, 1954.

[17] J. Krauskopf, "Discrimination and detection of changes in luminance." *Vision Res.,* vol. 20, pp. 671-677, 1980.

chapter 5

A comparison of results from parameter estimations of impulse responses of the transient visual system[1]

A.C. den Brinker

Abstract

Parameter estimations of a fourth-order linear model are applied to data from subthreshold measurements of impulse responses of the transient visual system. These impulse responses were obtained experimentally by several subjects, at two different background luminance levels and for different field sizes. The parameter estimations show consistent results over different subjects. For both different background levels and field sizes there are consequent changes in the estimated parameters. On the basis of these changes a proposal is made for a spatiotemporal model of the transient visual system.

5.1 Introduction

It is generally agreed that the human visual system processes stimuli in different parallel subsystems, called channels. In the temporal domain two channels are usually assumed: the *sustained* and the *transient* channel. The simplest model for a single channel is given in Figure 1, and consists of a linear filter L followed by an additive noise source N and a detection mechanism with threshold d. The linear filter characteristics depend on the (mean) background, the spatial dimension of the stimulus and surprisingly little on the subject, as will be shown.

By means of a perturbation technique it is possible to measure the impulse responses of the transient and sustained channel of the human visual system (Roufs and Blommaert, 1981). Such an experiment has been carried out by different subjects at different background levels (Roufs and Blommaert, 1981; Blommaert and Roufs, 1987) and for different field sizes. The results of these measurements show a triphasic impulse response for large field sizes (i.e. diameters larger than approximately 0.3 degree). This response is associated with the *transient* visual system (Roufs, 1974a; Roufs and Blommaert, 1981).

In this paper it is shown that these triphasic impulse responses can be adequately modelled as a fourth-order linear filter. In the Laplace domain this linear filter is described as a transfer function with two complex pole pairs, one zero
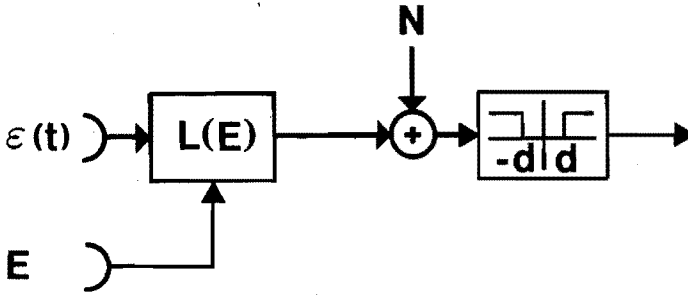
Figure 1: The model for the transient channel: a linear filter L, an additive noise source N, and a detection mechanism with threshold d.

and an amplification factor (chapter 4). In this article, the parameters and 90% confidence regions obtained by the estimation process described in chapter 4 are compared over the different experimental conditions under which the impulse response measurements were performed.

This comparison of estimated parameters (poles and zeros of the transfer function) of the linear filter might give information about the behaviour of the system with varying experimental conditions. In this way this analysis can give insight into the fundamental properties of the processing of visual stimuli, and might provide a link with the experimental results obtained by electrophysiology. As far as we know, this kind of research of systematic changes in parameters of a linear filter as a function of experimental conditions has not been performed before, except in more general terms, where characteristic quantities (cut-off frequency, sensitivity) have been experimentally determined as a function of background (Kelly, 1961; Roufs, 1972) and spatial dimension (Roufs and Bouma, 1980).

The estimated parameters show that there are relatively small intersubject variations of their values if the same background and the same spatial configuration of the stimulus are used. Over different background levels there is a consistent change in the measured impulse response. The measured impulse responses seem to be isomorphic (Roufs 1974a; Roufs and Blommaert, 1981). The change of the measured impulse response is reflected in a change of the estimated parameters of the fourth-order linear filter. From the fourth-order linear filter estimates it is found that for the largest part there is indeed a change in time scale. As a second minor effect a change in the lowpass behaviour occurs. Together this means that the impulse responses at different levels are indeed approximately isomorphic, though not precisely as Roufs (1974a) assumed.

Variation of the field size (for one subject and one background level) results in a change of the measured impulse response. These changes are reflected in the parameters of the estimated filter. It will be shown that only part of the estimated parameters vary with a change in spatial configuration. This implies that it is

possible to isolate the lateral and the afferent information spread contained in these impulse responses. On the basis of this finding a simple *spatiotemporal* model for the transient visual system is proposed.

In the last part of the article we will show that the impulse response data and the analysis of the behaviour of the parameters of the linear filter are in agreement with other experimental findings, most notably the measurements of the sensitivity versus the frequency of a sinusoid, the so-called De Lange curves.

5.2 Measurement data, the description of the fourth-order linear filter and evaluation of the fit

Available experimentally obtained impulse responses

The experimentally obtained impulse responses that are available and considered here are:
- impulse responses of seven subjects at a 1200 Td level for a 1 degree field,
- impulse responses of three subjects at a 100 Td level for a 1 degree field,
- impulse responses of two subjects at a 1200 Td level for different field diameters.

How these impulse responses are derived experimentally is not an issue in this paper (see Roufs and Blommaert, 1981). The measured impulse responses are estimated as a fourth-order linear filter with a transfer function described by two complex pole pairs and one zero. The parameter estimation technique is described elsewhere (chapter 4), and extended by estimates of the 90% confidence regions of the parameters. The estimates of the confidence region are only appropriate if the objective function in the optimization problem is (approximately) quadratic within these regions. In all cases a check was made on this assumption. In this paper we will concentrate on the results of these parameter estimations. In cases where estimated parameters are compared over different experimental conditions, and parameter shifts are supposed to result from the changed experimental conditions, support for this reasoning will be sought from the estimates of the confidence regions, insofar as these could be estimated.

The transfer function of the linear filter

As a linear model for the transient system a fourth-order filter is used, with transfer function $H(s)$ in the Laplace domain s. The transfer is given in threshold units d (see Fig. 1). The characteristics of the filter are described by its parameters (p_1, p_2, z, A, NF) according to

$$H(s) = NF \frac{A(s-z)}{(s-p_1)(s-p_1^*)(s-p_2)(s-p_2^*)}, \qquad (1)$$

where
NF	$=$	norm factor
A	$=$	an amplification factor
z	$=$	a zero of the transfer function
p_1, p_2	$=$	complex poles of the transfer function
*	$=$	the conjugate of a complex number.

The impulse response $h(t)$ can be calculated from $H(s)$ as

$$h(t) = NF \cdot A \sum_{i=1}^{2} \left\{ R_i \exp\{p_i t\} + R_i^* \exp\{p_i^* t\} \right\}, \qquad (2)$$

where R_i are the (complex valued) residues given by

$$R_1 = \frac{p_1 - z}{(p_1 - p_1^*)(p_1 - p_2)(p_1 - p_2^*)}, \qquad (3)$$

$$R_2 = \frac{p_2 - z}{(p_2 - p_1)(p_2 - p_1^*)(p_2 - p_2^*)}. \qquad (4)$$

Some examples of measured and estimated normalized impulse responses are shown in Figure 4 and will be discussed later. All estimated impulse responses mentioned in this article and not shown in Figure 4 can be found in chapter 4. As a result of the measurement technique the measured impulse response is basically scaled to an extremum equal to one, the absolute value being obtained separately. The amplification factor A is such that the fitted curve $H(s)/NF$ has an extremum exactly equal to one.

The filter $H(s)$ given by (1) is the transform of an impulse response that consists of a sum of damped sinusoids (2). If this description is to supply insight into the processing within the transient channel, it presupposes that different subsystems within this channel can *approximately* be described by impulse responses that are damped sinusoids. Conceptually, this is not unlikely: many physiological experiments and models describe feedback mechanisms (e.g., adaptive models; Shapley and Enroth-Cugell, 1984). Such mechanisms often show these oscillatory responses as a direct consequence of the feedback loop. In actual measurements of single neurons mostly biphasic impulse responses are found (e.g., Naka, 1982; Daly and Normann, 1985). If the real part of the poles is not too small with respect to its imaginary part, the impulse response associated with a complex conjugated pole pair can be considered as an approximation to these responses. From this point of view the filter (1) may not only provide descriptive formula of the impulse response, but may also be able to reveal the underlying properties of the temporal processing.

Estimated and measured noise

Given the experimental uncertainty the fits agree reasonably well with the measurements. This is shown numerically in Table 1. Here we have compared the

mean measured and the estimated noise given by the standard deviations. The mean measured standard deviation s_m is taken as

$$s_m^2 = \frac{1}{M} \sum_{i=1}^{M} s^2(t_i), \tag{5}$$

where
M = the number of samples,
t_i = the sampling moments of the impulse response, $1 \leq i \leq M$,
$s(t_i)$ = the measured standard deviation of the mean at t_i.

For the estimated standard deviation s_e we find (Bard, 1974; Wolberg, 1967)

$$s_e^2 = \frac{\Psi}{M - N}, \tag{6}$$

where
Ψ = sum of squared residuals at the final estimate,
M = number of measured samples,
N = number of free variables in the estimation process,
$\quad\quad N = 5$ (see chapter 4).

Table 1 shows that the estimated standard deviation is in most cases greater than the measured standard deviation. Some of the fits, notably FB and JW, are not adequately represented by the fourth-order filter. Probably a higher order filter would be better. However, averaged over different subjects the estimated standard deviation s_e is only about 8% larger than the measured standard deviation s_m. Therefore we argue that in most cases a fourth-order filter is a sufficiently elaborate model to represent the measured impulse responses. Furthermore we will show that, even in cases of poorer fits, the estimated fourth-order linear filters are similar to those estimated for other subjects under the same experimental conditions.

Apart from the above-mentioned estimations we also fitted the same fourth-order filter (1) with a bandpass restriction, i.e. $z = 0$. In the fits of the data to a bandpass filter only the complex pole pairs acted as degrees of freedom in the estimation process. The results of the bandpass estimates show that the fits to this model are not as good as those with z as a free parameter. Not only is the estimated standard deviation σ_b in all cases greater then σ_e (see Table 1), but also that these fits always overestimated the first (negative) phase. The reason for estimating a bandpass filter for the transient system is that in contrast to usual assumptions about the transient system (Roufs, 1974a), our model (given by eq.(1)) has spurious sustained activity; its response to a step function shows a large response at the onset, but also a small steady response for long durations after onset.

5.3 Intersubject variations of estimated parameters

First the intersubject variations of the estimation results for a 1 degree field without surround will be considered. The estimated parameters for seven subjects at

	back-ground (Td)	field size (deg)	s_m	s_e	s_b
JR74	1200	1	.120	.144	.157
JAJR	1200	1	.086	.099	.111
FB	1200	1	.074	.127	.—
JP	1200	1	.112	.131	.139
LT	1200	1	.139	.115	.131
HD	1200	1	.118	.143	.144
IH	1200	1	.106	.154	.156
LT	100	1	.109	.096	.180
HR	100	1	.113	.116	.217
JW	100	1	.170	.247	.252
HD	1200	0.28	.168	.145	.219
HD	1200	1.00	.118	.143	.144
HD	1200	5.50	.124	.111	.179
IH	1200	0.28	.153	.087	.106
IH	1200	0.50	.152	.126	.128
IH	1200	1.00	.106	.154	.156
IH	1200	5.50	.093	.078	.148

Table 1: Measured standard deviation s_m and the calculated standard deviation of the noise. The estimated noise for a model according to (1) is denoted by s_e; for the same model but now with $z = 0$ (a bandpass filter) the noise is denoted as s_b.

a 1200 Td background level and three subjects at 100 Td are shown in Table 2. The first columns contain the estimated parameters p_1, p_2 and z. The complex values p_1 and p_2 are split up into two real valued parameters:

$$p_i = \alpha_i + j\,\beta_i, \qquad\qquad i = 1,2 \qquad\qquad (7)$$

where $j = \sqrt{-1}$ and α_i, $\beta_i \in \Re$ $(i = 1, 2)$. α_i is the i-th damping parameter and β_i the i-th (radian) frequency parameter. The pole p_1 is the pole with the largest norm. The last two columns contain the amplification A and the norm factor NF. The amplification A was not a free parameter in the estimation process but was calculated to obtain an extremum of the impulse response equal to one (chapter 4). The norm factor NF gives the experimentally measured sensivity of the system to an impulse, and is expressed in units $Td^{-1}s^{-1}$. Together the parameters in Table 2 describe the system in threshold units d. The impulse response $h(t)$ can now be

given in these damping and frequency parameters by

$$h(t) = NF \cdot A \sum_{i=1}^{2} B_i \exp\{\alpha_i T\} \cos(\beta_i t + \phi_i) \tag{8}$$

where $B_i = 2 R_i \exp\{-j\phi_i\}$.

	α_1 (s^{-1})	β_1 (rad/s)	α_2 (s^{-1})	β_2 (rad/s)	z (s^{-1})	A (10^4s^{-2})	NF (Td^{-1}s^{-1})
JR74	-25.0	83.6	-15.4	42.1	6.87	-.946	0.68
JAJR	-27.6	93.8	-15.4	46.5	13.6	-1.07	0.90
FB	-20.5	101.	-12.9	54.1	19.2	-.874	1.2
JP	-22.5	94.1	-18.8	44.8	13.2	-1.04	1.09
LT	-20.4	94.3	-20.2	54.0	20.2	-.935	0.59
HD	-23.3	99.8	-19.3	51.8	11.8	-1.13	0.44
IH	-19.8	103.	-22.0	50.2	53.8	-.833	1.01
LT	-16.6	56.1	-20.8	26.6	20.1	-2.11	3.86
HR	-13.0	58.5	-14.1	28.0	32.9	-3.47	7.46
JW	-10.1	58.1	-11.8	28.8	17.8	-3.38	4.59

Table 2: Estimated parameters of the fourth-order linear filter for six subjects at a 1200 Td level and three subjects at a 100 Td level (upper and lower part of the table respectively). In all cases the stimulus diameter is 1 degree.

From Table 2 we see that the variation of the estimates over the different subjects is relatively small, given a specific background level. This is also shown in Figs. 2A and 2B. In Fig. 2A the estimated poles and zeros of seven subjects at the 1200 Td level are shown, in Fig. 2B the estimated poles for three subjects at 100 Td. From these plots it can be seen that there are only minor variations between subjects if identical spatial configuration and background level are used. All parameters p_1, p_2 and z cluster, at both 1200 (Fig. 2A) and 100 Td background (Fig. 2B). At 1200 Td there is one zero (for subject IH, see Table 2) which has an exceptional location with respect to the cluster formed by the other zeros. But then, this zero has a large variance as can be seen from the 90% confidence intervals shown in Fig. 5B (this figure will be discussed later).

Comparing Figs. 2A and 2B we see that a change in background level shows a much larger change in the estimated parameters than the intersubject variation at one level.
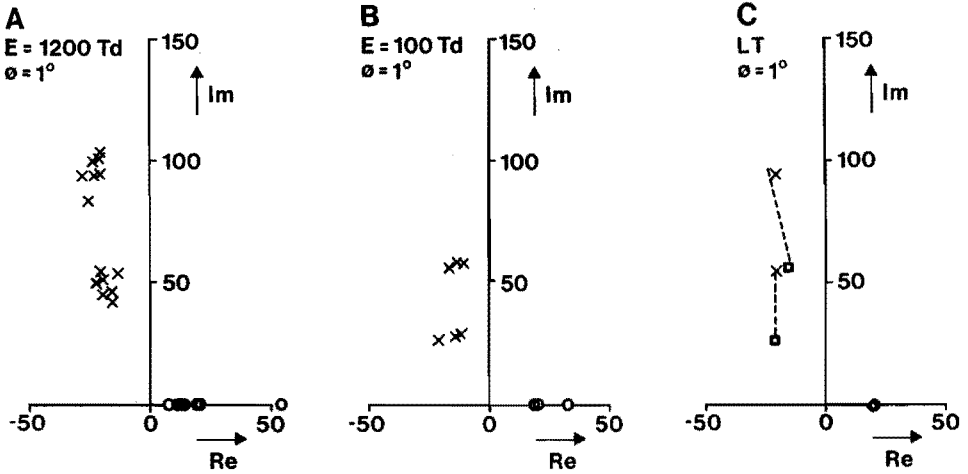
Figure 2: Pole-zero plots in the complex plane. Horizontal and vertical axes are the real and imaginary axes, respectively. The units are in s^{-1}. The lower part of the s-plane is not shown in this plot. **A.** Estimated parameters of all impulse responses at 1200 Td. The crosses and circles are the poles and zeros, respectively. **B.** Estimated parameters of all impulse responses at 100 Td. The crosses and circles are the poles and zeros, respectively. **C.** Estimated parameters of subject LT at 100 and 1200 Td. The crosses and circle are the poles and zero respectively, at 1200 Td. The squares and diamond are the poles and zero respectively, at 100 Td. The dotted lines give the direction of the movement of the poles p_1 and p_2 with variation in background (see text).

5.4 Changes in estimated parameters with background

In section 3 it was shown that at one background level for a certain spatial config-uration (1 degree field) the estimated parameters for different subjects have only minor variations. We now try to establish invariances over the two background conditions that were used in the experiments.

First we will argue that the zero z is nearly independent of the background. From Table 2 it can be seen that this parameter for different subjects lies roughly between 10 and 25 s^{-1} for both levels (except for IH). But, more important, the results for subject LT, from whom impulse responses at both levels are available, show an estimated zero that is nearly identical at both levels. A similar argument holds for the damping parameter α_2. This is also illustrated in Fig. 2C where the estimated poles and zeros of subject LT at both levels are simultaneously plotted.

As a second source of information on invariances over both background lev-els, we look at the *relative location* of these parameters in the s-plane, i.e. we

ignore the absolute values of the parameters, but consider the *ratio* of the different parameters.

This is tabulated in Table 3. The two last columns give the ratio $-\alpha_1/\beta_1$ and $-\alpha_2/\beta_2$. This ratio is a measure of the direction of these poles in the s-plane. In columns three and four the ratios α_1/α_2 and β_1/β_2 can be found, which relate the location of pole p_1 to pole p_2. The mean values of the relative location of the poles have also been calculated and are shown in Table 3. This averaging of estimated parameters over different subjects seems allowed, since the intersubject variations over one level are small in comparison to the variation of the parameters with background. However, we have to observe the necessary caution, since at the 100 Td level only three parameter sets are available, where one parameter set (JW) is derived from a data set which is rather noisy, and where the fit is not as good as one would like (see Table 1).

	back-ground	α_1/α_2	β_1/β_2	$-\alpha_1/\beta_1$	$-\alpha_2/\beta_2$
JR74	1200	1.63	1.99	.299	.365
JAJR	1200	1.80	2.02	.294	.330
FB	1200	1.58	1.87	.202	.239
JP	1200	1.20	2.10	.239	.418
LT	1200	1.01	1.75	.216	.374
HD	1200	1.21	1.92	.234	.373
IH	1200	0.90	2.06	.191	.438
mean	1200	1.33	1.96	.239	.362
LT	100	.796	2.11	.295	.782
HR	100	.923	2.09	.221	.501
JW	100	.858	2.01	.174	.409
mean	100	.857	2.07	.230	.564

Table 3: The relative location in the s-plane of the estimated parameters of the fourth-order linear filter. Six subjects at 1200 Td and three subjects at a 100 Td background level. In all cases the stimulus diameter is 1 degree.

From Table 3 it can be seen that the (mean) ratio of the imaginary parts of the two poles is nearly independent of the background level, and so is the ratio of the real and imaginary parts of pole p_1. This means that α_1, β_1 and β_2 change by an equal amount if the background level is changed from 100 Td to 1200 Td. The ratio α_1/α_2 and $-\alpha_2/\beta_2$ changes with background, so it appears that this parameter α_2 does not change by an equal amount as do the parameters α_1, β_1 and β_2. Indeed, this should be the case if α_2 is independent of the background level, as was argued before.

In Figure 2C all invariances in the parameters over the two background levels are illustrated in the pole-zero plots of subject LT at 100 and 1200 Td. The relative location of p_1 is approximately constant: for the two background levels the poles p_1 are (roughly) located on a straight line through the origin. For subject LT the ratio of the frequencies β_1 at 1200 and 100 Td and idem for β_2 is in the mean about 1.8. In Figure 3 the estimated impulse response of LT is plotted together with the estimated impulse response of LT at 100 Td with a time axis scaling for this last response by the same factor (1.8) as is found for the ratio of the estimated frequencies. From this we see that the responses of the transient system at different levels are nearly isomorphic with a small change in lowpass behaviour: the first negative phase is broader and slightly deeper, and the second negative phase is deeper for the higher background condition.
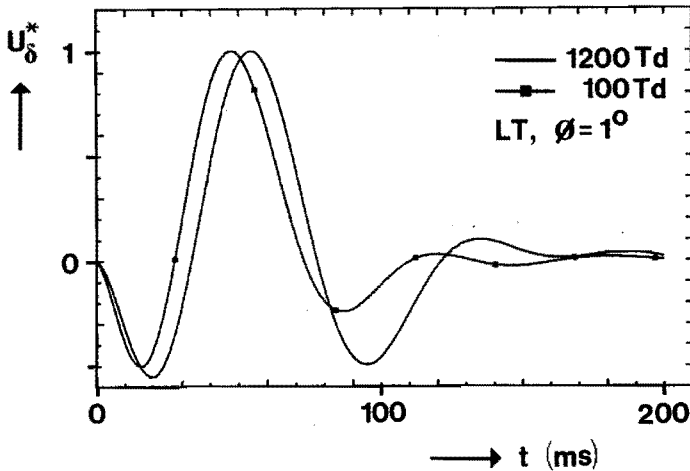
Figure 3: The estimated impulse responses of subject LT for a 1 degree field at 100 and 1200 Td. The time axis of the 100 Td impulse response is scaled with a factor 1.8 (see text).

In this way a comparison of results from parameter estimations of impulse responses can give insight into the changes in the parameters of the linear filter. It appears that this change in the parameters of the linear filter can be described by one multiplication factor only. This, however, has been established only for a change of background level from 100 to 1200 Td. On the other hand, the shift in the parameters may well reflect the general change of the parameters of the linear filter for any change in background level.

5.5 Changes in estimated parameters with variation of field size

The data that are available for different field sizes consist of impulse responses of two different subjects at 1200 Td. Subject HD measured three impulse responses for field diameters of 0.28, 1 and 5.5 degrees. From subject IH we have four impulse responses for field sizes of 0.28, 0.50, 1.0 and 5.5 degrees. The impulse response data and estimates are shown in Figure 4. All these impulse responses are triphasic, and as a general trend it can be seen that for larger field sizes the impulse responses become slightly faster.
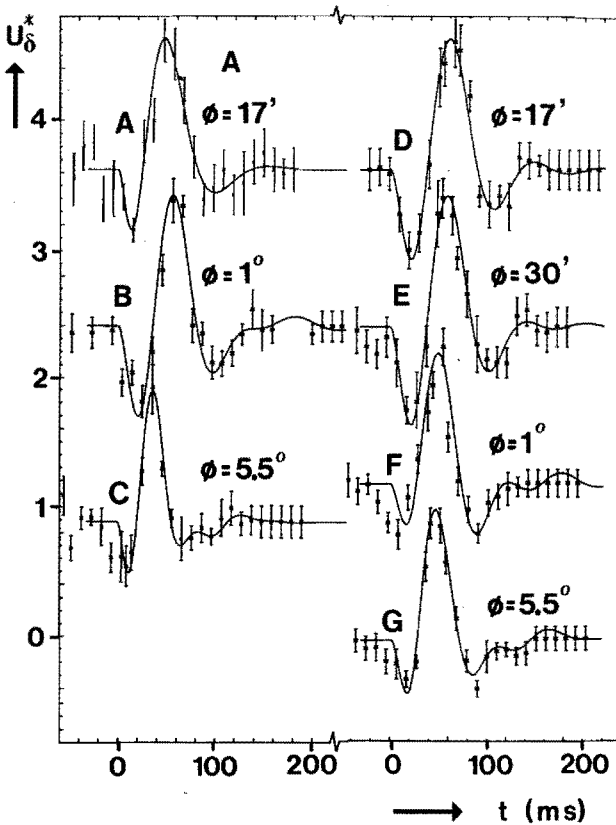

Figure 4: Measured and estimated normalized impulse responses U_δ^* at 1200 Td for HD (Figs. A, B and C are for field sizes 0.28, 1.0 and 5.5 degrees resp.) and IH (Figs. D, E, F and G are for field sizes 0.28, 0.50, 1.0 and 5.5 degrees resp.). For presentation purposes, all the figures except G are shifted along the vertical axis.

The estimated parameters are shown in Table 4. The estimated parameters of subject HD for a field with a diameter of 0.28 degrees were extremely unreliable. It was not possible to obtain variances and covariances of the estimated parameters. The results of the estimation process of the two subjects are also shown in Fig. 5 as confidence regions of the parameters in the *s*-plane. From Table 4 we see that the pole p_2 with the smallest norm is estimated to be almost equal over these field sizes for each subject. This is also reflected in Fig. 5, since the estimated (co-)variance regions of the pole p_2 all overlap. The other parameters vary with the field diameter. The pole p_1 moves approximately on a straight line parallel to the imaginary axis; the estimated frequency parameter β_1 decreases with decreasing field size. From Table 4 and Fig. 5 it can be seen that there is also a change in the parameter z with field size. This change in z is not as easily portrayed as is the case with β since there seems to be no monotonous relation between this parameter and field size.
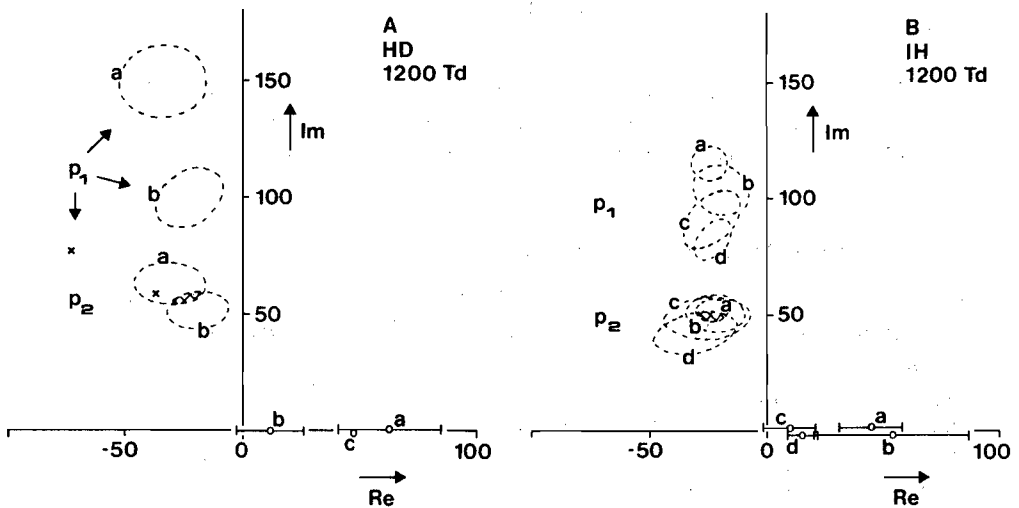
Figure 5: Pole-zero plots in the complex plane. Horizontal and vertical axes are the real and imaginary axes, respectively. The units are in s^{-1}. The lower part of the *s*-plane is not shown in this plot. The ellipses give estimates of the 90% confidence regions of the poles. The estimated poles are located in the centres of the ellipses. The zeros are indicated by a small circle and the bars give the 90% confidence intervals. **A.** Subject HD, 5.5 (a), 1 (b) and 0.28 (c) degrees field. **B.** Subject IH, 5.5 (a), 1 (b), 0.50 (c) and 0.28 (d) degrees field. For subject HD and a 0.28 degree field it was not possible to estimate reliable confidence regions; in this case the poles are given by crosses and the zero is indicated by a small circle denoted c.

The conclusion we draw from this is that only part of the behaviour of the

processing in the transient system is dependent on the spatial configuration of the stimulus. More specifically: the part of the processing of a linear filter that has spatiotemporal properties is reflected in the parameters $p_1 = \alpha_1 + j\,\beta_1$ and z.

	diam. ($^\circ$)	α_1 (s^{-1})	β_1 (rad/s)	α_2 (s^{-1})	β_2 (rad/s)	z (s^{-1})	A ($10^4 s^{-2}$)	NF ($Td^{-1}s^{-1}$)
HD	0.28	-72.9	77.3	-36.9	58.6	47.7	-2.36	0.15
HD	1.00	-23.3	99.8	-19.3	51.8	11.8	-1.13	0.44
HD	5.50	-34.6	150.	-31.0	62.9	63.1	-2.01	1.01
IH	0.28	-23.5	82.7	-31.4	42.5	15.3	-1.19	0.21
IH	0.50	-23.8	91.2	-25.9	48.4	9.64	-1.23	0.38
IH	1.00	-19.8	103.	-22.0	50.2	53.8	-.833	1.01
IH	5.50	-24.5	115.	-23.2	51.9	44.8	-1.17	2.07

Table 4: Estimated parameters of the fourth-order linear filter. Subject HD at 1200 Td and stimulus diameter 0.28, 1 and 5.5 degrees. Subject IH at 1200 Td and stimulus diameter 0.28, 0.50, 1.0 and 5.5 degrees.

5.6 Relation with other experimental data

We want to compare the results we obtained from the analysis of the shifts in the parameters of the fourth-order linear filter with other psychophysical data. An obvious choice is to look at the De Lange curves that have been given in the literature many times. However, we do have to make several remarks. The first is that we do not have the De Lange curves for the same subjects as those for whom the impulse responses were measured. Second, the amplitude spectrum of the Fourier transform of the estimated impulse response *cannot* be compared directly with a De Lange curve. In measuring a De Lange curve the experiment necessarily incorporates a stochastic effect. The detection of a sinusoid that is slowly switched on and off has a probability of being seen at each peak of the sinusoid. This will cause a lowering of the threshold because of 'probability summation' (Roufs, 1974b; Quick, 1974). To account for the probability summation the noise of the system has to be modelled, and the exact circumstances of the De Lange measurement have to be known. Furthermore, the De Lange characteristic will be an envelope of the frequency characteristics of the sustained and transient channel operating in parallel. The transient system is the highest tuned filter, so the high frequency side of the De Lange curve should be comparable with the amplitude spectrum of the Fourier transform of the estimated impulse response, after correction for the probability summation. Because of the above remarks the comparison of the estimated filters with the De Lange curve can be qualitative only.

It is well known (Kelly, 1971; Roufs, 1972) that the De Lange curves change to a higher peak and cut-off frequency at higher luminance levels. In Figure 6A several De Lange curves are shown with the background level as parameter (from Roufs, 1972). The same behaviour is found in our estimates too. Figure 6B shows the amplitude gain spectrum of the Fourier transform of the impulse responses of LT at 100 Td and 1200 Td. The vertical axis is not arbitrary but scaled according to the sensitivity (the norm factor NF) of the transient system to an impulse for both levels. An increase in background level results in a lower sensitivity, a higher peak frequency and a higher cut-off frequency in both Figure 6A and 6B.
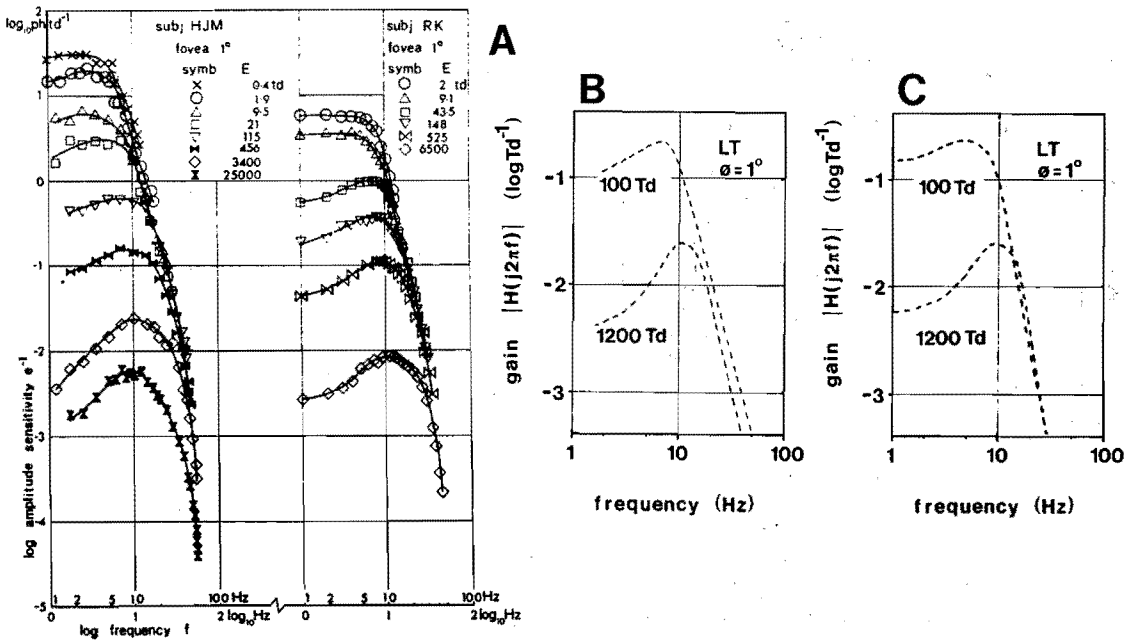
Figure 6: **A.** De Lange curves at different background levels for two subjects. Reprinted with permission from Vision Research 12, J.A.J. Roufs, Dynamic properties of vision.-I. Copyright 1972 Pergamon Journals Ltd. **B.** Amplitude spectrum of the Fourier transform of the impulse responses of LT at 100 Td and 1200 Td. The vertical axis is not arbitrary but scaled according to the sensitivity of the transient system to an impulse at these two levels. **C.** The amplitude spectra of the estimated impulse responses of subject LT (1 degree field) at 100 and 1200 Td. The spectra of the estimated impulse responses (Fig. 6) are both multiplied by the amplitude transfer function of a second-order filter (see text).

Except for the low frequency side, which we cannot compare with the simu-

lations from our model, as argued before, the effect of the variation of the field size on the De Lange curve is similar to the effect of the changing parameters of the impulse response as we have found (see Figure 7). An increase in field size changes the temporal characteristics to a higher sensitivity, a higher peak and a higher cut-off frequency (Roufs and Bouma, 1980). This is the same as is found in our analysis: the parameter p_1 changes to a higher norm, the impulse response is faster (see Figure 4) and the measured sensitivity to an impulse response is higher for more extended fields (see norm factors NF in Table 4).
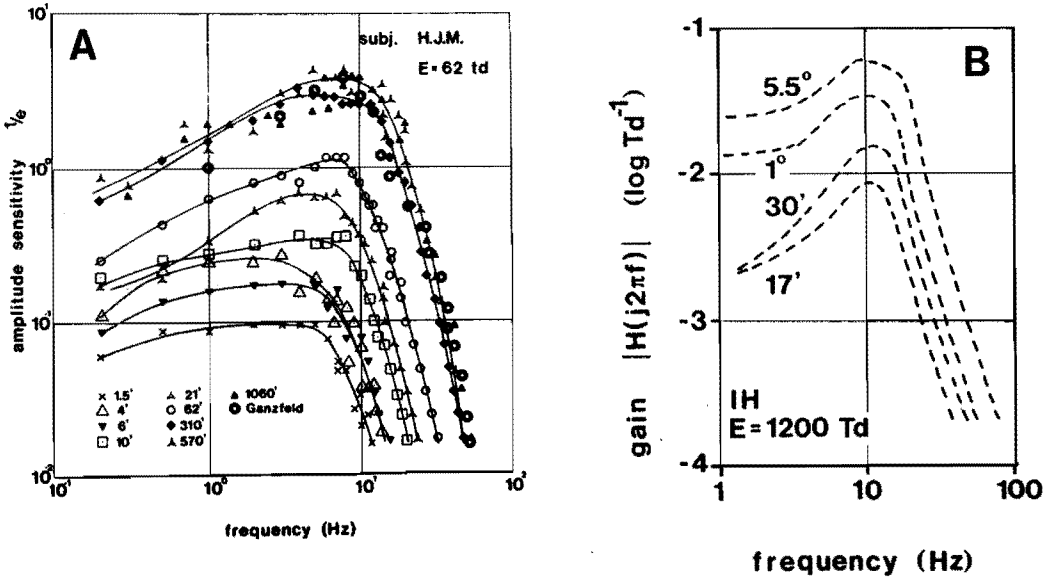

Figure 7: **A.** De Lange curves for different field diameters at a background of 62 Td, from Roufs and Bouma, 1980. Permission for reprint, courtesy Society of Information Display. **B.** Amplitude spectrum of the Fourier transforms of the estimated impulse responses of HD at 1200 Td for three different field sizes: from bottom to top 17', 1°, 5.5°. The vertical axis is not arbitrary but scaled according to the sensitivity of the transient system to an impulse for these field sizes at 1200 Td.

There is a qualitative difference between the amplitude spectrum of the proposed linear filter and the De Lange curves. The slope for high frequencies of the De Lange curves is steeper than the slope (0.9 log units/octave) in the linear model (1). Another difference between the De Lange curves and the calculated Fourier transforms at different background levels is that the high frequency asymptotes of the De Lange curves coincide. In the Fourier transform there is a difference in height of about 0.5 log units between the high frequency asymptotes for the 100 and 1200 Td levels. There are several reasons why a steeper slope was not incor-

porated in our model. First of all the impulse response to which the linear filter is fitted is adequately described by the fourth-order filter. To take more parameters into account would be contradictory to the parsimony principle. Furthermore it would probably mean introducing ill-conditioned parameters in our estimation process.

However there is a simple way of changing the linear filter (1) such that it fits the De Lange curves. In Figure 6C the Fourier transforms from Figure 6B are multiplied by a second-order process,

$$G(s) = \frac{p_3^2}{(s - p_3)^2}. \tag{9}$$

For the 1200 Td level we took $p_3 = 100$ s^{-1} and for the 100 Td level we scaled p_3 down by the same factor as in p_1, namely 1.8 (see Section 4). The value of the pole p_3 is not critical at all. It should be somewhere above the peak of the Fourier transforms of Figure 6B. Consequently, the two curves coincide for high frequencies (see Figure 6C). The high frequency fall-off in Figure 8 is now the same as was found experimentally, about 1.5 log units/octave (Kelly, 1971; Roufs, 1972). The estimated impulse response will hardly change after introducing this extra second-order process, since only the high frequency end (above the cut-off frequency) of the gain characteristic is modified. In the time domain the impulse response $g(t)$ of this extra filter is given by

$$g(t) = \mathcal{L}^{-1}\{G(s)\} = p_3^2 t \exp\{p_3 t\}, \tag{10}$$

where $\mathcal{L}^{-1}$ denotes the inverse Laplace transform.

Other experimental data that are consistent with the estimated impulse responses are threshold measurements of pulses with variable duration (Blommaert and Roufs, 1987) and the experimentally determined phase characteristic. The phase characteristic has been measured by a subthreshold summation technique and showed a linear phase relation for a 1 degree field at 1200 Td for frequencies from 1 to 25 Hz (Roufs e.a., 1984). The estimated parameters of the fourth-order filters are such that they give an approximately linear phase for that frequency range (see Appendix).

In conclusion we can state that the effects of background and field size variation are qualitatively the same in De Lange curves, impulse response measurements and in the estimated parameters of the fourth-order linear model. From the estimated parameters of our model we see that the effect of an increase in background level and an increase in field sizes has quite a different effect on the estimated parameters.

5.7 Discussion

In Section 2 our choice for the model was given. It was hoped that the filter (1) would give a good description of the available data, but also that it would allow

us to obtain insight into the temporal processing within the transient channel. However, the choice was also founded on its common usuage in engineering and its convenient mathematical formulation. It does not rule out the possibility that filters other then (1) can provide descriptions of the experimental data that are equally well, nor do we think that the observed shifts in the parameters is exclusively reserved to the choice of damped sinusoids as fundamental functions.

We have shown that the subthreshold measurements of the impulse response of the transient visual system can be adequately modelled in a fourth-order linear filter with two complex pole pairs and one zero in its transfer function. From this representation of the measured impulse responses predictions of the response of the system can be made for other stimuli (Blommaert and Roufs, 1987). But more important is that these fourth-order filters give insight into the processing of stimuli in the transient channel of the visual system for different mean luminance levels and different spatial configurations.

On the basis of the systematic parameter changes, we are able to propose a model for the transient system which provides an approach towards a description of the spatiotemporal processing. The model is shown in Figure 8, and is spatiotemporal in nature. It consists of two processing stages. The first step is a linear spatiotemporal filter L_1. This filter is not only dependent on the mean luminance E, but also on the spatial configuration, which we describe by its spatial frequency w. This is denoted as

$$L_1 = L_1(E, w). \qquad (11)$$

For the parameter p_1 which describes this filter L_1 the shift in the parameter caused by background variation and by field size variation can be separated, at least in a first-order approximation:

$$p_1(w, E) = \hat{p}_1(w)\, f(E), \qquad (12)$$

where $f(E)$ is a real valued function of the mean luminance E, and $\hat{p}_1$ is the value of p_1 for $f(E) = 1$. The separability of the effect of the mean luminance and field size was shown in our analysis for a 1 degree field only. However, such separability will probably exist for field sizes near 1 degree, where the transient activity is dominant and which is, therefore, very attractive from a modelling point of view.

The parameter z, the position of the zero, changes with field size, so this parameter should be incorporated in the spatiotemporal filter L_1. The complicating factor for this parameter is that there is no monotonous change with field size, as was observed for p_1.

The second step is a purely temporal linear filter L_2. In the transfer function (eq. (1)) this filter is reflected in the pole p_2, the pole with smallest norm. This pole is dependent on the mean luminance only. We denote the dependence as
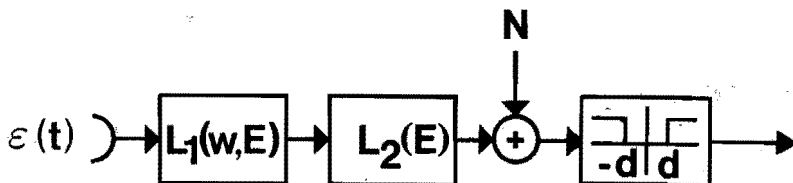
$$L_2 = L_2(E), \qquad (13)$$

Figure 8: Proposal for a spatiotemporal model, based on analysis of changes in estimated parameters from a fourth-order model that is fitted to subthreshold measurements of impulse responses. The filter L_1 is dependent on both mean luminance E and spatial characteristics of the stimulus, while the filter L_2 is dependent on the mean luminance only. The spatial dependence is denoted by w, the spatial frequency of the stimulus. The last stage is formed by a detector with threshold d.

where the mean luminance level is given by E.

The refinement of the fourth-order model, i.e. the introduction of a third stage characterized by p_3, can be easily incorporated in Figure 8. It was shown that p_3 changes with background level in the same way as p_1. Whether and how p_3 should change with field diameter, and consequently whether it belongs to L_1 or L_2, is something as yet to be explored.

For the spatiotemporal filter L_1 it is possible to construct a distributed electrical network as has been done in several studies for the electrical coupling between retinal cells (Bennet, 1977; Torre *et al.*, 1983). It was found that pole p_1 changes in such a way with field size that for larger fields the filter L_1 has a 'faster' impulse response. This corroborates the physiological findings of Detwiler *et al.* (1980), who found this for the rods in the retina of the snapping turtle. Possibly the filter L_1 is located in the retina. We hope to explore the possibilities of translating the foregoing behaviour of the poles and zeros with spatial extension into the behaviour of a linear distributed electrical network elsewhere (chapter 6).

In conclusion, we have analysed the behaviour of poles and zeros of linear filters that were fitted to impulse responses obtained under different experimental conditions. On the basis of the shifts that are observed in the poles and zeros upon a change in experimental conditions it is possible to obtain insight into the operation of the transient visual system. From our analysis a spatiotemporal model for the transient system evolved (Fig. 8). The main features of this model are linearity, simplicity and parsimonious use of parameters. Also it was shown that changes in background level and spatial extension of the stimulus have strikingly different effects on the parameters of the model, and that these two effects are probably separable. The model is in agreement with physiological data. As a consequence of

the simplicity of the model, it is suitable for detailing. This was shown by making a small modification such that the model matches the De Lange curves.

Acknowledgements

References

Bard Y. (1974) Nonlinear parameter estimation. New York: Academic Press.

Bennet M.V.L. (1977) Electrical transmission: a functional analysis and comparison to chemical transmission. In: Bethseda M.D., Handbook of Physiology. American Physiological Society.

Blommaert F.J.J., Roufs J.A.J. (1987) Prediction of thresholds and latency on the basis of experimentally determined impulse responses. Biol. Cyb. **56**, 329-344.

Daly S.J., Normann R.A. (1985) Temporal information processing in cones: effects of light adaptation on temporal summation and modulation. Vision Res. **25**, 1197-1206.

Detwiler P.B., Hodgkin A.L., McNaughton P.A. (1980) Temporal and spatial characteristics of the voltage response of rods in the retina of the snapping turtle. J. Physiol. **300**, 213-250.

Kelly D.H. (1961) Visual responses to time-dependent stimuli. I. Amplitude sensitivity measurements. J. Opt. Soc. Am. **51**, 422-429.

Kelly D.H. (1971) Theory of flicker and transient responses, I. Uniform fields. J. Opt. Soc. Am. **61**, 537-546.

Naka K.-I. (1982) The cells horizontal cells talk to. Vision Res. **22**, 653-660.

Quick R.F. (1974) A vector magnitude model of contrast detection. Kybernetik **16**, 65-67.

Roufs J.A.J. (1972) Dynamic properties of vision.-I. Experimental relationship between flicker and flash thresholds. Vision Research **12**, 261-278.

Roufs J.A.J. (1974a) Dynamic properties of vision.-IV. Thresholds of decremental flashes, incremental flashes and doublets in relation to flicker fusion. Vision Research **14**, 831-851.

Roufs J.A.J. (1974b) Dynamic properties of vision.-VI. Stochastic threshold fluctuations and their effect on flash-to-flicker sensitivity ratio. Vision Research **14**, 871-888.

Roufs J.A.J., Blommaert F.J.J. (1981) Temporal impulse and step responses of the human eye obtained psychophysically by means of a drift-corrected perturbation technique. Vision Research **21**, 1203-1221.

Roufs J.A.J., Bouma H. (1980) Towards linking perception research and image quality. Proc. SID **21**, 247-269.

Roufs J.A.J., Pellegrino van Stuyvenberg J.A., Piceni H.A.L. (1984) Phase and gain analysis of subthreshold-flicker and flash responses. Perception **13**, A15.

Shapley R.S., Enroth-Cugell C. (1984) Visual adaptation and retinal gain control. In: Osborne, N.N. and Chader, G.J. (Eds), Progress in Retinal Research Vol. 3. Oxford: Pergamon Press.

Torre V., Owen G., Sandini G. (1983) The dynamics of electrically interacting cells. IEEE Transac. Systems, Man and Cybernetics **SMC-13**, 757-765.

Wolberg J.R. (1967) Prediction Analysis. New York: D. Van Nostrand Co. Inc..

Appendix. Approximation of a linear phase characteristic
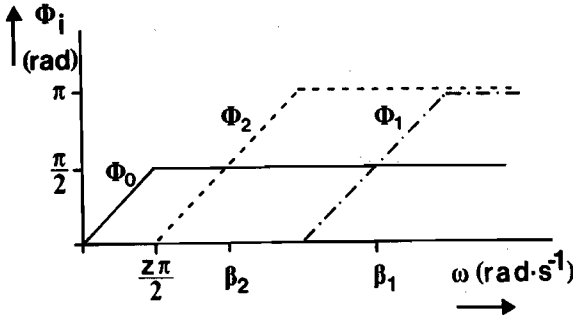
Figure 9: The phases ϕ_i ($i = 0, 1, 2$) of the fourth-order filter approximated by linear pieces (see text).

Consider the fourth-order filter given by (1). The zero z is assumed to be located in the right-half plane, the amplification factor A is assumed to be negative (see Table 2). We define the phase ϕ by

$$H(j\omega) = |H(j\omega)| \exp\{j\phi(\omega)\}.$$

The phase ϕ is split into three parts:

$$\phi = -\phi_0 - \phi_1 - \phi_2,$$

where

$$\phi_0 = \arctan\left(\frac{\omega}{z}\right),$$

$$\phi_1 = \arctan\left(\frac{\omega - \beta_1}{-\alpha_1}\right) + \arctan\left(\frac{\omega + \beta_1}{-\alpha_1}\right),$$

$$\phi_2 = \arctan\left(\frac{\omega - \beta_2}{-\alpha_2}\right) + \arctan\left(\frac{\omega + \beta_2}{-\alpha_2}\right).$$

Figure 10: The estimated phase characteristic of subject JP (1 degree field, 1200 Td). The parameters of the fourth-order filter are given in Table 1. The straight line depicts the relation $\omega\, t_{ex}$.

The phases ϕ_i for $i = 0, 1, 2$ are approximated by linear line pieces (see Figure 9) so that

$$\begin{aligned}
\arctan(\gamma) &= \gamma, & |\gamma| &\leq \pi/2, \\
\arctan(\gamma) &= sgn(\gamma)\,\pi/2, & |\gamma| &> \pi/2,
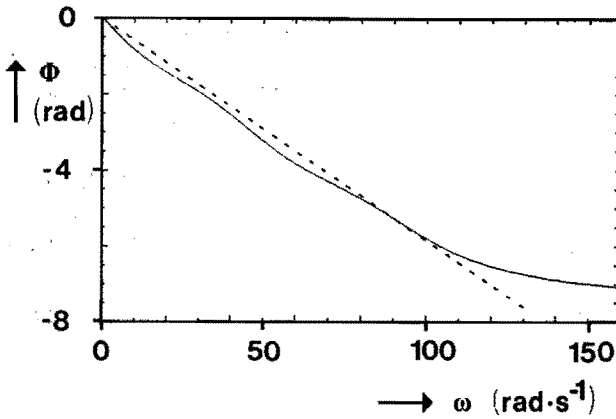\end{aligned}$$

where sgn denotes the sign of a variable. To obtain a linear phase ϕ for low frequencies in this first-order approximation of the phases ϕ_i the parameters (α_i, β_i, z) with ($i = 1, 2$) are dependent according to

$$z = -\alpha_1 = -\alpha_2,$$
$$\frac{\beta_2}{-\alpha_2} = \frac{\beta_1}{-2\alpha_1} = \pi.$$

From Table 2 we see that the phase characteristic of the fourth-order filter at 1200 Td and a 1 degree field is close to a first-order approximation of a linear phase for low frequencies. For other conditions (than 1200 Td and 1 degree field) this is not so. In Figure 10 the phase characteristic of subject JP (1200 Td, 1 degree field) is plotted with the parameters from Table 2. We see that the estimated phase is indeed close to a linear phase characteristic. The dotted line in the Figure 10 is the line $\omega\, t_{ex}$ where t_{ex} is the time of the occurrence of the extremum of the estimated impulse response. This line and the phase characteristic are very close. This is in accordance with the measurements of the phase characteristic as performed by Roufs *et al.* (1984).

chapter 6

A membrane model for spatiotemporal coupling[1]

A.C. den Brinker

Abstract

A model is proposed for spatiotemporal coupling within the transient visual system. The main features of the model are linearity, rotation symmetry and parsimonious use of parameters. The spatial transfer function of the model has a low-pass character with a cut-off frequency that depends on the temporal frequency. For the transient system the model can be completely parametrized using subthreshold measurements of impulse responses. The model is in agreement with physiological data on lateral information spread within the retina. The model was tested for predictions on flashed and sinusoidal stimuli and agrees in all major aspects with the experimental data.

6.1 Introduction

Much research on visual processing is focussed on the threshold behaviour of the visual system. By threshold behaviour is meant the magnitude of physical variables of the stimulus in order to be on the brink of being seen or not seen.

The importance of this kind of research is partly due to its applicability to technical realizations of visual information displays. Knowledge of the threshold behaviour can give criteria for the design of visual equipment. Two kinds of boundaries can be stated: one for the information that should be seen, the other for visual artefacts of the equipment that are allowable.

In order to use the experimental data on threshold behaviour for the above-mentioned purpose, a convenient way to represent these data is provided by a model which is adequate and yet as simple as possible. Unfortunately, the behaviour of the visual system of even small signals around some steady background level (as is usually the case for threshold experiments) is far from simple, or rather, is not well understood.

The processing of visual stimuli at threshold level is usually assumed to be performed in different pathways that are operating in parallel. In the temporal domain there are usually two channels operating in parallel postulated (Kulikowski and Tolhurst, 1973; Roufs, 1974; Breitmeyer and Ganz, 1976). These two channels are called the *sustained* and the *transient* channel, based on an electrophysiological concept (Cleland *et al.*, 1971). In some psychophysical studies (e.g., Mandler and Makous, 1984) three temporal channels are advocated.

---

[1]submitted to Biological Cybernetics

There is not only a difference in temporal characteristics of the different channels, but also in spatial features. In the spatial domain the number of different channels ranges from four (Wilson and Bergen, 1979) to (virtually) infinity (Koenderink and Van Doorn, 1978). It is generally accepted that a channel which is most sensitive to high-temporal frequencies is spatially low-tuned and vice versa (Breitmeyer and Ganz, 1976; Legge, 1978).

The *transient* system is tuned to high temporal and to low spatial frequencies (e.g., Legge, 1978). Associated with the transient system is the percept of agitation (Roufs, 1974). The different channels are assumed to be spatiotemporally coupled. This can be seen from the De Lange curves, where the threshold amplitude of a (gated) sinusoid is plotted versus its (temporal) frequency. For larger field sizes De Lange curves are obtained, which show higher cut-off and peak frequencies (Roufs and Bouma, 1980; see also Section 8). Since the transient system is most sensitive to large stimuli we expect to find the most pronounced spatiotemporal interaction in this channel. Furthermore, there is much experimental material available to model this channel (Roufs and Blommaert, 1981; Roufs and Bouma, 1980). For these reasons we have concentrated our research on spatiotemporal coupling on the transient system.

From physiological experiments there is also evidence of spatiotemporal coupling. Detwiler *et al.* (1978, 1980) found an information spread in the retina of the turtle that becomes faster for larger field sizes. This is similar to the psychophysical findings of the variation in the De Lange curves as shown in Roufs and Bouma (1980) and Section 8.

Many models have been proposed on either spatial or temporal behaviour. However, many phenomena cannot be accounted for in just a spatial or a temporal model, and spatiotemporal ones are scarce (Korn and von Seelen, 1972; Marko, 1981). In this article a spatiotemporal model is proposed, and it is argued that this model can account for several phenomena associated with the transient channel. Also a quantitative comparison of the model behaviour and experimental data is made in this article. Since the point of view that is taken in deriving a description for spatiotemporal interaction is fairly general, it is hoped that the model is also applicable to data outside of those discussed here.

The spatiotemporal model derived here is *not* derived from physiological data on the behaviour of single neurons. The reason for this is that, firstly, we do not know what would be the relevant data for this modelling, and secondly, that we want to model psychophysical behaviour, i.e. responses of a mass of neurons. How to relate single neuron activity to the activity of a mass of neurons would, in our view, involve too many assumptions. Instead, we start from a general partial differential equation, a kind of relation between input and output signals that is often used in physics to describe the behaviour of a thin medium. This kind of modelling is essentially a black-box approach to account for the behaviour of a layer of neurons (such as are found in the retina). How this may be realized is not relevant for the modelling of psychophysical data. Nevertheless, we will consider

an electrical network that can be described by the partial differential equation (PDE). In this way, a possible realization is shown and the parameters of the PDE are interpreted as physically realizable impedances.

A large number of restrictions is imposed on the PDE. One of these is linearity. Although the visual system as a whole does not act as a linear system (even at threshold level), there are indications that at least within a single channel linearity is applicable (De Lange, 1952; Roufs, 1974; Krauskopf, 1980; Roufs and Blommaert, 1981; Blommaert and Roufs, 1987). From the PDE a transfer function is derived, and the root locus diagrams of these transfer functions are discussed. It is shown that the model can be fully parametrized from subthreshold measurements of impulse responses of the transient visual system. This was done and the model was tested by comparison of predictions and experimental data on flashed and sinusoidal stimuli. There is a good agreement between these two although some refinements in the model seem necessarily.

6.2 A partial differential equation

The spatiotemporal interaction such as is found in visual processing is probably an operation performed in layers of neurons, e.g., horizontal or amacrine cells. Input and output signals are then essentially situated in the same plane, or may be separated by a small medium (a membrane). Partial differential equations are often used to describe the processing of signals within a membrane. The general form of such an equation is given by

$$\sum_{k=0}^{K} \sum_{l=0}^{L} \sum_{m=0}^{M} c_{k,l,m} \frac{\partial^k}{\partial x^k} \frac{\partial^l}{\partial y^l} \frac{\partial^m}{\partial t^m} u(x,y,t) = \tag{1}$$

$$\sum_{k=0}^{K'} \sum_{l=0}^{L'} \sum_{m=0}^{M'} d_{k,l,m} \frac{\partial^k}{\partial x^k} \frac{\partial^l}{\partial y^l} \frac{\partial^m}{\partial t^m} v(x,y,t), \tag{2}$$

where $v(x,y,t)$ and $u(x,y,t)$ are input and output signal, respectively. With this partial differention equation (PDE) the lateral information spread within the visual system is to be described.

To be able to solve a PDE given an input signal $v(x,y,t)$ the initial and boundary conditions have to be specified. We assume that the system is causal, that the spatial extension ranges from minus to plus infinity for x and y and that excitations that have bounded amplitudes cause responses with bounded amplitudes.

Further, we assume time invariance of the system: the parameters $c_{k,l,m}$ and $d_{k,l,m}$ $(k,l,m = 0,1,2,\cdots)$ are independent of t. Also we assume a processing which is locally space invariant. These assumptions lead to constants for $c_{k,l,m}$ and $d_{k,l,m}$. Contrary to the time invariance, the space invariance of the processing in the visual system is not a very common assumption. The reason for introducing this assumption is threefold. Firstly, we will concentrate on stimuli projected in the fovea. We assume processing's independence of location to be justified

within this area. Secondly, we are of the opinion that before introducing more complicated models the utility of very simple models to account for measurement data should be thoroughly explored. Thirdly, the assumption is in accordance with stack models (e.g., Koenderink and van Doorn, 1978), where in each layer homogeneous processing takes place. We assume that the transient system can be seen as a layer within such a stack model, presumably the layer with the largest receptive fields and the largest extent.

Next the PDE is assumed to be rotation-symmetrical. Although we know of physiological findings that contradict this assumption (e.g., orientation sensitivity), this restriction is imposed for the same reason as for the location-independent processing: the parsimony principle. Furthermore, there is psychophysical evidence of isotropic processing of visual stimuli by the transient system (Kelly and Burbeck, 1987). Rotation symmetry leads to the following restrictions on the parameters of the PDE:

$$K = L, \tag{3}$$

$$K' = L', \tag{4}$$

$$c_{2k+1,l,m} = c_{k,2l+1,m} = 0, \tag{5}$$

$$d_{2k+1,l,m} = d_{k,2l+1,m} = 0, \tag{6}$$

$$c_{k,l,m} = c_{l,k,m}, \tag{7}$$

$$d_{k,l,m} = d_{l,k,m}. \tag{8}$$

We also take $K' < K$ to ensure that the response tends to zero for stimuli with increasing spatial frequency.

The last restriction we make on the PDE is the choice of the highest partial differentiation with respect to time and space. From analysis of experimentally obtained impulse responses it was found that the spatiotemporal coupling in the transient system is of a second-order temporal nature in a first-order approximation (chapter 5, see also section 7). Therefore we take $M = 2$.

The lowest partial differentation with respect to x and y to obtain spatiotemporal coupling is $k + l \leq 2$. This restriction is again made from the point of view of parsimony. We now have a PDE with only temporal differentiations on the right-hand side. Consequently, the right-hand side does not contribute to any spatiotemporal coupling. Therefore, an input signal $i(x,y,t)$ is introduced, which is defined by

$$i(x,y,t) = \sum_{m=0}^{2} d_{0,0,m} \frac{\partial^m}{\partial t^m} v(x,y,t). \tag{9}$$

Replacing the right-hand side of the PDE by $i(x,y,t)$ gives no loss of generality with respect to the spatiotemporal character of the equation and is a somewhat more convenient description.

All the assumptions lead to a very simple PDE to describe the spatiotemporal

coupling:

$$\sum_{m=0,2}\left[-A_m\left\{\frac{\partial^2}{\partial x^2}+\frac{\partial^2}{\partial y^2}\right\}+B_m\right]\frac{\partial^m}{\partial t^m}u(x,y,t)=i(x,y,t),\qquad(10)$$

$$A_m=-c_{0,2,m}=-c_{2,0,m},\qquad(11)$$

$$B_m=c_{0,0,m}.\qquad(12)$$

Although this class of partial differential equations is very limited, it contains some equations that are often used in physical science. It comprises, for example, the diffusion and the wave equation. A combined diffusion and wave equation takes the form

$$-\left\{\frac{\partial^2 u}{\partial x^2}+\frac{\partial^2 u}{\partial y^2}\right\}+\frac{1}{v^2}\frac{\partial^2 u}{\partial t^2}+\frac{\beta}{v}\frac{\partial u}{\partial t}+\frac{\beta^2}{4}u=i(x,y,t),\qquad(13)$$

and is within the above-mentioned class of PDEs.

6.3 The transfer function

We assume that only signals $i(x,y,t)$ and $u(x,y,t)$ occur for which Fourier transforms with respect to the spatial variables and a Laplace transform with respect to the time variable exist. The Fourier transform $G_F(\omega_x)$ of a function $g(x)$ is taken as

$$G_F(\omega_x)=\mathcal{F}_x\{g(x)\}=\int_{-\infty}^{\infty}g(t)\exp(-j\,\omega_x x)\,dx\,,\qquad j=\sqrt{-1}.\qquad(14)$$

(The Fourier transform $G_F(\omega_y)$ of a function $g(y)$ is defined similarly.) The Laplace transform $G_L(s)$ of a causal function $g(t)$ is taken as

$$G_L(s)=\mathcal{L}_t\{g(t)\}=\int_{0}^{\infty}g(t)\exp(-s\,t)\,dt.\qquad(15)$$

The transforms $I(\omega_x,\omega_y,s)$ and $U(\omega_x,\omega_y,s)$ of the signals $i(x,y,t)$ and $u(x,y,t)$ are defined by

$$I(\omega_x,\omega_y,s)=\mathcal{F}_x\mathcal{F}_y\mathcal{L}_t\{i(x,y,t)\},\qquad(16)$$

$$U(\omega_x,\omega_y,s)=\mathcal{F}_x\mathcal{F}_y\mathcal{L}_t\{u(x,y,t)\}.\qquad(17)$$

Since in our case the spatial dimensions of the stimulus are expressed in degrees, the spatial angular frequencies ω_x and ω_y are expressed in dg^{-1}. With the help of these transforms the PDE is changed into an explicit relation between the input and output signal:

$$\sum_{m=0}^{2}\{A_m(\omega_x^2+\omega_y^2)+B_m\}s^m\,U(\omega_x,\omega_y,s)=I(\omega_x,\omega_y,s).\qquad(18)$$

The transfer function $H(\omega_x, \omega_y, s)$ is defined as the ratio of the transforms of response and excitation, so that

$$H(\omega_x, \omega_y, s) = \frac{U(\omega_x, \omega_y, s)}{I(\omega_x, \omega_y, s)} = \frac{1}{\sum_{m=0}^{2}\{A_m(\omega_x^2 + \omega_y^2) + B_m\}\, s^m}. \qquad (19)$$

With the transfer function $H(\omega_x, \omega_y, s)$ is associated a function $h(x, y, t)$, by

$$H(\omega_x, \omega_y, s) = \mathcal{F}_x \mathcal{F}_y \mathcal{L}_t\{h(x, y, t)\} \qquad (20)$$

The (causal) function $h(x, y, t)$ is called Green's function. Green's function gives the relation between excitation and response in the spatial and temporal domain by a convolution:

$$u(x, y, t) = h(x, y, t) * i(x, y, t), \qquad (21)$$

where $*$ denotes convolution over x, y and t.

As a consequence of the assumed rotation symmetry of the processing, the transfer function $H(\omega_x, \omega_y, s)$ is not dependent on ω_x and ω_y separately, but on the sum of squares of ω_x and ω_y. The (rotation-symmetric) spatial angular frequency w is therefore introduced by

$$w = \sqrt{\omega_x^2 + \omega_y^2}, \qquad (22)$$

and thus the transfer function is dependent on w and s

$$H(\omega_x, \omega_y, s) = H(w, s) = \frac{1}{\sum_{m=0}^{2}\{A_m\, w^2 + B_m\}\, s^m}. \qquad (23)$$

Similarly, Green's function $h(x, y, t)$ is rotation-symmetrical, and depends on the radius $r = \sqrt{x^2 + y^2}$, so that

$$h(x, y, t) = h(r, t). \qquad (24)$$

The relation between the transfer function $H(w, s)$ and Green's function $h(r, t)$ is given by a Hankel transform $\mathcal{H}_r$ and a Laplace transform:

$$H(w, s) = 2\pi\, \mathcal{H}_r \mathcal{L}_t\{h(r, t)\}, \qquad (25)$$

where the Hankel transform $G_H(w)$ of a function $g(r)$ is given by

$$G_H(w) = \mathcal{H}_r\{g(r)\} = \int_o^{\infty} g(r)\, r\, J_0(wr)\, dr, \qquad (26)$$

and where J_0 is the Bessel function of zeroth order and first kind.

From the transfer function $H(w, s)$ (eq. (23)) it can be seen that there are six free parameters: A_i and B_i for $i = 0, 1, 2$. Eigenfunctions of the system are Bessel functions J_0 in the spatial domain. In the temporal domain complex exponentials are the eigenfunctions. Thus, taking as input signal $i(x, y, t) = J_0(w_0\sqrt{x^2 + y^2})\cos(\omega_0 t)$ gives as response the signal $u(x, y, t)$, where

$$u(x, y, t) = |H(w_0, j\omega_0)|\, J_0(w_0\sqrt{x^2 + y^2})\cos(\omega_0 t + \phi), \qquad (27)$$

and where

$$\phi = \arg\{H(w_0, j\omega_0)\}. \tag{28}$$

Taking as input signal $i(x, y, t) = J_0(w_0\sqrt{x^2 + y^2})\,\delta(t)$ gives an output signal which is the product of the spatial modulation $J_0(w_0\sqrt{x^2 + y^2})$ of the input signal and a second-order impulse response $T(t)$ in time: $u(x, y, t) = J_0(w_0\sqrt{x^2 + y^2})\,T(t)$. The temporal modulation $T(t)$ is the inverse Laplace transform $\mathcal{L}^{-1}$ of the transfer function for $w = w_0$, so that

$$T(t) = \mathcal{L}^{-1}\left\{ \frac{1}{\sum_{m=0}^{2}\{A_m\, w_0^2 + B_m\}\, s^m} \right\}. \tag{29}$$

If the system described by (23) is to be stable, then the response of the system should be stable for arbitrary w. From (29) it is easy to see that the the polynomial of s has to be a Hurwitz polynomial for each w, so the signs of the parameters A_i, B_i $(i = 0, 1, 2)$ have to be identical. If the system is stable for arbitrary w, then the system is completely stable.

6.4 A membrane model

In this section an electrical network is proposed that behaves according to the class of PDEs (10) considered earlier, if adequate restrictions on its impedances are imposed (see next section). In this way, a possible realization of the class of PDEs is available and the parameters of the PDE can be interpreted and understood in a more physical representation. This realization of the PDE in the form of an electrical network has as a second advantage that it is possible to make a comparison with physiological models, since these are usually also modelled as electrical networks.

Consider a two-dimensional electrical network consisting of equal sections as shown in Figure 1. The input signal of the section at location $(m\Delta x, n\Delta y)$ is a current source $j(m\Delta x, n\Delta y, t)$, the output signal $\tilde{u}(m\Delta x, n\Delta y, t)$ is the potential at the node of the impedances. The admittance and the impedances are described as an admittance and impedances in the Laplace domain: $Y_1(s)$, $Z_1(s)$ and $Z_2(s)$. We take the admittance $Y_1(s)$ to be proportional to the area $\Delta x\Delta y$ of the section:

$$Y_1(s) = Y(s)\,\Delta x\Delta y. \tag{30}$$

$Y(s)$ is the parallel admittance of a unit area. The impedances $Z_1(s)$ and $Z_2(s)$ are taken to be proportional to the length of the sections and inversely proportional to the width, with the same proportionality factor

$$Z_1(s) = Z(s)\frac{\Delta x/2}{\Delta y}, \tag{31}$$

$$Z_2(s) = Z(s)\frac{\Delta y/2}{\Delta x}. \tag{32}$$

$Z(s)$ is the surface impedance of unit length and width. The impedance between two adjacent output signals is twice the sketched impedance, if similar sections are joined together. The current $j(m\Delta x, n\Delta y, t)$ is assumed to be proportional to the area of the section:

$$j(m\Delta x, n\Delta y, t) = \tilde{i}(m\Delta x, n\Delta y, t)\,\Delta x\,\Delta y. \qquad (33)$$

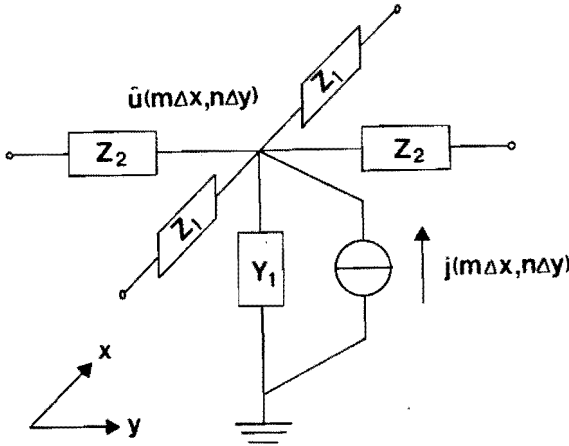The dimension of $\tilde{i}$ is the dimension of a current density.

Figure 1: Section of an electrical network suggested as a model for the spatiotemporal coupling in the visual system.

Consider an infinitely large network of sections as shown in Figure 1 in both dimensions x and y. Assume furthermore that the sections Δx and Δy are infinitely small. The electrical network becomes a distributed network with a current density $\tilde{i}(x,y,t)$ as input signal and a potential $\tilde{u}(x,y,t)$ as output. Both signals are continuous distributed signals as a function of both spatial coordinates.

The transforms $\tilde{I}(\omega_x,\omega_y,s)$ and $\tilde{U}(\omega_x,\omega_y,s)$ of the signals $\tilde{i}(x,y,t)$ and $\tilde{u}(x,y,t)$ are defined by

$$\tilde{I}(\omega_x,\omega_y,s) = \mathcal{F}_x\mathcal{F}_y\mathcal{L}_t\{\tilde{i}(x,y,t)\}, \qquad (34)$$

$$\tilde{U}(\omega_x,\omega_y,s) = \mathcal{F}_x\mathcal{F}_y\mathcal{L}_t\{\tilde{u}(x,y,t)\}. \qquad (35)$$

The transfer function $\tilde{H}(\omega_x,\omega_y,s)$ is taken as the ratio of transforms of the input and the output signal.

$$\tilde{H}(\omega_x,\omega_y,s) = \frac{\tilde{U}(\omega_x,\omega_y,s)}{\tilde{I}(\omega_x,\omega_y,s)} = \frac{Z(s)}{(\omega_x^2 + \omega_y^2) + Z(s)\,Y(s)}. \qquad (36)$$

From the transfer function $\tilde{H}(w,s)$ where $w = \sqrt{\omega_x^2 + \omega_y^2}$ it can be seen that

• for a stable network the ratio $Z(j\omega)\,Y(j\omega)$ may not be zero or negative real for any real value of ω,

• for spatiotemporal inseparable behaviour of the distributed network it is required that the ratio $Z(j\omega)\,Y(j\omega)$ depends on ω,

• the network is low-pass in its behaviour in the spatial angular frequency w (see Figure 2). The cut-off spatial frequency depends on the temporal angular frequency ω,

• the transfer function $\tilde{H}(w,s)$ of the distributed network of Figure 1 is the same as the transfer function $H(w,s)$ belonging to the PDE (10), if adequate restrictions are imposed on the surface impedance $Z(s)$ and the parallel admittance $Y(s)$.
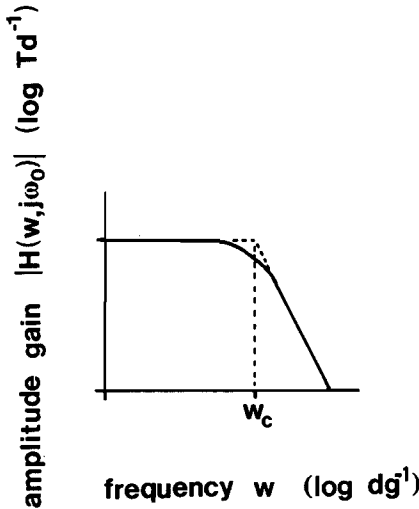
Figure 2: Amplitude characteristic $|H(w,j\omega_0)|$ as a function of the spatial frequency w. Peak value and cut-off frequency w_c of the transfer function depend on the temporal frequency ω_0. In the case that the model is used for the visual system, the units of the amplitude characteristic are in Td^{-1}.

6.5 The impedance and admittance of the electrical network

If the electrical network described by $\tilde{H}(w,s)$ is to be governed by the same relations between input and output signals as the class of PDEs (10) considered earlier, some restrictions have to be made on the impedance $Z(s)$ and the admittance $Y(s)$. Assume that $Y(s)$ and $Z(s)$ can be written as the ratio of two real

polynomials in s, by

$$Y(s) = C_Y \frac{\prod_{i=1}^{m_Y}(s - z_{Yi})}{\prod_{i=1}^{n_Y}(s - p_{Yi})}, \tag{37}$$

$$Z(s) = C_Z \frac{\prod_{i=1}^{m_Z}(s - z_{Zi})}{\prod_{i=1}^{n_Z}(s - p_{Zi})}, \tag{38}$$

where
C_Y , C_Z amplification factors ,
z_{Yi} , z_{Zi} zeros of the admittance and the impedance, respectively ,
p_{Yi} , p_{Zi} poles of the admittance and the impedance, respectively.

We assume that all zeros z_{Yi} of the parallel admittance and all poles p_{Zi} of the surface impedance are in the left-half of the complex plane. In so far as the poles and zeros of the admittance (and of the impedance) are not real-valued, these occur in complex conjugated pairs.

Substituting (37) and (38) in the transfer function $\tilde{H}(w, s)$ (eq.36) of the electrical network the following expression for the transfer is found:

$$\tilde{H}(w, s) = \frac{C_Y \prod_{i=1}^{n_Y}(s - p_{Yi}) \prod_{i=1}^{m_Z}(s - z_{Zi})}{C_w w^2 \prod_{i=1}^{n_Y}(s - p_{Yi}) \prod_{i=1}^{n_Z}(s - p_{Zi}) + \prod_{i=1}^{m_Y}(s - z_{Yi}) \prod_{i=1}^{m_Z}(s - z_{Zi})}, \tag{39}$$

where $C_w = C_Y/C_Z$. Comparing $\tilde{H}(w, s)$ to $H(w, s)$ (eq.23), it is easy to see which restrictions have to be imposed on the admittance $Y(s)$ and impedance $Z(s)$ to obtain equal transfer functions for both cases. We find that

$$n_Y = m_Z = 0, \tag{40}$$

$$m_Y = n_Z = 2. \tag{41}$$

From (40) and (41) it follows that $Y(s)$ and $Z(s)$ are active elements and cannot be synthesized as impedances consisting of passive resistors, capacitors and inductances. We do not think of this as a drawback of our model, since we do not assume that neurons act as passive elements (Koch, 1984). Furthermore, if v had not been replaced by i (9) then it would be possible to realize the membrane with passive elements. However, as argued before, for our purpose it is not necessary to have zeros in the transfer function that are independent of the spatial frequency. Thus, from the point of view of simplicity, these zeros are unwanted within the membrane model.

With the restrictions (40 and 41) on the impedance and admittance the transfer function $\tilde{H}(w, s)$ can be written as

$$\tilde{H}(w, s) = \frac{C_Y}{C_w w^2 \prod_{i=1}^{2}(s - p_{Zi}) + \prod_{i=1}^{2}(s - z_{Yi})}, \tag{42}$$

and for equivalence of $\tilde{H}(w, s)$ and $H(w, s)$ (eq. (23)) it is found that

$$A_2 = C_Z^{-1}; \quad A_1 = -2\,C_Z^{-1}(p_{Z1} + p_{Z2}); \quad A_0 = C_Z^{-1}\,p_{Z1}\,p_{Z2},$$
$$B_2 = C_Y^{-1}; \quad B_1 = -2\,C_Y^{-1}(z_{Y1} + z_{Y2}); \quad B_0 = C_Y^{-1}\,z_{Y1}\,z_{Y2}.$$

From these equations it is seen that the parameters of the PDE $(A_i, B_i, i = 0, 1, 2)$ can be interpreted as the zeros of a parallel admittance and the poles of the surface impedance of a distributed electrical network.

6.6 Root locus trajectory

It is common usage to characterize temporal behaviour by the poles of the model. Since the model considered here is a spatiotemporal one, a pole migration takes place: from (23) (and (42)) it can be seen that for each spatial angular frequency w the model acts as a second-order temporal filter. The range of (complex) values that the poles span as a function of the spatial angular frequency characterizes the model. This characteristic is a figure in the complex plane that is called the root locus diagram. As is shown in the following, the location of the poles in the complex plane forms a specific pattern, given the transfer function (23).

For any spatial frequency w the distributed network described by $\tilde{H}(w, s)$ acts as a second-order temporal filter. The temporal characteristics are described by the poles of the transfer function at w. The poles are the roots s of the quadratic characteristic equation of $\tilde{H}(w, s)$, which is given by

$$C_w w^2 \left\{ \prod_{i=1}^{2} (s - p_{Zi}) \right\} + \prod_{i=1}^{2} (s - z_{Yi}) = 0. \tag{43}$$

As stated before, the poles p_{Zi} (and zeros z_{Yi}), $i = 1, 2$ are both real-valued or form a complex-conjugated pair. The characteristic equation has also two real-valued or two complex-conjugated solutions.

For $w = 0$ the poles of $\tilde{H}(w, s)$ are the zeros of $Y(s)$, and for $w \to \infty$ the poles of $\tilde{H}(w, s)$ are the poles of $Z(s)$. The solutions s of the characteristic equation are a function of the spatial frequency w, and can be plotted in the s-plane similarly to what is usually done with feedback systems (Kuo, 1962). The same rules apply for the construction of a root locus trajectory in both cases.

If there are complex solutions of the characteristic equation (43), then these are located on a circle with centre on the real axis. The circles include the case of a circle with an infinitely large radius, i.e. a root locus which is (part of) a line parallel to the imaginary axis. In Figure 3 some examples of root locus trajectories of $\tilde{H}(w, s)$ are shown.

From psychophysical measurements it was found that larger fields (containing lower spatial frequencies) tend to temporal responses with faster oscillations. The De Lange curves have a higher peak and cut-off frequency for more extended field sizes (Granit and Harper, 1930; Roufs and Bouma, 1980; see also Section 8). Such behaviour is also found physiologically in the retina (Detwiler *et al.*, 1978, 1980).

Because of the oscillatory character of the system responses complex-valued poles are needed in the model. Furthermore, the imaginary part must increase with decreasing spatial frequency w, to account for faster responses for larger
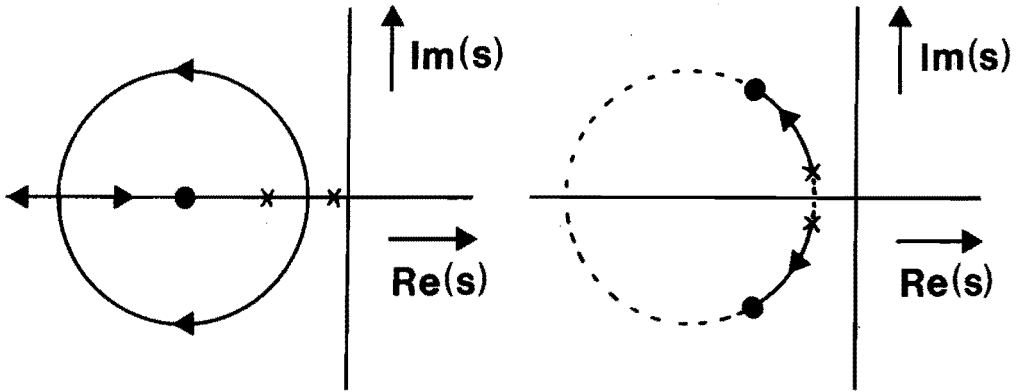
Figure 3: Two examples of root locus trajectories of $\hat{H}(w, s)$ as a function of the spatial angular frequency w. The crosses and the filled circles indicate the poles of the transfer function for $w = 0$ and $w = \infty$, respectively. The lines with the arrows indicate the direction of the pole migration with increasing w.

fields. Thus, contrary to cable models of nervous cells (Bennet, 1977) the surface impedances in our model cannot be taken as resistive elements. This would mean that a root locus is found with poles going to infinity for large spatial frequencies.

On similar grounds (poles going to infinity for $w \rightarrow \infty$) the combined wave and diffusion equation (13) must be rejected for a spatiotemporal model of the transient visual system. Such a PDE gives slower temporal responses for decreasing spatial frequency.

6.7 Parametrization of the membrane for the spatiotemporal coupling in the transient system

The question that arises is whether this spatiotemporal model can be fully parametrized from psychophysical measurements. If the model behaves similarly to the real system, we expect that by measuring the temporal behaviour of the system at several spatial frequencies the root locus of the spatiotemporal model can be found and from this the model can be parametrized, apart from a multiplication factor. Having the poles at three different spatial frequencies is sufficient to parametrize the model.

In chapter 4 and chapter 5 fourth-order linear filters were fitted to data from subthreshold measurements of impulse responses of circular discs with a completely dark surround (Roufs and Blommaert, 1981). These estimation procedures were also performed on data from two subjects at a 1200 Td background level for several

field sizes. The results of the parameter estimations on these impulse responses are shown in Figure 4A. In this figure the estimated 90% confidence regions of the poles and zeros are plotted. From Figure 4A it can be seen that one pole pair (the one with largest norm) is shifting, if we compare the estimates obtained from the impulse responses of discs of different size. The estimate of the other pole seems to be independent of the diameter of the stimulus.
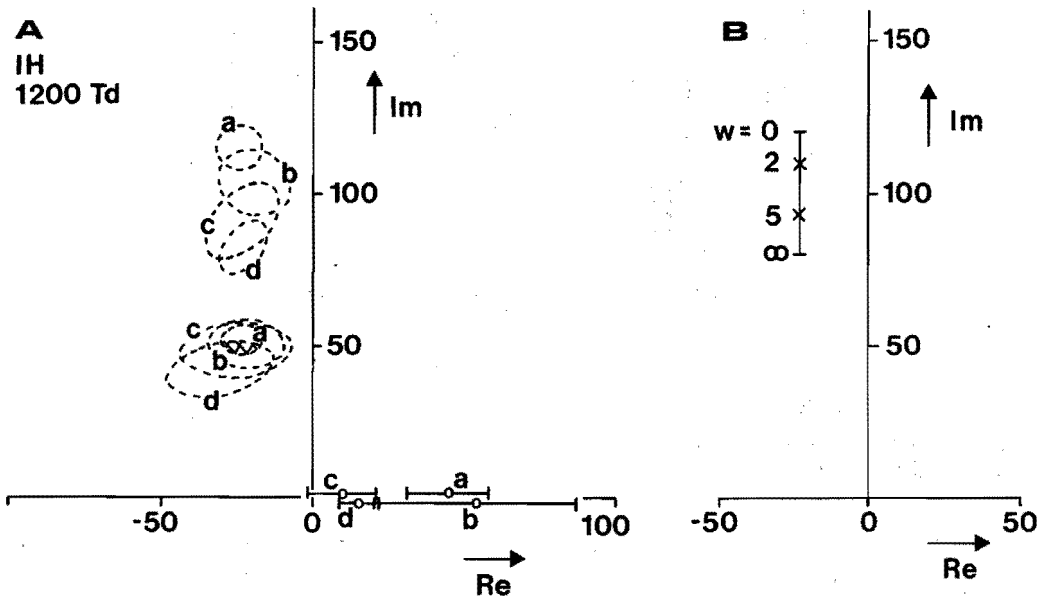
Figure 4: Pole-zero plots in the complex plane. Horizontal and vertical axis are the real and imaginary axis, respectively. The units are in s^{-1}. The lower part of the s-plane is not shown in this plot. A Pole-zero plot of filter parameters of a fourth-order linear filter determined from experimentally obtained impulse responses. Subject IH, 1200Td, for field diameters of 5.5 (a), 1.0 (b), 0.50 (c) and 0.28 (d) degrees. The ellipses give estimates of the 90% confidence regions of the poles. The estimated poles are located in the centres of the ellipses. The zeros are indicated by a small circle and the bars give the 90% confidence intervals. (Replot from chapter 4.) B Pole-zero plot of the membrane model as a function of the spatial frequency w (see text).

An impulse response described by such a location of the poles (Fig. 4A) is shown in Figure 5 for subject IH at 1200 Td and a 30' field diameter, together with the data of the experimentally determined impulse response (see Roufs and Blommaert, 1981).

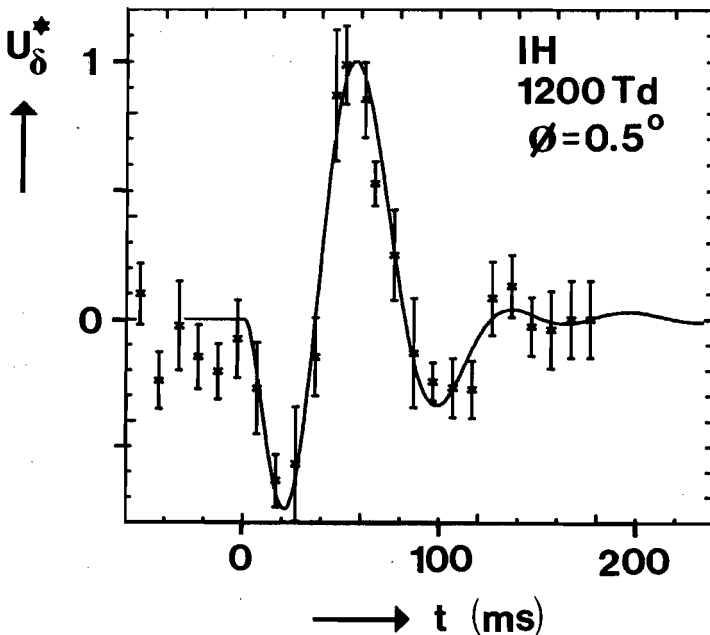Figure 5: Experimentally determined normalized impulse response and fitted fourth-order linear filter (see chapter 5). The bars through the experimental data points are twice the standard deviation of the mean.

In chapter 5 it was therefore argued that the transient system could be described by two second-order filters in cascade where only one of these filters contains lateral interaction. This is shown in Figure 6, the first filter is dependent on w, the spatial frequency, the second is not. Underneath the filters are sketches of an input signal (a pulse-like stimulus), the (internal) responses from the filters L_1 and L_2, and the signal in the detection mechanism. The response of the first filter is the response of a second-order filter but the exact form depends on the field size that is used. Convolution of this second-order filter response with the impulse response of the second filter gives an impulse response shown by r_2 (Figure 6). This signal is contaminated by noise and then compared with the threshold level.

The behaviour of the largest pole as a function of the diameter of the field is reminiscent of the root locus trajectory of the membrane model (see Section 6, Figure 3). But then the plot of Figure 3 is only applicable for (zero order) Bessel functions on a background with an infinite extension, while the estimated parameters in Figure 4A are derived from discs with a completely dark surround. In the latter case the transient system is probably not operating homogeneously over space, since the lateral interaction between neurons is presumably affected by some (local) measure of the mean luminance.
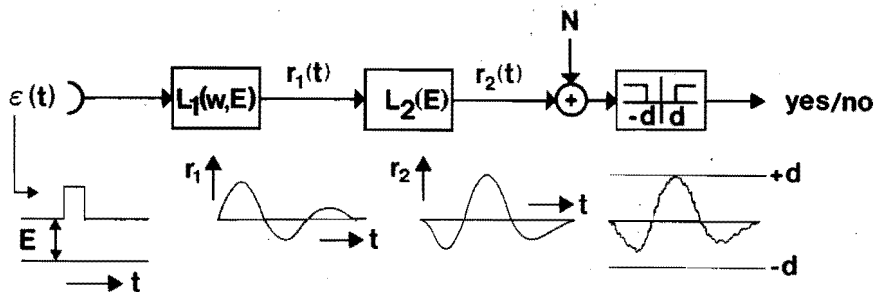
Figure 6: Spatiotemporal model of the transient visual system as suggested in chapter 5. The model consists of two linear filters, both dependent on the mean luminance E, where the first filter accounts for the spatiotemporal coupling, and the second filter is temporal only. Both filters are of a second-order temporal nature only. The last stage of the model is a detector with (symmetrical) threshold d. Underneath the sketched model a pulse-like input signal is shown, and the internal responses. The response of the first filter is a second-order filter response, where the parameters of this filter are dependent on the field diameter of the stimulus.

Still, we want to make use of this kind of psychophysical data, since it so clearly demonstrates the effects of spatiotemporal coupling, and since this effect is contained in so few parameters. To be able to test the membrane model, by incorporating the data from Figure 4A, some additional assumptions about the behaviour of the model have to be made. These assumptions are:
• the parameters of the membrane model ($Y(s)$ and $Z(s)$) are locally controlled by the background,
• in the case of a sharp light-dark border the admittance $Y(s)$ seen from the light area is (virtually) infinite.
This implies that for discs of a certain diameter D, $Y(s)$ and $Z(s)$ are constant within this area, and the boundary condition for the PDE is given by $u(x,y,t) = 0$, for $(x,y) \in$ border. This, in turn, means that at a light-dark border all lateral-going signals are totally reflected (with a negative sign). The two foregoing assumptions are without doubt idealizations, but may be adequate for a first-order approximation.

The first assumption stating that the processing in the transient system adapts to the background level is trivial, except for the statement that the membrane parameters are *locally* regulated. There is physiological evidence for this assumption: horizontal cells show summation of adaptation within an area smaller than their receptive fields (Itzhaki and Perlman, 1987).

The second assumption is inspired by two perceptual findings:
• detection of temporal events upon a disc with a completely dark surround takes

place at or near the centre, but never close to the border,

• if some short suprathreshold increment is given in the luminance of the disc, then a 'blob' is observed which peaks in the middle and is zero at the border.

In the case of a completely reflecting border, each rotation-symmetrical stimulus on the disc can be described as a Fourier-Bessel series (Watson, 1966), and the dynamics of the membrane within this disc area is described by the transfer function $\tilde{H}(w,s)$. For a stimulus with a diameter equal to the background, the main component in this series is the first component, which is a Bessel function J_0 (zeroth order, first kind) with spatial angular frequency

$$w = \frac{j_1}{D/2},\qquad(44)$$

where
j_1 is the first zero of this Bessel function $(J_0(j_1) = 0)$,
D is the diameter of the disc.
We therefore take as a first-order approximation that for a field of diameter D, the temporal behaviour of the membrane is dominated by the pole pair corresponding to the frequency $w = 2j_1/D$. Consequently, the largest pole in the estimated fourth-order filters of the impulse responses of discs (diameter D) with a completely dark surround is a pole that should be associated with a spatial frequency $w = 2j_1/D$.

In this way, impulse responses of discs with a completely dark surround of three different diameters (same subject and background level) can be used to parametrize the membrane model. Admittedly, this procedure to obtain parameters of the membrane from this impulse responses relies heavily upon some non-trivial assumptions. Nevertheless, we will show that this rough procedure can give some indication whether the simple membrane model presented in the foregoing can be used to describe the spatiotemporal coupling within the transient visual system.

6.8 Predictions from the model

Model parameters

Parameter estimations of fourth-order filters (chapter 5 and Figure 4A) have been applied to experimentally determined impulse responses (Roufs and Blommaert,1981; Blommaert and Roufs, 1987). The membrane parameters were derived from these estimates in the manner suggested in the previous section. It was found that the parameters of the membrane are (approximately) $C_w = 0.07$, $z_{Y1}, z_{Y2} = -23 \pm j120$ s^{-1} and $p_{Z1}, p_{Z2} = -23 \pm j70$ s^{-1}. The amplification factor C_a was taken to be unity. The root locus diagram is shown in Figure 4B and the resemblance with the behaviour of pole with the largest norm estimated from the impulse responses can be clearly seen from comparison with Figure 4A.

The second filter L_2 (Figure 6) is a second order temporal filter with transfer

function $H_2(s)$ (chapter 5):

$$H_2(s) = \frac{A\,(s - z)}{(s - p)(s - p^*)},\qquad(45)$$

where A is an amplification factor and p, p^* and z are the poles and zero of the transfer function. The parameter values of this filter were derived from the estimates performed on the impulse response over different subjects at 1200 Td and for 1° fields. These values were taken to be $p = -23 + j45$ s^{-1}, $z = 15$ s^{-1} and $A = 0.6 \cdot 10^8$.

For both the parameters in the membrane as for the parameters of filter L_2 rounded values were taken in view of the variances in the estimates from which these parameters were derived (see chapter 5). The model presented above is totally deterministic, no effects of probability summation (either in time or over space) are taken into account.

Predictions of the model with the above mentioned parameters were made of threshold-versus-duration curves and amplitude gain characteristics for fields of different sizes with a dark surround. These predictions will be compared in the sequel with experimental data. But first the experimental apparatus and procedure are described.

Apparatus and procedure

In both the threshold-versus-duration and the De Lange measurements, the stimulus was a centrally fixated circular field of diameter 0.25, 0.5, 1.0, 2.0 or 5.0 degrees with a dark surround. The stimulus was presented (monocularly) in Maxwellian view through an artificial pupil of 2 mm. The lights were generated by linearised glow modulators, operated around a suitable working point. The luminance of the background was set by means of neutral density filters. The modulation of the background was controlled electronically by function generators. The modulation was either a rectangular pulse of variable duration or a sinusoid with variable frequency. The duration of the sinusoid was 0.8 s and was slowly switched on and off by a ramp function which lasted for 0.25 s. The amplitude of the desired function could be adjusted using a dB step attenuator. The calibration of the dynamic stimuli was checked before every session by means of a photomultiplier tube, properly corrected with respect to spectral sensitivity.

A P800 mini computer guided the experiments. The subject had one knob to release the stimulus, which was delayed for 300 ms. The beginning of the stimulus was marked by an acoustic signal. "Yes" or "No" answers were directly fed into the computer. For a certain modulation amplitude 10 identical stimuli were presented successively and the detected percentage was determined by the computer and used for generating the next modulation amplitude. In each case, the 50% threshold amplitude was determined by linear regression from at least 2 amplitude values with detection chances between 20% and 80%. This was done

four times for each duration (in the threshold-versus-duration characteristic) or frequency (in the De Lange experiment). The durations and frequencies were presented in counterbalance (two sessions in counterbalance provide four estimates of the threshold amplitude).

Two subjects participated in all experiments: LT and BdB, both male and ages at the time of the experiment 36 and 30, respectively. Furthermore, subjects HD and IH (aged 28 and 43, respectively) also provided data on the normfactors. All subjects had normal acuity, although some of them used a slight correction.
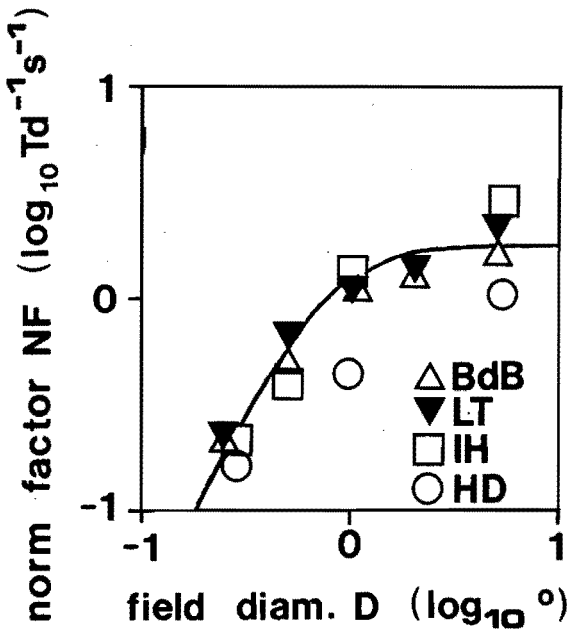
Figure 7: The norm factor of shortly flashed circular disc with a dark surround at a 1200 Td background level as a function the field diameter. The line is the prediction from the model (see text), the symbols represent the experimental data for different subjects as indicated.

Results

In the first experiment threshold-versus-duration curves were determined as a function of field size. Only a very limited number of durations was used in the measurement. Essentially, to determine the normfactor NF only one duration within Bloch's region is necessarily. The normfactor is the inverse of the energy of such

pulse to reach threshold:

$$NF = 1/(\varepsilon\,\vartheta), \tag{46}$$

where
ε the amplitude of the pulse at threshold level,
ϑ the duration of the pulse.
The thresholds of several pulses with a duration outside Bloch's region were also determined to check whether the threshold-versus-duration curves had a dip at intermediate durations. This was always the case for the field sizes that were used in the experiments and is interpreted as indication that the transient system determined the response. For smaller field sizes the sustained system starts to determine the response and (of course) cannot be used as verification of the model. Also the largest field size was taken as 5° in diameter to ensure that there are no areas stimulated very far outside the fovea (see also Discussion).

In Figure 7 the normfactor NF is plotted versus the field diameter. The model predicts a slope of 2 (on log-log basis) for small diameters and a constant level for large field sizes. The experimental data agrees nicely with the prediction, although one should maybe allow a subject dependent spatial integration. (Mainly the parameter C_w in the model determines the transition point from slope 2 to a constant level). Only data from subject HD do not seem to fit the predictions; this is probably due to the fact that for this subject large gaps in time existed between the measurements of the norm factors of different field sizes.

In Figure 8 De Lange curves are shown (subject BdB, 1200 Td background) for several field sizes. From this figure the top value (the sensitivity factor S) and the cut-off frequency f_h (0.3 log units below S) were taken as characteristic quantities of the high frequency side (and thus of the transient system). These data were replotted in Figure 9 as a function of field size, together with data from a second subject (LT, 1200 Td background level). The model predicts a slope 2 (on log-log basis) for the sensitivity factor of fields with a small diameter, and a constant sensitivity factor for large field sizes. The experimental data confirms this (Fig. 9A). The prediction is for all field sizes about 0.2-0.3 log units below the experimental data, an amount that can be easily attributed to probability summation over time (Roufs, 1974; Roufs and Pellegrino, 1976). The cut-off frequency (Fig. 9B) increases both in the model simulations and in the experimental data with an increase in field size (see also Granit and Harper, 1930; Roufs and Bouma, 1980). The model predicts values for the cut-off frequency that are too high in comparison to the experimental data. Apart from the fact that it is not always easy to make a good estimate of the cut-off frequency from the experimental data, this discrepancy was already noted before. The fourth-order estimates as derived from the impulse response measurements show a fall-off in their gain that is too slow (chapter 5) and consequently provide a too high estimate of the cut-off frequency (see also Discussion).
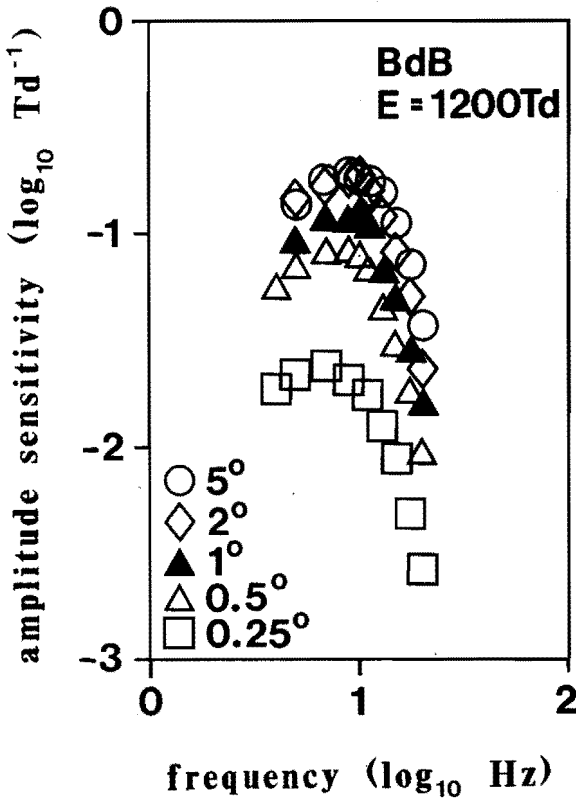
Figure 8: De Lange curves of subject BdB at 1200 Td background for different field sizes (as indicated in the figure).

6.9 Discussion

In this article a linear model is presented as a model for spatiotemporal coupling within the transient visual system. The model is described by a PDE. This PDE is of a very simple form because of the many restrictions imposed on it (linearity, time and space invariance, rotation symmetry, low order of the PDE). The many restrictions are simultaneously the weak and strong features of the model. The strong point is the simplicity and the parsimony in parameters of the model. The weak point is the set of many major assumptions which have to be made regarding the model in order to obtain such a simple description.

The model does not agree with the current idea of local processing of visual stimuli. But then, the model presented here should account for the transient system,

Figure 9: **A** The sensitivity factor S and **B** the cut-off frequency f_h as a function of the of the field diameter. The line represents the prediction from the model (see text), the symbols show the experimental data for two different subjects.

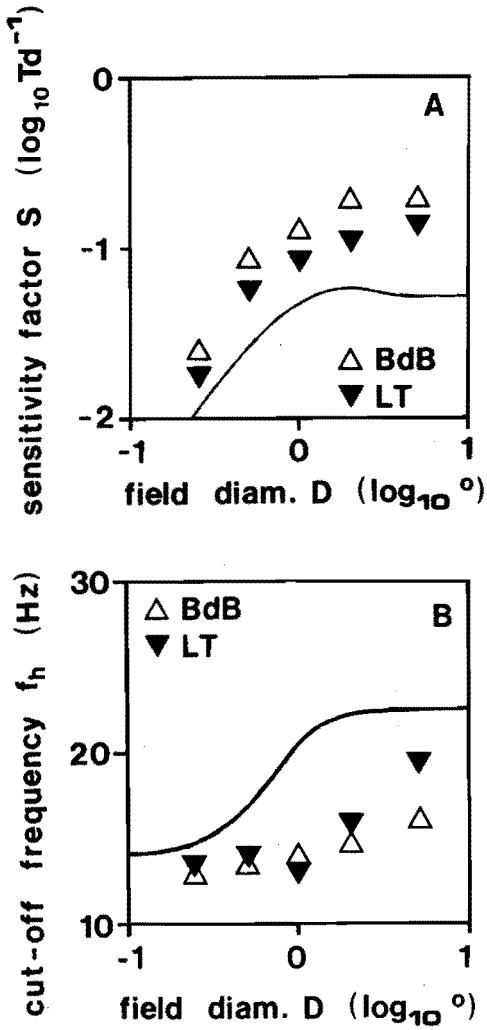i.e. the channel with the largest spatial interactions. We suppose that approximation with an infinitely outstretched processing over space is a good approximation to that with a large yet finite window.

The PDE can be seen as belonging to a distributed electrical network. The system is low-pass in the spatial domain, for each temporal frequency. Alternatively, the filter is of a second-order temporal nature for each spatial frequency. The temporal behaviour of the model with variation of the spatial modulation can be seen from a root locus trajectory. The model can be fully parametrized given a proper root locus trajectory.

In chapter 5 parameter estimations of subthreshold measured impulse responses were discussed. From these kinds of psychophysical measurements the suggested spatiotemporal model can be parametrized. This results in a simple spatiotemporal model for the transient visual system as is shown in Figure 6 and consists of the membrane model in cascade with a temporal filter (of second-order) and a detection unit. The model can be completely parametrized from the estimated fourth-order linear filters of the experimentally determined impulse responses leaving no free parameters in the model.

The membrane behaviour is qualitatively similar to physiological findings in the rod network (Detwiler *et al.*, 1980). The rationale of such coupling as suggested by Detwiler *et al.* (1978, 1980) is a trade-off between the need for large spatial integration and long temporal integration in order to obtain an internal response level (for signals with small amplitude) that is large enough to exceed the internal noise level.

The membrane model was quantitatively tested by comparing predictions of normfactors, sensitivity factors and cut-off frequencies to experimental data. Making allowances for the fact that the model is deterministic, the model performed in accordance with the experimental results over a limited range of (relatively large) stimulus dimensions presented foveally. Only the cut-off frequency of the model was always found to be too high in the model. This is a consequence of the fourth-order that were used as the starting point of the parametrization of the model. An easy way to overcome this problem is to use higher order filters as a model for the impulse response as argued in chapter 5. In the model presented here this would mean that instead of using a second-order filter for the temporal filter L_2 a higher order temporal filter would be more adequate.

From the simulations of the model it was also found that the location of the maximum in the spatial domain varied with the dimension of the stimulus. For small field sizes ($< 1°$) the response of the membrane is completely dominated by the first Bessel function from the series that are associated with the disc, and consequently the maximum is always located in the middle of the disc. For larger field diameters the simulations showed that the maximum occurred somewhere between the centre and the border of the disc. This is in agreement with the perceptual observation that for larger field sizes the detection occurs somewhere off-centre.

The model is open for further detailing. The responses from the membrane may be considered as rough approximations to actual occurring retinal cell responses. We did not refine the membrane responses in this way since in the first place we are interested in psychophysical modelling and, secondly, given the presented results, we do not think that such approach is very fruitful. For psychophysical modelling some refinements are needed. For instance, the predicted temporal frequency fall-off of the model is rather low (0.9 log unit per octave) in comparison with the De Lange characteristics. Furthermore, it may be worthwhile to confront the membrane model with the matched filter model we presented elsewhere (chapter 3). The idea behind the latter model would be that response of the membrane is transmitted to the cortex, presumably a process in which a large amount of noise is introduced. If cortical cells act in such a way as to minimize these noise influences and if the system acts linearly around threshold level (De Lange,1952; Krauskopf, 1980; Roufs and Blommaert, 1981; Blommaert and Roufs, 1987), then the temporal filter should have the characteristics of a matched filter (chapter 3). In this way not only an appropriate fall-off of the gain characteristic can be obtained and presumably a better prediction of the cut-off frequency, but simultaneously this would provide a functional interpretation of the filter L_2 (see Figure 6).

Another possibility for further research lies in extending the membrane properties to extra-foveal phenomena by introducing slowly varying admittance and impedance values $(Y(s), Z(s))$ as a function of eccentricity. Also, the behaviour of these parameters with background level may yield interesting interpretations. In this way maybe phenomena as found by Rovamo and Raninen (1984) and Raninen and Rovamo (1986) can be accounted for within the model.

Acknowledgements

References

Bennet (1977) Electrical transmission: a functional analysis and comparison to chemical transmission. In: Bethseda, MD, Handbook of Physiology. American Physiological Society.

Blommaert F.J.J., Roufs J.A.J. (1987) Prediction of thresholds and latency on the basis of experimentally determined impulse responses. Biol. Cyb. 56, 329-344.

Breitmeyer B.G., Ganz L. (1976) Implications of sustained and transient channels for theories of visual pattern masking, saccadic suppression, and information processing. Psychol. Review 83, 1-36.

Cleland B.G., Dubin M.W., Levick W.R. (1971) Sustained and transient neurones in the cat's retina and lateral geniculate nucleus. J. Physiol. **217**, 473-496.

Detwiler P.B., Hodgkin A.L., McNaughton P.A. (1978) A surprising property of electrical spread in the network of rods in the turtle's retina. Nature **274**, 562-565.

Detwiler P.B., Hodgkin A.L., McNaughton P.A. (1980) Temporal and spatial characteristics of the voltage response of rods in the retina of the snapping turtle. J. Physiol. **300**, 213-250.

Granit R., Harper P. (1930) Comparative studies in peripheral and central retina. II. Synaptic reaction in the eye. Am. J. Physiol. **95**, 211-228.

Itzhaki A., Perlman I. (1987) Light adaptation of red cones and L1-horizontal cells in the turtle retina: effect of background spatial pattern. Vision Res. **27**, 685-696.

Kelly D.H., Burbeck C.A. (1987) Further evidence for a broadband, isotropic mechanism sensitive to high-velocity stimuli. Vision Res. **27**, 1527-1537.

Koch C. (1984) Cable theory in neurons with active, linearized membranes. Biol. Cyb. **50**, 15-33.

Koenderink J.J., Doorn A.J. van (1978) Visual detection of spatial contrast; influence of location in the visual field, target extent and illuminance level. Biol. Cyb. **30**, 157-167.

Korn A., von Seelen W. (1972) Dynamische Eigenschaften von Nervennetzen im visuellen System. Kybernetik **10**, 64-77.

Krauskopf J. (1980) Discrimination and detection of changes in luminance. Vision Res. **20**, 671-677.

Kulikowski J.J., Tolhurst D.J. (1973) Psychophysical evidence for sustained and transient detectors in human vision. J. Physiol. **232**, 149-162.

Kuo B.C. (1962) Automatic Control Systems. Englewood Cliff N.J.: Prentice-Hall.

Lange H. de (1952) Experiments on flicker and some calculations on an electrical analogue of the foveal system. Physica **18**, 935-950.

Legge G.E. (1978) Sustained and transient mechanisms in human vision: temporal and spatial properties. Vision Res. **18**, 69-81.

Mandler M.B., Makous W. (1984) A three-channel model of temporal frequency perception. Vision Res. **24**, 1881-1887.

Marko H. (1981) The z-model - a proposal for spatial and temporal modeling of the visual threshold perception. Biol. Cyb. **39**, 111-123.

Raninen A., Rovamo J. (1986) Perimetry of critical flicker frequency in human rod and cone vision. Vision Research **26**, 1249-1255.

Roufs J.A.J. (1974a) Dynamic properties of vision-IV. Thresholds of decremental flashes, incremental flashes and doublets in relation to flicker fushion. Vision Res. **14**, 831-851.

Roufs J.A.J. (1974b) Dynamic properties of vision.-VI. Stochastic threshold fluctuations and their effect on flash-to-flicker sensitivity ratio. Vision Research **14**, 871-888.

Roufs J.A.J., Blommaert F.J.J. (1981) Temporal impulse and step responses of the human eye obtained psychophysically by means of a drift-correcting perturbation technique. Vision Res. **21**, 1203-1221.

Roufs J.A.J., Bouma H. (1980) Towards linking perception research and image quality. Proc. Soc. Inf. Displ. Eng. **21**, 247-270.

Roufs J.A.J., Pellegrino van Stuyvenberg J.A. (1976) Gain curve of the eye to subliminal sinusoidal modulation of light. IPO Annual Progress Report **11**, 49-63.

Rovamo J., Raninen A. (1984) Critical flicker frequency and M-scaling of stimulus size and retinal illuminance. Vision Research **24**, 1127-1131.

Watson G.N. (1966) A treatise on the theory of Bessel functions. Cambridge: University Press.

Wilson H.R., Bergen J.R. (1979) A four-mechanism model for threshold spatial vision. Vision Res. **19**, 19-32.

chapter 7

Changes with background in the linear model of the transient visual system[1]

A.C. den Brinker

Abstract

There is evidence that the transient channel of temporal human vision behaves as a linear filter for small excursions around a steady background level. The linear filter characteristics depend on the background level.

From experimentally obtained impulse responses of the transient channel the linear filter can be modelled and parametrized. This has been done for two different background levels. The two sets of estimated parameters at these two levels show a shift in the parameters which can be described by a single multiplication factor. This result was extrapolated to arbitrary background levels by postulating that each change in background level can be described by a multiplication factor. This leads to an assumption on the variation of the parameters of the linear filter of the transient channel with changes in the background level.

This assumption is tested by simulating the system for different parameter sets of the linear filter. The simulations give a good agreement with experimental data on threshold-versus-duration curves and De Lange curves. The (minor) quantitative differences in simulations and experimental data can be explained.

7.1 Introduction

The temporal behaviour of the visual system at threshold level is usually assumed to be adequately described by two channels working in parallel (Roufs, 1974a; Breitmeyer and Ganz, 1976; Green, 1984). These channels are called the *sustained* and the *transient* channel. Psychophysical evidence shows that both channels act linearly for small changes around a steady background level (Krauskopf, 1980; Roufs and Blommaert, 1981; Blommaert and Roufs, 1987). The sustained channel is in the temporal frequency domain tuned to low frequencies, the transient to high frequencies.

The impulse response of the *transient* system can be described as a fourth-order linear filter (chapter 4) and its parameters can be estimated from impulse responses measured by a perturbation technique (Roufs and Blommaert, 1981; Blommaert and Roufs, 1987). The interesting part of modelling (apart from being

---

able to make predictions) is the possibility it offers to give insight into the way data are processed in the system. In chapter 5 a fourth-order linear filter was used as a model for the transient system. There it was found that the parameters of this filter changed in a characteristic way if either a change in background level or spatial extension of the stimulus was introduced in the experiment. This made it possible to implement a refinement on the assumption of isomorphic impulse responses of the transient channel at different background levels (Roufs, 1974a; Roufs and Blommaert, 1981). Also a simple spatiotemporal model was presented on the basis of the shifts in estimated parameters with diameter of the stimulus. Here we will concentrate on the changes in the parameters of a linear model for the transient channel that are found from experiments at different background levels.

In chapter 5 a fourth-order linear filter was used to model the transient system. It was found that such a model provides an agreeable fit with the experimental data, and with reliably estimated parameters. Furthermore it was shown that some of the parameters were independent of background level, while others changed with background. However, it was also shown that the fourth-order linear filter did not agree with data on sensitivity versus frequency of a sinusoid (TMTF, Temporal Modulation Transfer Function, also called De Lange curve), since the fall-off of this linear filter was essentially too low. A sixth-order filter can provide the necessary fall-off and is therefore more appropriate.

Therefore we restart the modelling of the transient system by fitting a sixth-order linear filter to the experimentally determined impulse response data. Again it is found that the estimated parameters show very small intersubject variation, if the same experimental conditions are used. On the other hand, background variations provide substantial shifts in the estimated parameters.

We will introduce a (simple) description of how parameters of the sixth-order linear filter might change with background level. By simulation this postulated change in parameters is confronted with experimental data. Sensitivity factors, cut-off frequency and critical duration can be calculated from the model and compared with experimental data. The results show a good agreement between the suggested parameter change and the experimental data. Quantitative differences will be discussed and explained.

7.2 Filter description

The model used for the transient system is shown in Figure 1. The input signal is a variation $\varepsilon(t)$ of the retinal luminance (the background E), expressed in Trolands. The linear filter L is described by its impulse response $U_\delta(t)$. The relation between $\varepsilon(t)$ and $r(t)$ is given by a convolution according to

$$r(t) = \int_0^t \varepsilon(\tau) U_\delta(t - \tau) d\tau. \tag{1}$$

An input signal is detected if there exists a t such that

$$|r(t) + n(t)| \geq d. \tag{2}$$

In conditions relevant for this analysis (photopic levels and not too small diameters, ≈ 1 degree) there is experimental evidence which justifies the assumption that the signal threshold d is symmetrical for dynamic stimuli (Roufs, 1974b; du Buf, 1987), as is expressed in (2) and Figure 1.
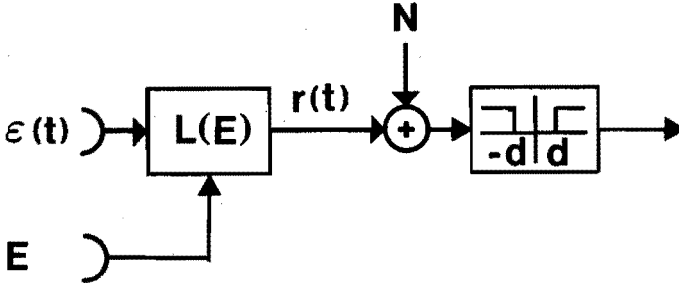

Figure 1: Model for the transient system of the human visual threshold perception. $\varepsilon(t)$ is the input signal, L is a linear filter, N a noise source and the last stage is a detector mechanism with threshold d. The linear filter L is dependent on the background luminance E.

The internal threshold d is a quantity that is not accessible via any psychophysical measurement. However, all internal responses can be expressed in this threshold. Rewriting (1) we obtain

$$r(t)/d = \int_0^t \varepsilon(\tau) \frac{U_\delta(t-\tau)}{d} \, d\tau. \tag{3}$$

We now define the normalized impulse response

$$U_\delta(t)/d = NF \cdot U_\delta^*(t), \tag{4}$$

where
$U_\delta^*(t)$ = the amplitude-normalized impulse response
         (i.e. the peak is normalized),
NF = the norm factor.

The norm factor NF is the reciprocal of the amplitude factor needed for a Dirac excitation in order to obtain an internal response that reaches the threshold d. This is open to measurement and can be approximated by the measurement of the amplitude ε_ϑ of a pulse with duration ϑ, where ϑ is small with respect to the time constants of the system. The norm factor is then given by

$$NF = \frac{1}{\varepsilon_\vartheta \, \vartheta}. \tag{5}$$

Note that the norm factor can be measured by any ϑ within Bloch's region.

The noise $n(t)$ can be measured with respect to its distribution function by measuring the psychometric function of, for instance, an impulse. Like the situation with the norm factor, the noise can be measured in threshold units only. This noise can then be modelled as a normal distribution, a log-normal distribution (Roufs, 1974b) or a Weibull distribution (Weibull, 1951). However, measurement of the noise is still problematic, because of large drift effects (Roufs and Blommaert, 1981; Watson, 1982; Blommaert and Roufs, 1987), and because different experimental procedures (method of constant stimuli, two alternative forced choice methods) seem to yield different experimental results (Nachmias, 1981; McKee *et al.*, 1985).

The amplitude-normalized impulse response $U_\delta^*(t)$ can be obtained psychophysically by using a perturbation technique (Roufs and Blommaert, 1981). This experimentally determined normalized impulse response $U_\delta^*(t)$ can be modelled using a fourth-order linear causal filter (chapter 4) by

$$\mathcal{L}\{U_\delta^*(t)\} = \hat{H}(s) = \frac{A\,(s-z)}{(s-p_1)(s-p_1^*)(s-p_2)(s-p_2^*)}, \tag{6}$$

where

$\mathcal{L}$ denotes the Laplace transformation,

$p_1,\ p_2$ are the (complex) poles of the transfer function $\hat{H}(s)$,

$p_1^*,\ p_2^*$ are complex conjugates of the poles p_1 and p_2 respectively,

z is the zero of the transfer function $\hat{H}(s)$,

A denotes a multiplication factor such that $\hat{H}(s)$ is the
           Laplace transform of a normalized impulse response.

However, in this article we will take a sixth-order linear filter as our model for the transient system, since it is not possible to reconcile De Lange data (TMTF, Temporal Modulation Transfer Function) with a fourth-order filter (chapter 5). The model now used is a simple elaboration of (6), where two (complex conjugated) poles (p_3, p_3^*) are added. The transfer function $\hat{H}(s)$ becomes

$$\mathcal{L}\{U_\delta^*(t)\} = \hat{H}(s) = \frac{A\,(s-z)}{\prod_{i=1}^{3}(s-p_i)(s-p_i^*)}. \tag{7}$$

Assuming that all the poles are simple, the impulse response $U_\delta^*(t)$ can be expressed as

$$U_\delta^*(t) = \sum_{i=1}^{3}\left\{R_i \exp\{p_i t\} + R_i^* \exp\{p_i^* t\}\right\}, \tag{8}$$

where R_i (i=1,2,3) are the (complex valued) residues given by

$$R_i = \frac{A\,(p_i - z)}{(p_i - p_i^*)\prod_{k=1,k\neq i}^{3}(p_i - p_k)(p_i - p_k^*)}, \qquad i = 1,2,3. \tag{9}$$

and R_i^* is the complex conjugate of R_i.

Apart from problems with respect to the noise characteristics, the system as shown in Figure 1 is completely open to psychophysical experiments, except for the threshold itself. Therefore we use a transfer function $H(s)$ which is expressed in threshold units:

$$H(s) = \mathcal{L}\left\{\frac{U_\delta(t)}{d}\right\} = NF\,\mathcal{L}\{U_\delta^*(t)\}, \tag{10}$$

which according to (7) leads to

$$H(s) = NF\frac{A\,(s-z)}{\prod_{i=1}^{3}(s-p_i)(s-p_i^*)}. \tag{11}$$

Basically, (8) expresses that the impulse response consists of a sum of damped sinusoids. There are several reasons for choosing this set of fundamental functions. To start with, it is a mathematical convenient description that is often used in engineering. The filter is of finite order and so the model is a lumped system. Secondly, these kind of responses provide a good description of many physical systems, including feedback systems. Transmission between nerve cells is often described as a feedback mechanism, and the linear part of responses of nerve cells is usually described by biphasic impulse responses (Naka, 1982; Daly and Normann, 1985). If the real part of a pole is not too small with respect to the imaginary part, the response associated with a pole pair (p_i, p_i^*) can be considered to be an approximation to these kind of responses. In this way it was hoped that fitting the chosen filter (7) to the impulse response data is more than mere curve fitting, but might be helpful in exposing underlying mechanisms.

7.3 Estimated sixth-order linear filters

The filter $\hat{H}(s)$ (eq. (7)) was fitted to the experimentally determined impulse responses (Roufs and Blommaert, 1981; Blommaert and Roufs, 1987). The results of the fits for different subjects at 1200 and 100 Td for 1 degree fields without surround are shown in Table 1. First of all the estimated standard deviation s_{e6} is shown, given by (Bard, 1974)

$$s_{e6} = \frac{\Psi_6}{M-N} \tag{12}$$

where
Ψ_6 = the sum of squared residuals at the optimal parameter set,
M = number of measured data points,
N = number of degrees of freedom in the fit ($N = 7$, three complex conjugated pole pairs and one zero).

Next the mean measured standard deviation s_m is shown. This was calculated according to

$$s_m^2 = \frac{1}{M}\sum_{i=1}^{M} s^2(t_i), \tag{13}$$

where $s(t_i)$ is the measured standard deviation of the mean at the i-th sampling moment t_i. For comparison we also tabulated the estimated standard deviation s_{e4} of the fourth-order filters (from chapter 5).

subject	JR74	JR	FB	JP	LT	HD	IH	LT	HR	JW
background (Td)	1200	1200	1200	1200	1200	1200	1200	100	100	100
s_{e6}	.118	.074	.105	.112	.119	.125	.138		.114	.243
s_m	.120	.086	.074	.112	.139	.118	.106	.109	.113	.170
s_{e4}	.144	.099	.127	.131	.115	.143	.154	.096	.124	.247
α_1 (s^{-1})	-10.9	-12.0	-10.4	-15.0	-15.1	-15.4	-15.6		-17.8	-9.9
β_1 (s^{-1})	36.0	39.0	47.4	37.8	44.9	42.9	37.6		25.0	22.1
α_2 (s^{-1})	-14.6	-16.9	-15.1	-18.5	-15.2	-17.4	-15.9		-18.6	-9.7
β_2 (s^{-1})	66.8	70.7	82.1	73.4	82.2	83.7	77.9		45.5	44.1
α_3 (s^{-1})	-11.6	-13.4	-11.1	-12.0	-19.0	-15.4	-10.8		-14.6	-6.8
β_3 (s^{-1})	114.1	118.2	131.1	117.3	125.1	143.8	117.6		69.2	65.4
z (s^{-1})	12.4	6.6	12.9	7.2	14.9	10.5	29.4		27.9	8.8
A (10^8s^{-4})	-.412	-.495	-.575	-.543	-.635	-1.080	-.440		-.108	-.052
NF $(\text{Td}^{-1}\text{s}^{-1})$	0.68	0.90	1.20	1.09	0.59	0.44	1.01	3.86	7.46	4.59

Table 1: Results of the fits of a sixth-order filter to experimentally determined impulse responses of the transient visual system.

From comparison of s_{e6} and s_{e4} we find that there is an improvement of the fit with a sixth-order linear filter over a fourth-order filter. Only for subject LT at 1200 Td do we find that the reduction of Ψ does not weigh up to the increase in free parameters: s_{e6} is larger than s_{e4}. But then, in this case the estimated standard deviation of the fourth-order fit is already smaller than the measured standard deviation. The improvement of s_{e6} over s_{e4} is greater for the 1200 Td data than for the 100 Td case. The estimated standard deviation s_{e6} agrees nicely with the mean measured one (s_m), indicating that good fits to the experimental data are provided by the filter (7).

Below the estimated standard deviations we find in Table 1 the estimated parameters p_1, p_2, p_3 and z. The poles are split into two real valued parameters:

$$p_i = \alpha_i + j\,\beta_i, \qquad i = 1,2,3, \qquad j = \sqrt{-1}, \qquad (14)$$

where α_i is the i-th damping parameter and β_i the i-th angular frequency parameter. In all cases the indexes for p were taken such that $|p_1| < |p_2| < |p_3|$.

All poles (p_1, p_2, p_3) and the zero z for the estimated filters at 1200 Td each cluster in a specific region in the s-plane, as is shown in Figure 2A. Roughly

A
1200 Td
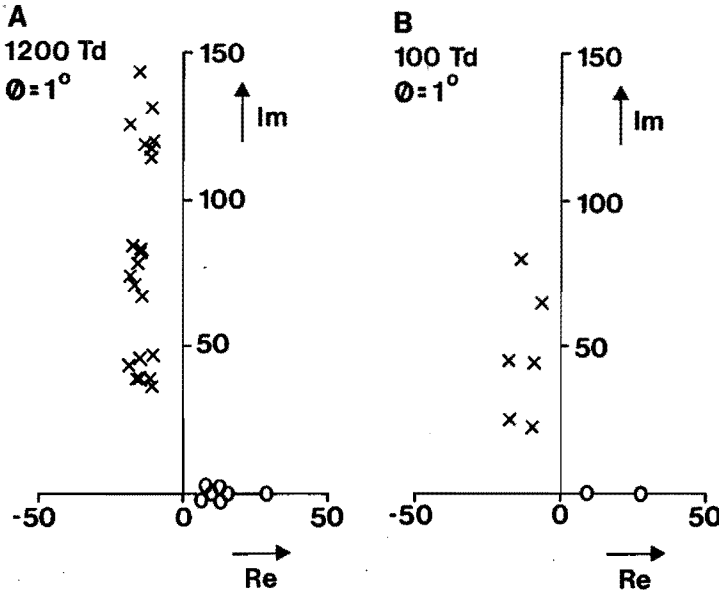**∅ = 1°**

B
100 Td
∅ = 1°

Figure 2: Pole-zero plot of the estimated parameters of the sixth-order linear filter. The horizontal and vertical axes are the real and imaginary axes respectively. Units along the axis are expressed in s^{-1}. The lower half of the s-plane has been omitted in the plot. The crosses and circles are the estimated poles and zeros, respectively. **A.** Estimated poles and zeros of 1 degree fields at 1200 Td for seven subjects. **B.** Estimated poles and zeros of 1 degree fields at 100 Td for two subjects.

speaking, we could introduce $\alpha_1 = \alpha_2 = \alpha_3 = -z = -15$, and $\beta_3 = 1.5\beta_2 = 3\beta_1 = 120$ as a smoothed parameter set of a "standard" subject at 1200 Td.

For the 100 Td level we have data sets of three subjects. For one of these sets (subject LT) the pole p_3 was shifted to very large values in the estimation process: $|p_3| \gg |p_2|, |p_1|$. In that case the estimate obtained is essentially a fourth-order filter. In other words, we could not fit a sixth-order filter to these data. In this case too the estimated standard deviation of the fourth-order fit is already smaller than the measured standard deviation, indicating a very accurate fourth-order fit.

For the 100 Td level the location of the poles and zeros is not as clear as for the 1200 Td level. First of all there are only two subjects for which the parameters could be estimated, the improvement from fourth to a sixth-order filter is only small, one data set (JW) is extremely noisy, and the 90%-confidence region in the s-plane around each pole is considerably larger for the sixth than for the fourth-order estimates. (At 1200 Td the confidence region around each pole in the sixth-order estimates is about as large as for the fourth-order.)

It seems that a sixth-order filter is easier to fit at high than at low background

levels: at lower levels there is less improvement in the estimated standard deviation and the confidence regions are increasing going from a fourth to a sixth-order estimation. This means that care has to be taken in drawing conclusions about shifts in the parameters if we are to base these (also) on the results of the estimated parameters at 100 Td.

Nevertheless, if the parameters at the 100 Td level are plotted (Fig. 2B) in the same way as for the 1200 Td case (Fig. 2A), it can be seen that the norm of pole p_i is smaller in the 100 than in the 1200 Td case, but the structure of the poles is strikingly the same: $\beta_3 \approx 1.5\beta_2 \approx 3\beta_1$. However, as already mentioned, we have to be careful with such observations since especially pole p_3 is not as well-conditioned as one would like.

Now we postulate the following: the parameters α_1, α_2 and z are independent of background level, and the parameters α_3, β_1, β_2 and β_3 each change by the same proportional amount with a change in background. This ad hoc postulated change is similar to what was found for the parameters of the fourth-order filter, and is a refinement on the assumption of isomorphous impulse responses at different background levels (see furtheron), where the refinement consists of a change towards a filter with a more pronounced bandpass character for higher background levels (see chapter 5). We will confront this postulate with data of threshold-versus-duration curves and with De Lange characteristics in the sequel of this paper. But first we will show that starting from the estimated parameters of LT at 1200 Td, given the postulated shift, we are able to obtain a good representation of the 100 Td experimental data of the impulse response (of the same subject LT). Essentially, we are performing an estimation with one free parameter: the shift in several parameters.

If the parameters α_3, β_1, β_2 and β_3 (LT, 1200 Td) are multiplied by a factor $\mu = 0.56$, an impulse response is obtained which is similar to the experimental data of LT at 100 Td, as is shown in Figure 3. Plotted here are the impulse response of the estimated sixth-order filter together with the experimental data points at 1200 Td (top curve), and the impulse response from the shifted parameters together with the 100 Td data (bottom curve). The estimated standard deviation for the 100 Td level is $s_e = 0.125$, and is close to the mean measured standard deviation s_m (see Table 1).

This postulated parameter shift gives not only a good fit to the data of subject LT (100 Td), but also an interpretation of why a sixth-order filter is harder to estimate from the experimental data at lower than at higher background levels. The ratios α_1/β_1 and α_2/β_2 (the damping ratios) are smaller at lower background levels, and consequently the amplitude spectrum associated with these poles changes into a more low-pass characteristic for lower backgrounds. Therefore the activity of pole p_3 (and p_3^*) in the amplitude spectrum falls more and more in the cut-off caused by the other poles, and less in the dominant frequency range of the spectrum. This means that, at the lower backgrounds, the pole-pair (p_3, p_3^*) only influences how fast (or slow) the impulse response starts. This, in turn, is hard to
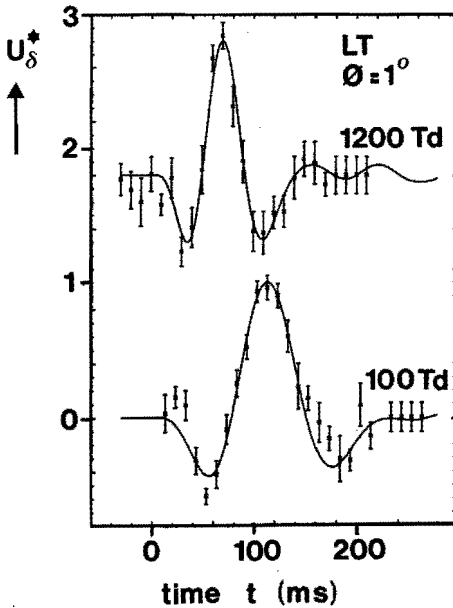
Figure 3: Experimentally determined normalized impulse responses and estimated impulse responses from a sixth-order linear filter. Subject LT for a 1 degree field without surround at 100 and 1200 Td. For clarity, the 1200 Td curve is shifted upward over 1.8 units.

estimate from an impulse response measurement in which the starting moment is unknown (as is the case with the perturbation technique).

7.4 Parameter changes with background

In the foregoing it was shown that the parameters of a sixth-order filter at 1200 Td can be shifted in such a way that the filter forms a description of the 100 Td measurement data. We postulate this as a general property of the transient system and will confront this with other experimental data. In mathematical notation the postulate reads:

$$p_1(E) = \hat{\alpha}_1 + j\,\hat{\beta}_1\,\mu(E), \qquad (15)$$

$$p_2(E) = \hat{\alpha}_2 + j\,\hat{\beta}_2\,\mu(E), \qquad (16)$$

$$p_3(E) = \hat{\alpha}_3\,\mu(E) + j\,\hat{\beta}_3\,\mu(E), \qquad (17)$$

$$z(E) = \hat{z}, \qquad (18)$$

$$A \cdot NF = \hat{A} \cdot \hat{NF}, \qquad (19)$$

where $\mu(E)$ is a real valued function of the background E, and $\hat{\alpha}_1$, $\hat{\beta}_1$, $\hat{\alpha}_2$, $\hat{\beta}_2$, $\hat{\alpha}_3$, $\hat{\beta}_3$, $\hat{z}$, $\hat{A}$ and $\hat{NF}$ are the filter parameters for that value of E for which $\mu(E) = 1$.

These relations ((15) to (18)) state that p_3 moves along a line through the origin, that p_1 and p_2 move along a line parallel to the imaginary axis, and that the location of z in the s-plane is constant. They also state that all the shifts in parameters occur by the same factor. The only degree of freedom that is left is the relation $\mu(E)$. Taking $A \cdot NF$ constant ensures that the high frequency asymptotes of the filter for all μ coincide.

The function $\mu(E)$ is a monotonically increasing function, as can be seen from the De Lange curves (Figure 8A) and the assumed parameter shifts ((15) to (18)). The De Lange curves are tuned to higher frequencies for higher background levels E. From (15) to (18) it is also clear that any increase in μ is an increase in the bandwidth. From this we conclude that $\mu(E)$ is a monotonically increasing function, whose numerical relation is yet to be established.

Note that the suggested parameter shift is somewhat more complicated than the isomorphy of the impulse responses at different background levels, as was suggested by Roufs (1974a), Roufs and Blommaert (1981) and Blommaert and Roufs (1987). If the impulse responses at different background levels were isomorphous all the poles and zeros would be shifting along straight lines through the origin.

However, in the suggested parametric shift ((15) to (18)) there is still a large amount of isomorphy. This can be seen from Figure 4, where the normalized impulse response of LT is plotted at 100 Td ($\mu = 1$, the same as for the bottom curve of Fig. 3) and for $\log \mu = -0.2$ and $+0.2$, using the sixth-order filter. The main change in these impulse responses is still a change in the scale of the time axis (as would be the case for isomorphy), but there is also a change in the depth of the negative phases with respect to the positive, which in fact can also be noted in the experimental data on impulse responses in Fig. 16 of Roufs and Blommaert (1981).

7.5 Simulations of the model with parametric changes

We start the simulations by taking the parameter values of the sixth-order linear filter $F(s)$ for LT at 100 Td and subsequently calculating the poles according to ((15) to (18)) for several μ factors. The response of the system can now be calculated to an arbitrary stimulus $\varepsilon(t)$.

Threshold-versus-duration curves

In Figure 5 the threshold-versus-duration curves for the system are plotted at 100 Td, and for different μ values. This plot agrees with experimental data (e.g., Blommaert and Roufs, 1981). From Figure 5 we take two characteristic quantities: the critical duration T_{ca} (which is the duration ε at the intercept of the two asymptotes for short and long duration) and the sensitivity factor F_a (which is the inverse of the amplitude ε_l for long durations; see Roufs (1974a) and Blommaert and Roufs (1987)). The critical duration T_{ca} and the sensitivity factor F_a can
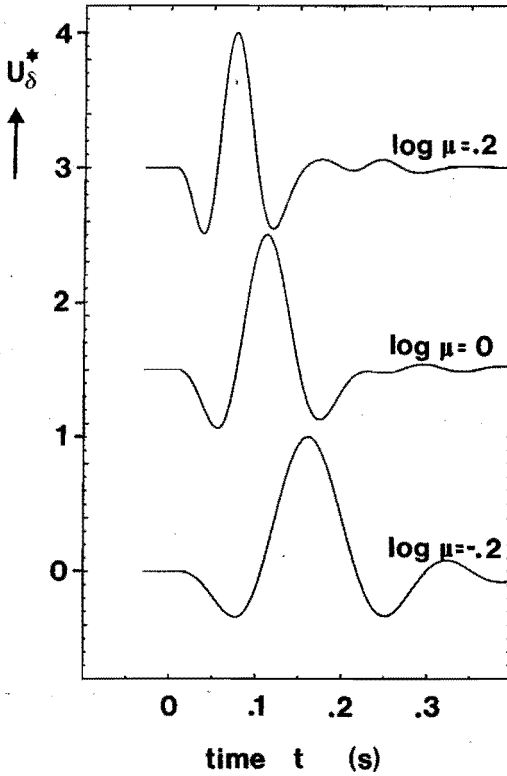
Figure 4: Normalized impulse response from sixth-order model for three different multiplication factors μ. For $\mu = 1$ the impulse response stems from the parameters of the sixth-order filter for subject LT at 100 Td for a 1 degree field without surround. For clarity, the curves for $\log \mu = 0$ and 0.2 have been shifted upward over 1.5 and 3.0 units, respectively.

thus be plotted as a function of the shift μ of the parameters with respect to the 100 Td level. From simulations like those in Figure 5 it can be shown that for $\log \mu \in [-0.5, 0.5]$ the relation between F_a and μ can be approximated as a linear one on a log-log basis, by

$$\log F_a = k_1 \log \mu + C_1, \tag{20}$$

where $k_1 = -4.2$ and $C_1 = -0.9$. Both values (k_1, C_1) are subject-dependent. Note that the value of k_1 is close to the relation that is expected from a parameter shift for isomorphy (see Appendix).

Figures 6A and 6B show experimental data of the sensitivity factor F_m and the critical duration T_{cm}, respectively, as a function of the background level E (re-
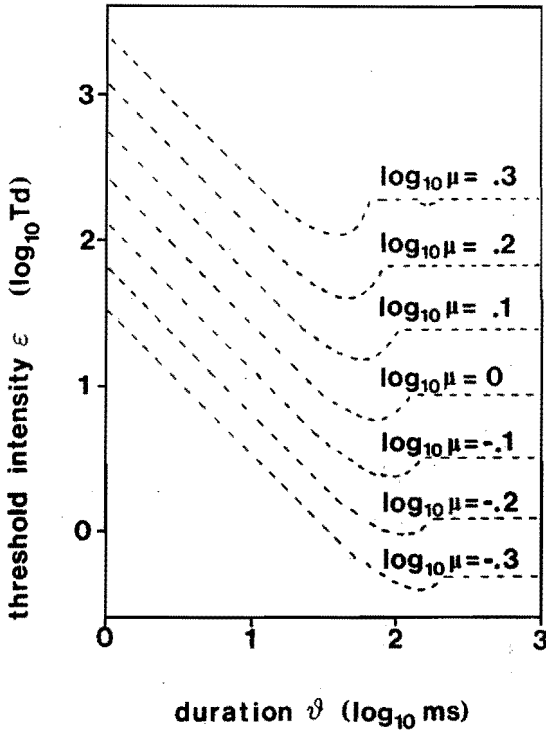
Figure 5: Threshold-versus-duration curves for the 100 Td level ($\mu = 1$) and for several parametric shifts μ (see text). Subject LT, 1 degree field.

plot from Roufs, 1972). T_{cm} and F_m are experimentally obtained values according to the Graham and Kemp (1938) definition. In these definitions the dip in the threshold-versus-duration curves is not recognized (Roufs, 1974a). Therefore the values of T_{cm} and F_m will be estimated larger than T_{ca} and F_a for the same experimental data. Furthermore, if the transient system acts in accordance with the suggested parameter shift, the difference between estimates of the critical duration and the sensitivity according to these two definitions will be larger at higher background levels. Nevertheless, as a first-order approximation, we will regard the experimental data from Figures 6A and 6B as if they reflected T_{ca} and F_a, respectively.

The experimental data can be approximated by

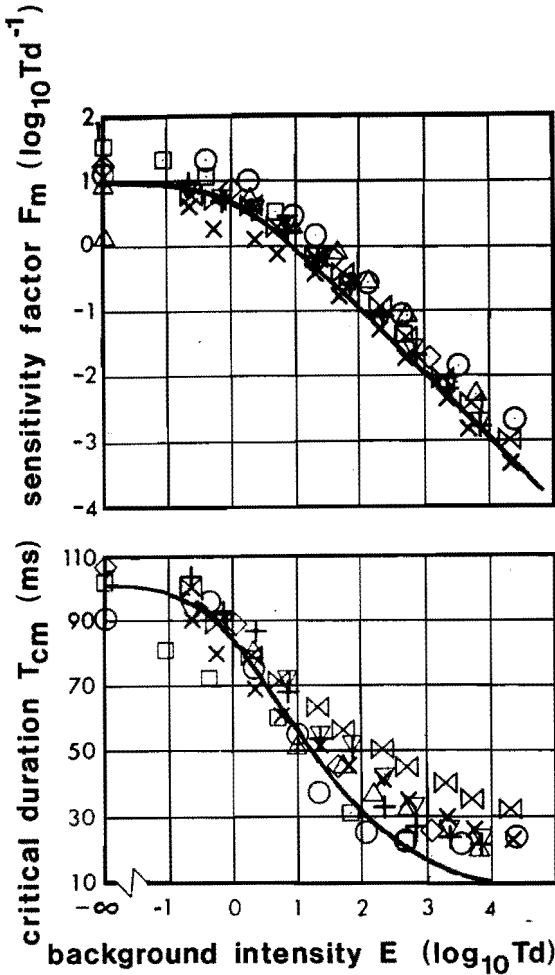$$\log F_m = k_2 \log \left(1 + \frac{E}{E_0}\right) + C_2, \tag{21}$$

Figure 6: **A.** Experimental data on the sensitivity factor F_m as a function of E. The continuous line is the sensitivity F_a according to the sixth-order model, using (22). **B.** Experimental data on the critical duration T_{cm} versus the background level E. The continuous line gives the critical duration T_{ca} as a function of the background intensity E, according to (22). Both figures are replots from Roufs (1972). Different symbols indicate different subjects.

where $k_2 = -0.91$ (Roufs, 1972) and $E_0 \approx 1$ Td. The numerical value of E_0 was taken 1 Td for convenience, but might be a value that depends on the subject. This relation (21) is an approximation of the experimental data of Figure 6A for not too large E ($E < 1000$ Td, see discussion).

In order to have agreement between the experimental data and the simulated

model, and on the assumption that F_m is a suitable approximation of F_a, we find that the function $\mu(E)$ must obey the following relation:

$$\log \mu = k \, \log \left(1 + \frac{E}{E_0}\right) + C, \qquad (22)$$

where $k = k_2/k_1 = 0.22$ and where $C = -0.44$ (which follows from the requirement that $\mu = 1$ for $E = 100$ Td). This relation is shown in Figure 7.
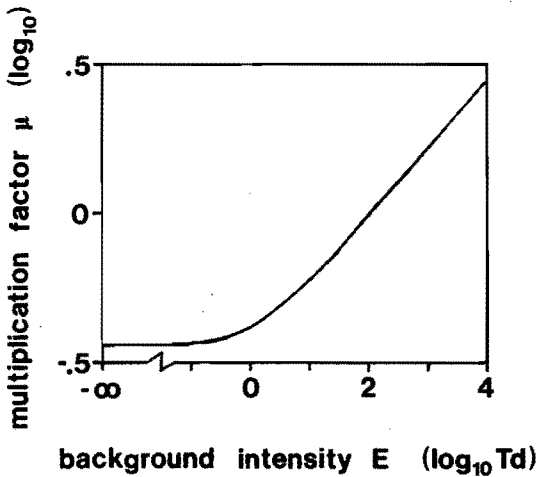

Figure 7: The relation between the parameter shift μ and the background level E. Starting points are the 100 Td parameters of LT, 1 degree field ($\log \mu = 0$).

With relation (22) the model simulations of the sensitivity and critical duration as a function μ can be plotted as functions of the background level E. These are shown as the continuous lines in Figures 6A and 6B.

The measured sensitivity and simulations of the model are in good agreement with the given choice of relation between μ and E (eq.(22)). In Fig. 6B the measured critical duration T_{cm} is plotted together with the simulated behaviour of T_{ca}. For low background levels there is a good agreement between these data. For higher background levels (10-1000 Td) the continuous line T_{ca} takes on smaller values than (most of) the measured T_{cm}, which is also predicted in the model, since at these higher background levels a significant difference in these two values is caused by the fact that the dip in the threshold-versus-duration curve is increasing. Above 1000 Td the behaviour of T_{ca} and that of T_{cm} do not agree, even if the

difference in definition of critical duration is taken into account. This is presumably due to the fact that at these background levels the system is unable to adapt the time constants of the system (e.g., Fig. 8 in Kelly, 1961), which means that we are extrapolating our predictions too far (see also the Discussion).

De Lange curves

A classic measurement in psychophysical vision research is the measurement of a De Lange curve, which is a plot of the reciprocal of the detection amplitude (or modulation depth) of a sinusoidal stimulus versus the frequency of the sinusoid. Some experimental data are shown in Figure 8A (from Roufs, 1972). In such De Lange curves the filter characteristics of the transient system are reflected. But, contrary to what is often assumed (Gorea and Tyler, 1986; Georgeson, 1987; Stork and Falk, 1987), the gain characteristics of the linear filter of the model (Figure 1) do *not* equal a De Lange curve.

The reason for this is twofold. We assumed a two-channel model. The De Lange curve reflects the activity in both channels and is usually regarded as the envelope of the gain characteristics of the sustained as well as of the transient system (Roufs, 1974a; Roufs and Blommaert, 1981). Since the sustained channel is low-tuned and the transient one high-tuned, we can only compare the high frequency side of the De Lange curve with the high frequency side of the gain characteristics of the transient channel. Secondly, since our model (Figure 1) includes a noise source N, the detection is *not* deterministic and the De Lange curve will reflect part of the stochastic behaviour. Experimentally, it is well known that the detection amplitude of a sinusoid depends on how long the sinusoid is presented to the observer (Roufs, 1974b; Roufs and Pellegrino van Stuyvenberg, 1976).

At different background levels the stochastics are much the same. The Crozier coefficient, which is the ratio of the standard deviation σ of the noise N and the threshold d, is constant over a large range of background levels (Roufs, 1974b). The reduction of the threshold amplitude as a consequence of the stochastic nature of the model should therefore be equal at different background levels, assuming that the same experimental conditions are used.

Bearing the above remarks in mind, we can compare some actually measured De Lange curves (Figure 8A, from Roufs, 1972) with the gain characteristics of the linear filter of the transient channel (Figure 8B). Unfortunately, we do not have the De Lange curves of subject LT for the same experimental conditions as the impulse responses. Furthermore, in the experiments that were performed to obtain Figure 8A, an unlimited inspection time was used. This means we do not know how to account for the probability summation quantitatively at different frequencies. Nevertheless a qualitative comparison can be made.

Similar to the threshold-versus duration curves we now look at the gain curves of the linear filter with varying μ (Figure 8B), and from these we choose the cut-off frequency f_c (frequency with a gain 0.3 log unit below the peak value) and the
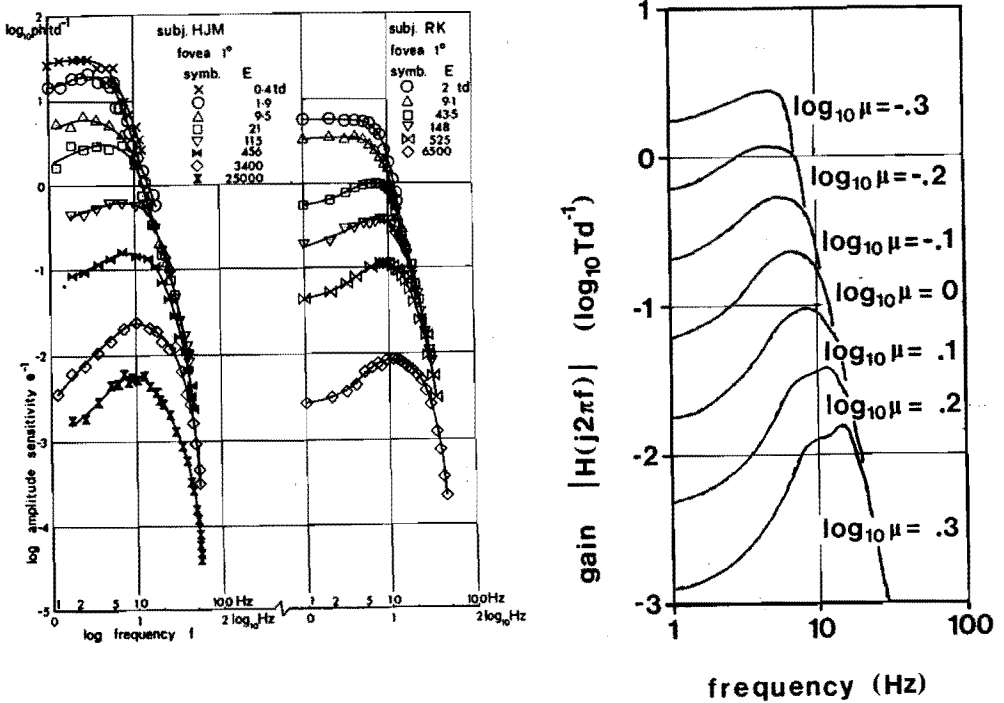
Figure 8: **A.** De Lange curves for two different subjects at different background levels. Reprinted with permission from Vision Research **12**, J.A.J. Roufs, Dynamic properties of vision.-I, copyright 1972, Pergamon Journals Ltd. **B.** Gain characteristic $|H(j2\pi f)|$ of the linear filter L for the sixth-order model for several multiplication factors μ, subject LT, 1 degree field (see text).

sensitivity S (the peak of the curve) as characteristic quantities. These are plotted in Figure 9A and 9B versus the background level E, according to (22), together with experimental data (replot from Roufs, 1972). The shapes of these curves are in nice agreement. The difference between the calculated and the experimental sensitivity S is about 0.4 log unit, which is about the difference one would expect from probability summation (Roufs and Pellegrino van Stuyvenberg, 1976; Roufs et al., 1984). The behaviour of the cut-off frequencies predicted from the model is in agreement with the experimental results, but the continuous line is slightly lower than the experimental data. This difference may be caused by the fact that the relation between μ and E may not be as appropriate as it seems (given the

difference in definition of the sensitivities F_a and F_m).
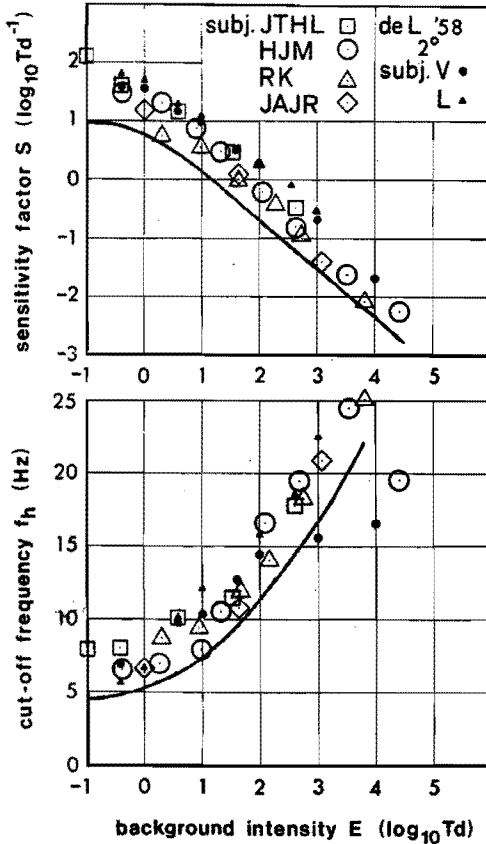
Figure 9: **A.** Experimental data on the sensitivity factor S versus the background level E. The continuous line gives the sensitivity factor S as a function of the background intensity E, according to (22). **B.** Experimental data on the cut-off frequency f_h as a function of the background level E. The continuous line gives the cut-off frequency f_h as a function of the background intensity, according to (22).

The difference between the low-frequency parts of the gain characteristics and the De Lange curves of 1 degree fields without surround is larger than would be expected as an effect of probability summation. This is in agreement with the two-channel assumption: the sustained system determines the sensitivity for this frequency range.

In Figure 10 the value of the low-frequency asymptote predicted from the model is shown versus E, again using relation (22). For background levels between 1 and 1000 Td the DC component is approximately inversely proportional to the background level, as is shown by the dotted line in Figure 10. Around these background levels the modulation depth for low frequencies, given by $m^{-1} = H(0) E$, is about 6.
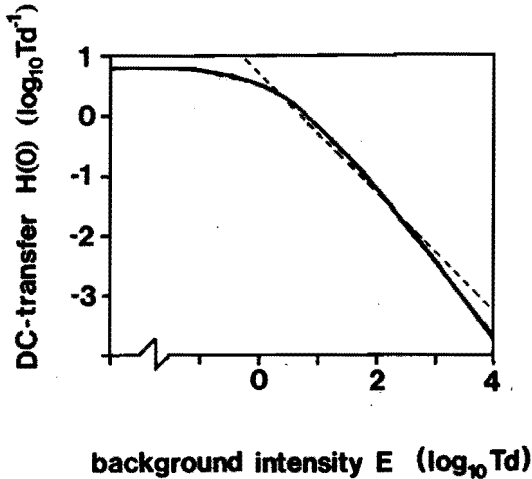

Figure 10: DC component of the gain characteristics of the linear filter of the transient system as a function of the background level E according to the sixth-order filter $H(s)$. The dotted line gives the relation $H(0) \propto 1/E$.

7.6 Discussion

In this article a sixth-order linear filter is proposed for the transient channel of the visual system. The parameters of this filter can be estimated from an experimentally obtained normalized impulse response. The sixth-order filter describes the impulse response as a summation of damped sinusoids (8). In the previous sections we argued that by this choice the parameters of the filter appear to change with background level according to a simple mathematical formulation. However, there may be other basic functions that perform as well as a description of the impulse responses. Furthermore, it does not rule out the possibility that other choices of basic functions can provide an equally neat description of changes of the parameters with background.

Some of the parameters of the filter (7) at different background levels are assumed to be independent of the background level, the others are assumed to have the same proportional shift going from one background level to another. This parameter shift is assumed to account for background levels somewhere between

1 and 1000 Td. For low background levels (beneath 1 Td) the system seems to be independent of the background level (for small excursions). There seems to be no adaptation to the stimulus (background), probably as a consequence of the fact that the limiting factors in detection are not governed by the stimulus condition but by the internal noise (Shapley and Enroth-Cugell, 1984). Between 1 and 1000 Td the system seems to adapt to the background by changing the time constants of the filter. The gain factor of the filter $A \cdot NF$ (see eq.(7)) is invariant. Above 1000 Td the system no longer changes, except for its sensitivity. This can be seen from the De Lange curves at high background levels; the high frequency asymptotes do not coincide any longer at high background levels. This is an effect for which the assumed model could account by postulating a saturation effect in the shift of the poles and zeros of the transfer function at these levels. This saturation effect in the shift of the poles should probably be attributed to the limited speed of transfer of information in and between neurons. A refinement of the model would consist in adapting the gain factor for backgrounds where the time constants (the poles and zeros) can no longer be adjusted. This would agree with Figure 6B, where it is shown that the critical duration seems to level off to some steady value, and also with Figures 8A and 6A, where it can be seen that there is still a steady drop in the sensitivity factors F and S. We did not incorporate this refinement because of a lack of experimental data for these high levels.

The assumed parameter shift was evaluated by comparing the performance of the filter for block stimuli of variable duration with experimental data. The model could be made to agree with the experimental data by means of an adequate relation between the parameter shift μ and the background level E. This derived relation is not quite accurate because the simulation and the experimental data essentially used different definitions for the sensitivity factor F and the critical duration T_c. But as a first order approximation this relation between the parameter shift and the background level should suffice.

Comparison of the gain characteristics of the linear filter and De Lange curves showed that the qualitative performance of the model agrees well with the experimental data. The quantitative difference can presumably be attributed to probability summation, but it is an effect that has to be evaluated by more careful experiments. Part of the difference might also be caused by the inaccuracy in the relation $\mu(E)$.

The proposed parameter shift is a convenient one since as far as the parameters change with background, they change by the same proportional amount. However, equally convenient parameter shifts (like isomorphy) cannot be ruled out on the basis of the experimental data used here (sensitivity factors, critical duration and cut-off frequency). On the other hand, the experimental data of Swanson *et al.* (1987) on threshold-versus-duration curves show more pronounced dips for higher background levels. This agrees with the suggested parameter shift (see Figure 5B), and argues against the isomorphy assumption. Also, the impulse response which Roufs and Blommaert (1981) measured at 2 Td seems to have less pronounced

negative phases than those at 1200 Td, which is also in agreement with our simulations (see Figure 4). The behaviour of the system was also tested for parameter shifts in which all poles were located on straight lines along the imaginary axes, i.e. (17) replaced by $p_3(E) = \hat{\alpha}_3 + j\,\hat{\beta}_3\,\mu(E)$. With an appropriate choice of $\mu(E)$ the behaviour is vastly similar to the one proposed earlier, and no preference for one or the other can be made on the now available data.

As already argued, the low-frequency sides of the De Lange curves of 1 degree fields without surround do not agree with the gain characteristics of the linear filter of the transient system, presumably because of the interfering interaction of the sustained system at these frequencies. However, the simulation seems to agree with the experimental results of Kelly (1961) for edgeless fields. A possible explanation is that edgeless fields do effectively suppress the sustained system in such a manner that the De Lange curves of these fields reflect the transient channel only. However, there is a difference of about 0.4 log unit between these experimental results and our simulations. At these low frequencies it is not clear whether such a difference can be attributed to probability summation.

The model considered here is a black box model only; a relation was found between the parameters of the model and the background level, but its actual (physiological) realization is still questionable. To obtain insight into possible mechanisms for realizing such parameter changes with background, it may be worth looking at electrical equivalents of sixth-order filters that can give this kind of behaviour.

The potentials of an analysis of the behaviour of the transient system in a linear model described by poles and zeros are not fully explored in this paper. We will only briefly touch upon this by making two suggestions for interpretation of the estimated filters.

The first interpretation is as follows. The sixth-order filter can be thought of as resulting from a cascade of filters. Suppose the sixth-order filter characteristics evolve from two filters in cascade, the first described by the pole pair (p_2, p_2^*) and the second by the other poles plus the zero z. It can be shown that the impulse response of the second filter resembles that of a filter that is matched to an incoming signal which is equivalent to the impulse response of the first filter. This means that this system is optimal for detection of fast changing input signals if the (main part of) noise that is introduced in the processing is white, additive and is introduced in between the two filters. The latter could be the case if the filter (p_2, p_2^*) is located in the retina and noise is introduced in the transmission of the responses from the retina to the cortex, and the second filter is the detection unit in the cortex. We hope to present such an analysis elsewhere.

A second possible interpretation is to see the sixth-order linear filter as stemming from three parallel pathways, which act as linear filters, each characterized by one pole pair. The responses of these filters are then linearly combined. This scheme is reminiscent of the proposal made by Kelly (1962), who argued that the De Lange characteristic of edgeless fields are built up from three separate colour-

sensitive pathways. Moreover, these three parallel filters would be most sensitive to (about) 7, 13 and 20 Hz at 1200 Td (namely $|p_1|/2\pi$, $|p_2|/2\pi$ and $|p_3|/2\pi$, respectively), which is in reasonable agreement with the findings of Kelly (1962) at a background level of 850 Td. In that interpretation the pole pairs (p_1, p_1^*), (p_1, p_1^*) and (p_3, p_3^*) would be associated with the blue-, green- and red-sensitive channels, respectively. But contrary to the arguments of Kelly (1962), our scheme would imply that each of the pathways is adaptable with respect to its time constants. This interpretation too needs careful consideration.

The suggested parameter shift, along with the assumption of coinciding high-frequency asymptotes, has an almost equal common low-frequency modulation over different background levels. Alternatively, the suggested parameter shift, along with the assumption of a constant low-frequency modulation depth, will give (almost) coinciding high-frequency asymptotes. The latter can be realized by a feedback mechanism which tries to achieve a constant DC response. This leads to a model for the transient visual system described by a closed-loop adaptive filter. This is an attractive possibility since it would imply that we do not need an independent mechanism to measure the background level E in order to set the parameters of the transient system (see Figure 1). Also, the artificial difference between background level E and the variation on this background $\varepsilon(t)$ is cancelled, as shown in Figure 11. The output of filter $H(s)$ is the input of a lowpass filter with cut-off frequency f_c somewhere below $z/2\pi$. The output of this lowpass filter is a measure of the lowpass component of the output of filter $H(s)$. This signal can be compared with some reference level, and, depending on the output of the comparator, the parameters can be adjusted to higher or lower values. How fast this adaptive process is depends to a great extent on the cut-off frequency of the lowpass filter. If this cut-off frequency f_c is about equal to $z/2\pi$, then this scheme (Figure 11) reflects a very fast adaptive mechanism.

If such a closed-loop adaptive filter exists in the transient system, then it is also clear why there is a separate mechanism, the sustained system, to process low temporal frequencies: the suggested adaptive filter is inherently unable to give information about the low temporal frequencies.

An interesting device for further research is the closed-loop adaptive filter. For instance, if we were to extrapolate the model to account for suprathreshold experiments by replacing the threshold device by a memoryless compressive nonlinearity (Roufs and Pellegrino van Stuyvenberg, 1979) we would undoubtedly predict the Broca-Sulzer phenomenon (this being inherently present in the impulse response; see de Ridder, 1987). Also, it is possible that the adaptive model can account for the shift in the Broca-Sulzer effect at low background levels, and for its stationary behaviour (independent of flash luminance) at higher background levels, as was found in the brightness-matching experiments reported by de Ridder (1987).

In conclusion we state that sixth-order linear filters can explain subthreshold measurements of impulse responses, threshold-versus-duration curves and De Lange
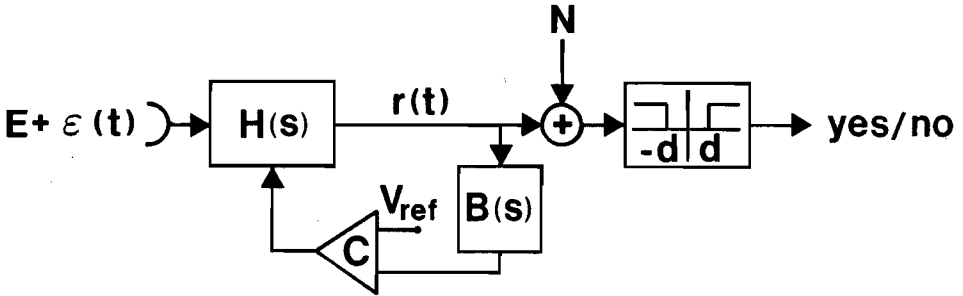
Figure 11: A closed loop adaptive filter as a model for the transient visual system. The model consists of a sixth-order linear filter $H(s)$, a lowpass filter $B(s)$ and a comparator C. The output of the lowpass filter is a measure of the low frequency component of the signal $r(t)$. The output of the comparator is used to adjust the parameters of $H(s)$.

data (with respect to the high-frequency side), for stimuli of larger extension (≈ 1 degree in diameter). All these data are associated with the transient visual system. At different background levels the system is able to change its parameters (time constants), which change can be described in a very simple way. Furthermore, this behaviour seems congruent with a closed-loop adaptive filter, where the steady output is used as a control signal. This adaptive filter might be able to give interpretations of various experimental psychophysical data that have not been discussed here, and may provide a link with physiological research.

Acknowledgements

Appendix. Changes of parameters for isomorphic impulse responses

Roufs (1971a) and Roufs and Blommaert (1981) suggested that impulse responses of the transient system at different levels are isomorphic. Using the sixth-order filter $H(s)$ as a model for the transient system the parametric shift $\mu(E)$ would be $p_i(E) = \hat{p}_i\,\mu(E)$, where $i = 1, 2, 3$, $z(E) = \hat{z}\,\mu(E)$, $A = \hat{A}$ and $NF = \hat{NF}\,\mu^{-5}(E)$, where μ is a multiplication factor depending on the background level E, and where $\hat{p}_1$, $\hat{p}_2$, $\hat{p}_3$, $\hat{z}$, $\hat{A}$ and $\hat{NF}$ are the parameters of the sixth-order filter for

which $\mu(E) = 1$. Further this would mean that $F_a \propto \mu^{-5}$, $T_{ca} \propto \mu^{-1}$, $S \propto \mu^{-5}$ and $f_h \propto \mu^1$. Similar to (22) we now obtain

$$\log \mu = k \, \log \left(1 + \frac{E}{E_0}\right) + C$$

where $k = 0.91/5$, $C = 0.36$ (subject LT) and (for convenience) $E_0 = 1$ Td. Since the numerical values (k, C) in this relation are close to the ones for the proposed non-isomorphic shift, figures of sensitivity factors, critical duration and cut-off frequency versus the background E will have a close resemblance to Figures 6 and 9.

References

Bard, Y. (1974) Nonlinear parameter estimation. New York: Academic Press.

Blommaert F.J.J., Roufs J.A.J. (1987) Prediction of thresholds and latency on the basis of experimentally determined impulse responses. Biol. Cyb. **56**, 329-344.

Breitmeyer B.G., Ganz L. (1976) Implications of sustained and transient channels for theories of visual pattern masking, saccadic suppression and information processing. Psychol. Rev. **83**, 1-36.

Buf J.H.M. du (1987) Spatial characteristics of brightness and apparent-contrast perception. Thesis, Eindhoven University of Technology.

Daly S.J., Normann R.A. (1985) Temporal information processing in cones: effects of light adaptation on temporal summation and modulation. Vision Res. **25**, 1197-1206.

Graham C.H., Kemp E.H. (1938) Brightness discrimination as a function of the duration of the increment sensitivity. J. gen. Physiol. **21**, 635-650.

Georgeson M.A. (1987) Temporal properties of spatial contrast vision. Vision Res. **27**, 765-780.

Gorea A., Tyler C.W. (1986) New look at Bloch's law. J. Opt. Soc. Am. A **3**, 52-61.

Green M. (1984) Masking by light and the sustained-transient dichotomy. Perc. and Psychophysics **35**, 519-535.

Kelly D. H. (1961) Visual responses to time-dependent stimuli. I. Amplitude sensitivity measurements. J. Opt. Soc. Am. **51**, 422-429.

Kelly D. H. (1962) Visual responses to time-dependent stimuli. IV. Effects of chromatic adaptation. J. Opt. Soc. Am. **52**, 940-947.

Krauskopf J. (1980) Discrimination and detection of changes in luminance. Vision Res. **20**, 671-677.

McKee S.P., Klein S.A., Teller D.Y. (1985) Statistical properties of forced-choice psychometric functions: Implications of probit analysis. Perc. and Psychophys. **37**, 286-298.

Nachmias J. (1981) On the psychometric function for contrast detection. Vision Res. **21**, 215-223.

Naka K.-I. (1982) The cells horizontal cells talk to. Vision Res. **22**, 653-660.

Ridder H. de (1987) Dynamic properties of human brightness perception. Thesis Eindhoven University of Technology.

Roufs J.A.J. (1972) Dynamic properties of vision.-I. Experimental relationship between flicker and flash thresholds. Vision Res. **12**, 261-278.

Roufs J.A.J. (1974a) Dynamic properties of vision.-IV. Thresholds of decremental flashes, incremental flashes and doublets in relation to flicker fusion. Vision Res. **14**, 831-851.

Roufs J.A.J.(1974b) Dynamic properties of vision.-VI. Stochastic threshold fluctuations and their effect on flash-to-flicker sensitivity ratio. Vision Res. **14**, 871-888.

Roufs J.A.J., Blommaert F.J.J. (1981) Temporal impulse and step responses of the human eye obtained psychophysically by means of a drift-correcting perturbation technique. Vision Res. **21**, 1203-1221.

Roufs J.A.J., Pellegrino van Stuyvenberg J.A. (1976) Gain curve of the eye to subliminal sinusoidal modulation of light. IPO Annual Progress Report **11**, 56-63.

Roufs J.A.J., Pellegrino van Stuyvenberg J.A. (1979) On the Broca-Sulzer effect: concerning the brightness of time dependent stimuli. IPO Annual Progress Report **14**, 79-87.

Roufs J.A.J., Piceni H.A.L., Pellegrino van Stuyvenberg J.A. (1984) Phase and gain of the visual transient system. IPO Annual Progress Report **19**, 49-56.

Shapley R., Enroth-Cugell C. (1984) Visual adaptation and retinal gain control. In: Osborne, N.N. and Chader, G. J. (Eds.): Progress in Retinal Research, Vol. 3. Oxford: Pergamon Press.

Stork D.G., Falk D.S. (1987) Temporal impulse responses from flicker sensitivities. J. Opt. Soc. Am. A **4**, 1130-1135.

Swanson W.H., Ueno T., Smith V.C., Pokorny J. (1987) Temporal modulation sensitivity and pulse-detection thresholds for chromatic and luminance perturbations. J. Opt. Soc. Am. A **4**, 1992-2005.

Watson A.B. (1982) Derivation of the impulse response: comments on the method of Roufs and Blommaert. Vision Res. **22**, 1335-1337.

Weibull W. (1951) A statistical distribution function of wide applicability. J. Appl. Mech. **18**, 292-297.

Symbols used

This list gives the important symbols and notations (usually occuring in more
than one chapter). All other symbols are restricted to one chapter only, and its
definition can be found there.

Mathematical operations:

$\mathcal{E}$ expected value
$\mathcal{F}$ Fourier transform
$\mathcal{H}$ Hankel transform
$\mathcal{L}$ Laplace transform

List of symbols:

α_i real part of pole p_i
β_i imaginary part of pole p_i
β parameter in the Weibull distribution
ε amplitude of a stimulus (mostly indexed)
ϑ duration of a rectangular pulse
θ_i i-th estimated parameter
θ_i^o true value of the i-th parameter
μ multiplication factor
σ standard deviation (indexed)
$\phi(f)$ phase spectrum
Ψ objective function of the optimization process
Ψ_{xy} cross-correlation of the functions x and y
ω temporal angular frequency
ω_x, ω_y spatial angular frequencies

List of symbols (cont.):

A	amplification factor
d	(internal) threshold level
D	diameter of a disc
E	background intensity
f	temporal frequency
f_c	cut-off frequency
F_a, F_m	sensitivity factors (from threshold-versus-duration curves)
$H(s)$	transfer function of a linear filter
j_i	i-th zero-crossing of the Besselfunction J_0
J_0	Besselfunction (zeroth order, first kind)
M	number of samples
n	order of a linear filter
$n(t)$	noise signal
N	number of free variables in the optimization process
NF	norm factor
p_i	i-th pole of the transfer function
q	proportionality factor in the perturbation experiments
$r(t)$	response of some linear filter
R_i	residual (belonging to pole p_i)
s	complex variable in the Laplace domain
s_m^2	measured variance
s_e^2	variance estimated from the regression
S	sensitivity factor (from a De Lange curve)
t	time variable
t_i	i-th sampling moment
t_{ex}	time delay between the onset of an impulse and the occurence of the extremum of the impulse response
T_c, T_{ca}	critical duration
U_δ^*	amplitude normalized impulse response
U_s^*	amplitude normalized step response
w	spatial angular frequency
$Y(s)$	admittance
z_i	zeros of a transfer function
$Z(s)$	impedance

Summary

The research presented in this thesis concerns the dynamic and spatial properties of the human visual system for threshold excitations around a steady background level. In agreement with current ideas about the behaviour of this system the point of view is adopted that the system processes stimuli in different parallel pathways. The research was concentrated on one of these pathways: *the transient channel*. The aim of this thesis is to provide a simple and accurate model for the behaviour of this system.

First of all, this calls for a discussion (Chapter 1) which stimuli are considered to be mediated by this channel, and thus which experimental data can be used for modelling. An important issue for modelling is the linearity or nonlinearity of the processing. Arguments are presented why it is hard to distinguish certain nonlinear models from the linear ones on the basis of the available experimental material (Chapter 2). Nevertheless, it is shown that a statistical test can be performed on the data from perturbation experiments. This test reveals that the (nonlinear) Rashbass model can be rejected as a candidate for a model of the transient visual system and supports the linearity assumption for this channel (Chapter 2).

The foregoing provided a basis for using data from threshold measurements to estimate linear models. The next thing to do is to make a choice for a specific linear model. Several models are considered in this thesis. All of these were parametrized from subthreshold measurements of the impulse response of the transient channel. Test on the models were made by prediction of threshold-versus-duration curves and by comparison of predicted gain characteristics to experimental data on the sensitivity of the visual system to sinusoidal stimuli.

The first linear model presented in an explicit form is mainly based on the functional argument that the system performs a noise suppression with respect to its internally generated noise. The model is a chain of filters according to the matched filter principle (Chapter 3). The model agrees with the experimental data although some refinements are required.

A fourth-order linear filter is also presented as a model for the transient channel. Since this model has more degrees of freedom than the one discussed previously it marks a more general approach. Unfortunately, since there are more parameters and since the number of samples of experimental data is rather limited, special care has to be taken to ensure a well-defined estimation procedure of the parameters of this model. The technique of this process is described in Chapter 4.

The results obtained by the above mentioned estimation procedure are presented in detail in Chapter 5. A comparison of estimated parameters over different experimental conditions (subject, background level, and field size) is performed. This comparison shows that the estimated model is (virtually) subject independent, whereas both variation of background level and variation of field size reveal systematic shifts in the estimated parameters.

The changes in the estimated parameters of the fourth-order model with varia-

tion in field size are shown to be consistent with a model containing a membrane exists (Chapter 6). The membrane behaves as a spatiotemporal operator. In this way all models as were estimated at the same background level but for different field sizes are incorporated into one larger model. This model can be completely parametrized from the earlier estimates of fourth-order temporal filters. This means that starting from purely temporal modelling of the transient channel, a quantitative estimate is derived for the spatial properties of this channel.

The fourth-order linear filters (and thus the membrane model) show a fall-off in the gain characteristic that is considered too small. Therefore sixth-order filters were taken as a model and estimated for one degree fields at two different background levels (Chapter 7). As was the case for the fourth-order filters, the parameters of the sixth-order changed systematically with background. These shifts in the parameters are consistent with a closed-loop adaptive filter. The properties of such a filter were tested for arbitrary background levels and showed a good agreement with experimental data on flashed and sinusoidal stimuli. In this way all the estimated linear models at different background levels but for the same field size were shown to be compatible with one highly nonlinear model.

All models, the matched-filter model, the membrane model, and the adaptive filter, provide more integrated views on the operation of the transient visual system. An important advantage of these models is furthermore that they are fully quantitatively specified. As is discussed in the last two Chapters of this thesis it is hoped that these models can be integrated and extended to obtain further insight into the processing of visual stimuli by the human eye.

Samenvatting

Het onderzoek in dit proefschrift betreft de dynamische en spatiale eigenschappen van het menselijk visuele syteem voor drempelexcitaties rond een vast achtergrondnivo. In overeenstemming met de huidige ideeen omtrent het gedrag van dit systeem is het standpunt ingenomen dat de verwerking in het systeem gebeurt middels verschillende parallelle processen. Het onderzoek is beperkt tot één van deze processen: de verwerking van stimuli door het *transiënte kanaal*. De bedoeling van dit proefschrift is om simpele en adequate modellen te genereren ter beschrijving van dit proces.

Daartoe wordt allereerst bediscussieerd (Chapter 1) welke stimuli door dit kanaal verwerkt worden, en dus welke experimentele gegevens geschikt zijn ter modellering. Een belangrijk aspect betreffende dit kanaal is de (niet-)lineairiteit van de verwerking. Er wordt aangetoond dat op grond van voorhanden zijnde meetgegevens het principieel moeilijk is om te discrimineren tussen bepaalde niet-lineaire modellen en de klasse van lineaire modellen. Desalnietemin bleek het mogelijk een statistische toets uit te voeren voor meetgegevens met de storing-stechniek. Deze toets wijst het (niet-lineaire) Rashbass model af, en ondersteunt de lineairiteits-hypothese voor het transiënte kanaal (Chapter 2).

Op grond van het voorgaande is gekozen voor het gebruik van meetgegevens van drempelexcitaties om lineaire modellen te schatten. Het lineaire model dient dan gekozen te worden. Verschillende modellen worden beschouwd in dit proefschrift. Alle modellen werden geparametriseerd op grond van onderdrempelige metingen van de impulsresponsie van het transiënte kanaal. De modellen zijn getest met betrekking hun predictieve waarde voor drempel tegen pulsduur karakteristieken en door vergelijking van de voorspelde amplitude-karakteristieken met experimentele gegevens van de gevoeligheid van het systeem voor sinusoïdale stimuli.

Het eerste expliciet geformuleerde lineaire model is voornamelijk gebaseerd op het functionele veronderstelling dat het systeem een optimale signaal-ruis verhouding heeft; invloeden van intern optredende ruis worden door het systeem zelf zoveel mogelijk onderdrukt. Het model bestaat uit een cascade van filters volgens het matched-filter principe (Chapter 3). Het model voldoet aan de experimentele gegevens, maar behoeft enige verfijningen.

Tevens is een vierde orde filter gebruikt als model voor het transiënte kanaal (Chapter 4). Daar dit model meer vrijheidsgraden bezit dan het voorgaande, heeft dit model de kenmerken van een meer algemene aanpak. Ongelukkigerwijs levert een groter aantal vrijheidsgraden extra problemen in een schattingsproces, vooral omdat er slechts een zeer beperkt aantal meetgegevens van de impulsresponsie beschikbaar zijn. Daarom is er extra aandacht besteed om een goed gedefinieerde optimalisatieprocedure voor dit doel te ontwikkelen. Deze techniek is beschreven in Chapter 4.

De resultaten verkregen met de bovengenoemde techniek worden gepresenteerd in Chapter 5. De geschatte parameters zijn vergeleken over de verschillende exper-

imentele condities (proefpersoon, achtergrondnivo, en grootte van de stimulus). Deze vergelijking toont aan dat het geschatte model (praktisch) proefpersoononafhankelijk is, en dat de geschatte parameters systematisch verschuiven met zowel achtergrondnivo als stimulusgrootte.

De verschuiving in de geschatte modelparameters als functie van de stimulusgrootte kan vertaald worden naar een model met een membraan (Chapter 6). Kenmerk van het membraan is dat het zich gedraagt als een systeem waarin ruimtelijke en temporele eigenschappen gekoppeld optreden. Op deze manier zijn de geschatte modellen van verschillende veldgroottes maar bij hetzelfde achtergrondnivo geïntegreerd in een enkel groter model. Dit membraan model kan volledig geparametriseerd worden op grond van de eerder uitgevoerde schattingen van vierde orde filters. Dit houdt tevens in dat uit puur temporele analyses het spatiale gedrag van het transiënte kanaal bepaald kan worden.

De vierde orde modellen (en dus ook het membraan model) geven een hoogfrequent afval die in vergelijking met experimenteel materiaal te laag is. Daarom zijn ook zesde orde filters geschat als model voor het temporele gedrag van 1° velden. Gegevens met betrekking tot twee verschillende achtergrondnivo's waren beschikbaar. Ook hier blijkt, net als bij de vierde orde modellen, dat de geschatte parameters systematisch met nivo meevariëren. De vastgestelde parameterverschuiving komt overeen met de karakteristieken van een adaptief filter. De eigenschappen van zo'n filter zijn bepaald voor willekeurige achtergrondnivo's en komen overeen met experimentele gegevens betreffende pulsvormige en sinusoïdale stimuli. Op deze manier is aangetoond dat het gedrag van het transiënte kanaal op verschillende achtergrondnivo's maar voor dezelfde veldgrootte overeenkomt met het gedrag van een hogelijk niet-lineair filter.

Alle beschouwde modellen, het matched-filter model, het membraan model, en het adaptieve filter, geven een meer geïntegreerde kijk op de werking van het transiënte kanaal. Het belang van het onderzoek ligt mede in het feit dat deze modellen volledig quantitatief gespecificeerd zijn. Zoals besproken in de laatste twee hoofdstukken van dit proefschrift hoopt de schrijver dat de gepresenteerde modellen geïntegreerd en nog uitgebreid kunnen worden om zodoende het inzicht in de verwerking van visuele excitaties door het menselijke oog verder te vergrootten.

Curriculum vitae

17 december 1957	geboren te Heerlen.
aug. 1970 - mei 1976	Sophianum te Vaals, Atheneum B.
sept. 1976 - aug. 1983	Technische Hogeschool Eindhoven, Elektrotechniek. Afstudeerrichting: Theoretische Elektrotechniek. Afstudeeronderwerp: Een incoherent polychromatisch beeldbewerkingssysteem op basis van achromatische Fouriertransformatoren.
sept. 1983 - mei 1984 sept. 1984 - maart 1985	Wetenschappelijk assistent verbonden aan de afd. Elektrotechniek der THE, en werkzaam in de vakgroep 'Meten en Regelen' binnen het projekt 'Netvliesmodellen'.
april 1985 - sept. 1986	Assistent onderzoeker TH Eindhoven binnen de vakgroep 'Meten en Regelen' aan de afdeling der Elektrotechniek. Werkzaam binnen de interafdelingswerkgroep 'Netvliesmodellen' met onderzoeksonderwerp 'Modellen van spatiotemporele kontrastverwerking in het visuele systeem'.
sinds okt. 1986	Universitair docent verbonden aan de faculteit der Elektrotechniek van de TUE in de vakgroep 'Theoretische Elektrotechniek'.

Stellingen

I

Het idee dat proefschriften alleen bewijzen wat iedereen al wist getuigt op zijn minst van een onterechte ontkenning dat quantitatieve analyses nieuwe en verbeterde inzichten kunnen genereren.

J. Blokker (1980) Mij hebben ze niet.
Amsterdam: De Harmonie.

II

Tussen een De Lange karakteristiek en een amplitude-overdracht grafiek van een lineair model voor het visuele systeem bestaat ten gevolge van ruis en de aanwezigheid van meerdere niet-lineair samenwerkende kanalen, een verschil dat niet genoegzaam onderkend wordt.

Dit proefschrift.

III

Het gegeven dat de menselijke visuele detectie van eenvoudige visuele stimuli veelal gemodelleerd wordt met passieve filters betekent niet dat de werkelijke optredende verwerking een passieve zaak is.

A.B. Watson (1986) Temporal sensitivity.
In: Handbook of Perception and Human Performance. Vol. I.
Sensory Processes and Perception.
Eds. K.R. Boff, L. Kaufman and J.P. Thomas.
New York: Wiley.

IV

Door het begrip "artificieel" aan "intelligentie" te koppelen is er begripsmatig geen vooruitgang geboekt op de inhoud van deze laatste term.

P. Vroon (1980) Intelligentie.
Baarn: Ambo.

V

De onbekendheid van de holografie gekoppeld aan haar illusoir karakter belemmert de ontwikkeling van de mogelijkheden van dit medium op het kunstzinnige vlak.

G. Saxby (1988) Practical Holography.
London: Prentice Hall.

VI

Door een omschrijving van de criteria waaraan stellingen dienen te voldoen zoals in artikel 17, lid 4 van het promotieregelement 1987 der TUE, bestaat het gevaar dat provocerende stellingen onverdedigbaar verklaard worden.
Promotieregelement 1987.
Technische Universiteit Eindhoven.

VII

Alle stellingen die op zichzelf terugslaan dienen bij promoties geweerd te worden.

Bert den Brinker

Eindhoven, 17 maart 1988.